NASA CR-145214

(NASA-CR-145214) A USER'S GUIDE FOR V174, A PROGRAM USING A FINITE DIFFERENCE METHOD TO ANALYZE TRANSONIC FLOW OVER OSCILLATING WINGS Final Report (Boeing Commercial Airplane Co., Seattle) 98 p HC A05/MF A01 G3/02
N78-12013
Unclas
53595

A User's Guide for V174 – A Program Using a Finite Difference Method to Analyze Transonic Flow Over Oscillating Wings

T. D. Butler, W. H. Weatherill,
J. D. Sebastian, and F. E. Ehlers

Boeing Commercial Airplane Company
Seattle, Washington

Prepared for
Langley Research Center
under contract NAS1-14204

National Aeronautics and
Space Administration

1977

1 Report No NASA CR-145214	2 Government Accession No	3 Recipient's Catalog No.
4 Title and Subtitle A USER'S GUIDE FOR V174 A PROGRAM USING A FINITE DIFFERENCE METHOD TO ANALYZE TRANSONIC FLOW OVER OSCILLATING WINGS		5 Report Date December 1977
		6 Performing Organization Code
7 Author(s) T. D. Butler, W. H. Weatherill, J. D. Sebastian, and F. E. Ehlers		8 Performing Organization Report No
		10 Work Unit No
9 Performing Organization Name and Address Boeing Commercial Airplane Company P.O. Box 3707 Seattle, Washington 98124		11 Contract or Grant No NAS1-14204
		13 Type of Report and Period Covered
12 Sponsoring Agency Name and Address Langley Research Center National Aeronautics and Space Administration Washington, D.C. 20546		14 Sponsoring Agency Code Final Report
15 Supplementary Notes		

16 Abstract

This document describes the design and usage of a pilot program using a finite difference method for calculating the pressure distributions over harmonically oscillating wings in transonic flow. The procedure used is based on separating the velocity potential into steady and unsteady parts and linearizing the resulting unsteady differential equation for small disturbances. The steady velocity potential, that must be obtained from some other program, is required for input. The unsteady differential equation, as solved here, is linear, complex in form with spatially varying coefficients. Since sinusoidal motion is assumed time is not a variable. The numerical solution is obtained through a finite difference formulation and a line relaxation solution method.

17 Key Words (Suggested by Author(s))		18 Distribution Statement	
Unsteady flow Transonic flow Oscillating wings Oscillating Airfoils Flutter		Unclassified - unlimited Subject category 02	
19 Security Classif (of this report) Unclassified	20. Security Classif (of this page) Unclassified	21. No of Pages 95	22 Price*

*For sale by the National Technical Information Service, Springfield, Virginia 22151

CONTENTS

Page

1.0 SUMMARY 1
2.0 INTRODUCTION 1

3.0 SYMBOLS AND ABBREVIATIONS 4

4.0 DISCUSSION 6

5.0 COMPUTER PROGRAM USAGE 13
- 5.1 Machine Requirements 13
- 5.2 Operating System 13
- 5.3 Storage Allocation 13
- 5.4 Timing 13
- 5.5 File I/O 13
  - 5.5.1 File Utilization 13
  - 5.5.2 File Formats 15
- 5.6 Control Cards 16
- 5.7 Program Input 17
  - 5.7.1 General Remarks 17
  - 5.7.2 Limitations 18
  - 5.7.3 Data Stacking 18
- 5.8 Program Output 22
  - 5.8.1 Program Results 22
  - 5.8.2 Program Diagnostics 22

6.0 COMPUTER PROGRAM DESCRIPTION 24
- 6.1 Overlay Structure 24
- 6.2 Common Block Usage 25

APPENDIX A 27

APPENDIX B 39

REFERENCES 95

FIGURES

No.		Page
1	Schematic of Mesh for Three-Dimensional Problem	2
B-1	Program V174	39
B-2	Subroutine DISP	45
B-3	Subroutine PLANE	47
B-4	Subroutine CPR	51
B-5	Subroutine DELT	53
B-6	Complex Function DELPHI	53
B-7	Program INIT	54
B-8	Subroutine AIRFOIL	58
B-9	Subroutine MESH	61
B-10	Subroutine INCOND	62
B-11	Subroutine STDST	63
B-12	Program COLLAX	65
B-13	Subroutine TRIDIAG	68
B-14	Subroutine MATRXCF	69
B-15	Program ROWLAX	73
B-16	Subroutine FOURDG	77
B-17	Subroutine SRMATCF	78
B-18	Program FARFLD	84
B-19	Complex Function FCNX	91
B-20	Complex Function FCNYZ	92
B-21	Complex Function LAGUER	93

A USER'S GUIDE FOR V174
A PROGRAM USING A FINITE DIFFERENCE METHOD
TO ANALYZE TRANSONIC FLOW OVER OSCILLATING WINGS

T. D. Butler, W. H. Weatherill,
J. D. Sebastian, and F. E. Ehlers
Boeing Commercial Airplane Company

1.0 SUMMARY

This document describes the design and usage of a pilot program for calculating pressure distributions over harmonically oscillating wings in transonic flow. The procedure is based on separating the velocity potential into steady and unsteady parts and linearizing the resulting differential equation for the unsteady flow by assuming small disturbances. The steady velocity potential distribution, which must be obtained from some other program, is required for input. The differential equation for the unsteady flow is linear, complex in form, with spatial varying coefficients that are dependent on the steady velocity potential distribution. Time is not a variable in the program since sinusoidal motion is assumed. The numerical solution is obtained through a finite difference formulation and a line relaxation solution procedure.

This program may be used for wings with arbitrarily, swept leading- and trailing-edges. The leading edge may be curved. However, the trailing edge must be straight. The program uses a rectangular array of mesh points.

2.0 INTRODUCTION

This document describes the design and usage of the FORTRAN IV digital computer program V174. This pilot program was written as part of a research effort to develop a method of computing the transonic perturbation flow about a harmonically oscillating three-dimensional wing.

Based on the finite difference procedures of references 1 through 3, the program computes the solution of the unsteady velocity potential and the resulting unsteady pressure distributions. It requires as input the potential distribution from a steady state transonic small perturbation program (ref. 4). Conservative differencing is used for subsonic points and nonconservative differencing for supersonic points and across shocks. Figure 1 shows the geometry used for the program.

The program is set up to calculate the deflections and slopes for a control surface mode, a pitch mode, or a flapping mode. The control surface, which is located at the trailing edge, may be either partial or full span. Although a modal amplitude theta (θ) is input, the printed pressure coefficients are for unit amplitude motion. Other motions may be treated by modifying the appropriate boundary condition subroutine.

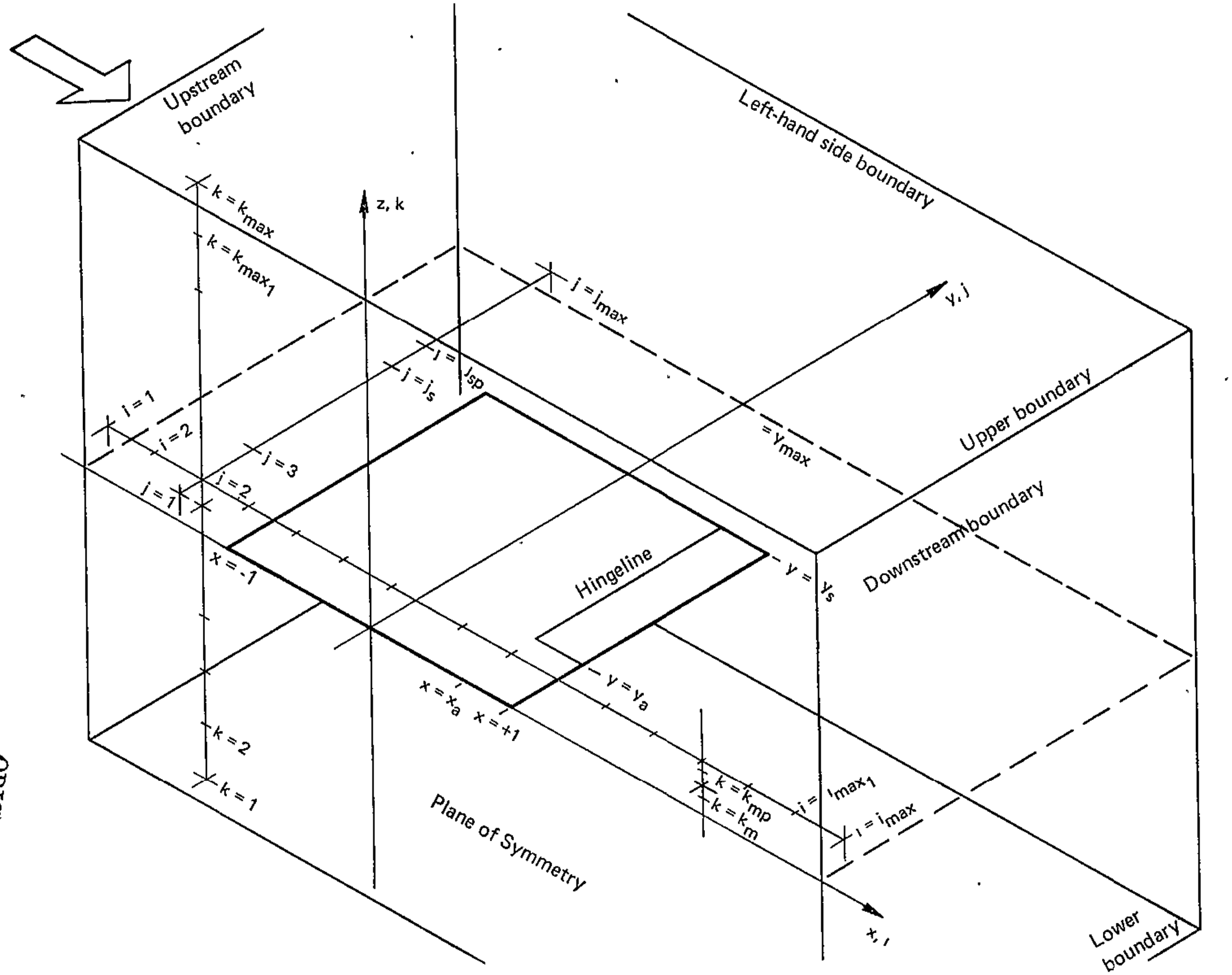

Figure 1.—Schematic of Mesh for Three-Dimensional Problem

Included in this document are:

- Description of equations used in the program
- Description of user I/O and scratch file formats
- List of program limitations
- Description of computer program usage
- Data stacking procedures
- Description of program output, normal and diagnostic
- Sample problem input/output
- Description of program structure and routines used

Features of this program include options to:

- Analyze flat plates or wings with thickness
- Use row or column line relaxation
- Begin the iterative solution from a previous solution of the same dimensions
- Analyze wings with swept leading and trailing edges
- Take advantage of autosymmetry in the case of a wing at zero angle of attack and with a symmetrical thickness distribution to substantially reduce the number of nodes
- Use over- and under-relaxation factors to reduce the number of iterations to convergence
- Determine iteration print intervals
- Determine far-field updating intervals

3.0 SYMBOLS AND ABBREVIATIONS

a,b	coefficients for y,z differences corresponding to second deriatives, with appropriate subscripts (eq. (3))
b	root semichord of wing
c,d	coefficients for x difference corresponding to second derivative (eq. (3))
$c_{k1},c_{k2},c_{k3},c_{k4}$	equation (28)
$c_{s1},c_{s2},d_{s1},d_{s2}$	equation (13)
c_1,d_1,c_2,d_2	coefficients for second-order accurate difference corresponding to first derivative (eq. (3))
E	coefficients in difference equations with appropriate subscripts
F_{ij}	equation (6)
f(x,y,t)	instantaneous wing shape defined by $z_0 = \delta f(x,y,t)$
f_0	undisturbed wing or airfoil shape
f_1	unsteady contribution to wing or airfoil shape
h	$z_{k_{m+1}} - z_{k_m}$
i	$\sqrt{-1}$
i, j, k	x,y,z subscripts for points in the mesh
M	freestream Mach number
U	freestream velocity
x_a	coordinate of control surface hinge line
x,y,z	scaled coordinates $(x_0, \mu y_0, \mu z_0)$ for the three-dimensional problem
$\bar{x},\bar{y},\bar{z}$	coordinates defined in equation (18)
x_ℓ,x_t	coordinates of leading and trailing edges
x_0,y_0,z_0	physical coordinates, made dimensionless with the root semichord
x_1',y_1',z_1'	variables of integration

y_t	coordinate of wingtip
β	$\sqrt{1 - M^2}$
γ	ratio of specific heats for air
ΔC_p	jump in pressure coefficient
Δx_1	$x_i - x_{i-1}$
Δx_2	$x_{i-1} - x_{i-2}$
$\Delta\varphi_1$	jump in φ_1 at plane of wing or vortex wake
δ	thickness ratio or measure of camber and angle of attack
δ_1	$x_2 - x_1$
δ_2	$x_{i_{max}} - x_{i_{max}-1}$
ϵ	$(\delta/M)^{2/3}$
λ_1	$\omega M/(1 - M^2)$
μ	scale factor on y_0 and z_0, $\mu = \delta^{1/3} M^{2/3}$
ϕ	unscaled perturbation velocity potential
φ_0 or Phi_0	steady scaled perturbation velocity potential
φ_1 or Phi_1	unsteady scaled perturbation velocity potential
φ_{1_w}	wake integral defined in equation (21)
χ	acceleration or pressure potential
ψ	fundamental source solution of integral equation for evaluation of far-field boundary conditions
ω	angular reduced frequency (semichord times frequency in radians per second divided by the freestream velocity, $\omega b/U$)

ORIGINAL PAGE IS
OF POOR QUALITY

4.0 DISCUSSION

The finite difference equations for three-dimensional unsteady transonic flow are given by Ehlers in reference 1. At interior points where the steady flow is subsonic, we have

$$a_{z_k}\varphi_{1_{ijk-1}} - \left(a_{y_j} + b_{y_j} + a_{z_k} + b_{z_k} + E_1 + E_2 - q_{ijk}/2\right)\varphi_{1_{ijk}} \tag{1}$$

$$+ b_{z_k}\varphi_{1_{ijk+1}} = -E_1\varphi_{1_{i+1jk}} - E_2\varphi_{1_{i-1jk}} - a_{y_j}\varphi_{1_{ij-1k}} - b_{y_j}\varphi_{1_{ij+1k}}$$

and at points where the steady flow is supersonic,

$$a_{z_k}\varphi_{1_{ijk-1}} - \left(a_{y_j} + b_{y_j} + a_{z_k} + b_{z_k} - E_3 - q_{ijk}/2\right)\varphi_{1_{ijk}} \tag{2}$$

$$+ b_{z_k}\varphi_{1_{ijk+1}} = (E_3 + E_4)\varphi_{1_{i-1jk}} - E_4\varphi_{1_{i-2jk}} - a_{y_j}\varphi_{1_{ij-1k}} - b_{y_j}\varphi_{1_{ij+1k}}$$

where:

$$a_{z_k} = \frac{1}{(z_{k+1} - z_{k-1})(z_k - z_{k-1})} \qquad a_{y_j} = \frac{1}{(y_{j+1} - y_{j-1})(y_j - y_{j-1})} \tag{3}$$

$$b_{z_k} = \frac{1}{(z_{k+1} - z_{k-1})(z_{k+1} - z_k)} \qquad b_{y_j} = \frac{1}{(y_{j+1} - y_{j-1})(y_{j+1} - y_j)}$$

$$E_1 = c_i u_{i+\frac{1}{2}jk} - i\omega c_{1_i}/\epsilon$$

$$E_2 = d_i u_{i+\frac{1}{2}jk} + i\omega d_{1_i}/\epsilon$$

$$E_3 = c_{i-1} u_{i-\frac{1}{2}jk} - i\omega c_{2_i}/\epsilon$$

$$E_4 = d_{i-1} u_{i-\frac{3}{2}jk} - i\omega d_{2_i}/\epsilon$$

$$c_i = \frac{1}{(x_{i+1} - x_{i-1})(x_{i+1} - x_i)} \qquad c_{1_i} = (x_i - x_{i-1})\cdot c_i$$

$$d_i = \frac{1}{(x_{i+1} - x_{i-1})(x_i - x_{i-1})} \qquad d_{1_i} = (x_{i+1} - x_i)\, d_i$$

$$u_{i+\frac{1}{2}jk} = K - (\gamma+1)(\varphi_{0_{i+1jk}} - \varphi_{0_{ijk}})/(x_{i+1} - x_i)$$

$$u_{i-\frac{1}{2}jk} = K - (\gamma+1)(\varphi_{0_{ijk}} - \varphi_{0_{i-1jk}})/(x_i - x_{i-1})$$

$$c_{2_i} = \frac{1}{x_i - x_{i-1}} + \frac{1}{x_i - x_{i-2}}$$

$$d_{2_i} = -d_{1_{i-1}}$$

Equations (1) and (2) are equations (24) and (27) from reference 1.

The boundary conditions on the upper and lower wing surfaces lead to the following equations for subsonic flow at finite difference points immediately below the wing, $k = k_m$

$$a_{z_{k_m}} \varphi_{1\,ijk_m-1} - \left(a_{y_j} + b_{y_j} + a_{z_{k_m}} + E_1 + E_2 - q_{ijk_m}/2\right) \varphi_{1\,ijk_m} \tag{4}$$

$$= -E_1 \varphi_{1\,i+1jk_m} - E_2 \varphi_{1\,i-1jk_m} - a_{y_j} \varphi_{1\,ij-1k_m} - b_{y_j} \varphi_{1\,ij+1k_m} - h_1\, b_{z_{k_m}} F_{ij}^{(L)}$$

and points immediately above the wing, $k = k_m + 1$

$$-\left(a_{y_j} + b_{y_j} + b_{z_{k_m+1}} + E_1 + E_2 - q_{ijk_m+1}/2\right) \varphi_{1\,ijk_m+1} + b_{z_{k_m+1}} \varphi_{1\,ijk_m+2} \tag{5}$$

$$= -E_1 \varphi_{1\,i+1jk_m+1} - E_2 \varphi_{1\,i-1jk_m+1} - a_{y_j} \varphi_{1\,ij-1k_m+1} - b_{y_j} \varphi_{1\,ij+1k_m+1} + h_1\, a_{z_{k_m+1}} F_{ij}^{(U)}$$

where

$$F_{ij}^{(L)} = f_{1_x}^{(L)} (x_i, y_j) + i\omega f_1^{(L)} (x_i, y_j) \tag{6}$$

$$F_{ij}^{(U)} = f_{1_x}^{(U)} (x_i, y_j) + i\omega f_1^{(U)} (x_i, y_j)$$

The (L) and (U) refer to upper and lower wing surfaces, respectively. The equations similar to equations (4) and (5) at supersonic points can be written down analogously.

The total harmonic deflection of the wing is written as

$$z_0 = \delta f(x,y,t) = \delta \left\{ f_0 (x,y) + f_1 (x,y)\, e^{i\omega t} \right\} \tag{7}$$

The steady velocity potential (φ_0) is calculated from the steady deflection shape (f_0),while the unsteady potential (φ_1) is calculated from the harmonic mode shape $f_1(x,y)$.

Over the wake, the condition that the trailing vortex sheet supports no pressure,

$$\frac{\partial \Delta\varphi_1}{\partial x} + i\omega\Delta\varphi_1 = 0 \tag{8}$$

results in a term being added to the right-hand side of equations (1) and (2). For finite difference points just below the wing plane ($k = k_m$), the additional term is

$$b_{z_{k_m}} \Delta\varphi_{1\,ij} \tag{9}$$

and for points just above the wing plane ($k = k_m + 1$), the term is

$$-a_{z_{k_m+1}} \Delta\varphi_{1\,ij} \tag{10}$$

where

$$\Delta\varphi_{1\,ij} = \Delta\varphi_{1\,i_1+1j}\, e^{-i\omega(x_i - x_{i_1+1})} \tag{11}$$

and $\Delta\varphi_{1i_1+1j}$ is the jump in velocity potential at the first point aft of the wing trailing edge at station j determined so as to satisfy the Kutta condition on the trailing edge. The addition of equations (9) and (10) implicitly satisfies the conditions. The normal velocity is continuous across the wake.

The finite difference equation for the jump in φ_1 across the wing to the second order in mesh size is

$$\Delta\varphi_1 = \varphi_1^{(U)} - \varphi_1^{(L)} = \varphi_{1\,ijk_m+1} - \varphi_{1\,ijk_m} - c_{s1}\left(\varphi_{1\,ijk_m+2} - \varphi_{1\,ijk_m+1}\right)$$

$$- c_{s2}\left(\varphi_{1\,ijk_m} - \varphi_{1\,ijk_m-1}\right) - \left(d_{s1}\, F_{ij}^{(U)} + d_{s2}\, F_{ij}^{(L)}\right) \tag{12}$$

where

$$c_{s1} = \frac{1}{4s_1(s_1+1)} \qquad c_{s2} = \frac{1}{4s_2(s_2+1)}$$

$$d_{s1} = \frac{h(2s_1+1)}{4(s_1+1)} \qquad d_{s2} = \frac{h(2s_2+1)}{4(S_2+1)} \tag{13}$$

$$s_1 = \left(z_{k_m+2} - z_{k_m+1}\right)/h \qquad s_2 = \left(z_{k_m} - z_{k_m-1}\right)/h$$

$$h = z_{k_m+1} - z_{k_m} \tag{14}$$

Two integral relations are used to satisfy the far-field boundary conditions on the outer boundaries of finite difference mesh. The first for the velocity potential is

$$\varphi_1(x_1,y_1,z_1) = \frac{1}{4\pi}\int_{-y_t}^{+y_t}\int_{x_\ell(y_1')}^{x_t(y_1')}\left[\Delta\varphi_1\ \psi_{z_1'} - \psi\Delta\varphi_{1_{z_1'}}\right]dx_1'\,dy_1'$$

$$+\frac{1}{4\pi}\int_{-y_t}^{+y_t} e^{i\omega x_t(y_1')}\,\Delta\varphi_{1_t}(y_1')dy_1'\int_{x_t(y_1')}^{\infty} e^{-i\omega x_1'}\,\psi_{z_1'}\,dx_1'$$

$$+\frac{1}{4\pi}\int_V\left\{(\gamma+1)\varphi_{0_{x_1'}}\,\varphi_{1_{x_1'}}\,\psi_{x_1'} - i\omega(\gamma-1)\varphi_1\ \psi\varphi_{0_{x_1'x_1'}}\right\}dv' \qquad (15)$$

and the second for the pressure function is

$$P(x_1,y_1,z_1) = \varphi_{1_{x_1}} + i\omega\varphi_1 \qquad (16)$$

$$= \frac{1}{4\pi}\int_{-y_t}^{+y_t}\int_{x_\ell(y_1')}^{x_t(y_1')}\left[\Delta\varphi_1\ \chi_{z_1'} - \chi\Delta\varphi_{1_{z_1'}}\right]dx_1'\,dy_1'$$

$$-\frac{1}{4\pi}\int_{-y_t}^{+y_t} e^{\,i\omega x_t(y_1')}\Delta\varphi_{1_t}(y_1')\psi_{z_1}(x_t(y_1')-x_1, y_1-y_1', z_1)\,dy_1'$$

$$+\frac{1}{4\pi K}\int_V\left\{(\gamma+1)\varphi_{0_{x_1'}}\,\varphi_{1_{x_1'}}\,\chi_{x_1'} - i\omega(\gamma-1)\varphi_1\ \chi\varphi_{0_{x_1'x_1'}}\right\}dv' \qquad (17)$$

defining

$$\bar{x} = x_1 - x_1',\ \bar{y} = y_1 - y_1',\ \bar{z} = z_1 - z_1' \text{ and } R = \sqrt{\bar{x}_1^2 + \bar{y}^2 + \bar{z}^2}$$

$$\psi(\bar{x},\bar{y},\bar{z}) = \frac{e^{\,i\lambda_1(M\bar{x} - R)}}{R}$$

$$\psi_{z_1'} = \frac{\bar{z}}{R}(1/R + i\lambda_1)\psi$$

$$\psi_{x_1'} = \left[i\lambda_1 M - \frac{\bar{x}}{R}(1/R + i\lambda_1)\right]\psi \qquad (18)$$

ORIGINAL PAGE IS OF POOR QUALITY

$$\chi = \psi_{x_1} + i\omega\psi$$

$$\chi = \left[i\lambda_1 M - \frac{\overline{x}}{R}(1/R + i\lambda_1) + i\omega \right] \psi$$

$$\chi_{z_1'} = -\frac{\overline{z}}{R}\left\{\left[\frac{3\overline{x}}{R^2} - i\lambda_1 M - i\omega\right](i\lambda_1 + 1/R) - \lambda_1{}^2\,\overline{x}/R\right\}\psi \tag{18}$$

Equations (15) and (17) have been simplified for the program. First, as noted in the two-dimensional derivation

$$\frac{\partial \Delta\varphi_1}{\partial z_1} = \Delta\left(\frac{\partial \varphi_1}{\partial z_1}\right) = 0 \tag{19}$$

and thus the second integral in the first term of both equations (15) and (17) is zero. Second, the third term, which is the volume integral and has not been of significance in the two-dimensional problem, has been dropped. Third, since we are interested in the far-field, we approximate $x_1 - x_1'$ and $y_1 - y_1'$ with y_1 so that the terms of ψ and χ may be moved outside the integral sign. The evaluation of wake integral in equation (15) is discussed in detail in the next section. The equation for the velocity potential on the far-field (eq. (15)) for $x_a = 1.0$ is

$$\varphi_1(x_1, y_1, z_1) = \frac{1}{4\pi}\psi_{z_1'} \int_{-y_t}^{+y_t} \int_{x_\ell(y_1')}^{x_t(y_1')} \Delta\varphi_1 \, dx_1' dy_1' + \varphi_{1_w}$$

$$+ \frac{1}{4\pi K}\int_V \left\{(\gamma+1)\,\varphi_{0_{x_1'}}\,\varphi_{1_{x_1'}}\,\psi_{x_1'} - i\omega(\gamma-1)\varphi_1\,\psi\varphi_{0_{x_1'x_1'}}\right\} dv' \tag{20}$$

where

$$\varphi_{1_w} = \frac{1}{4\pi}\int_{-y_t}^{+y_t} \Delta\varphi_{1_t}(y_1')\, I_w(y_1, z_1, y_1')\, dy_1' \tag{21}$$

with the trailing edge defined as a straight line by the functions $f(y_1') = a|\,y_1'\,|$, the function I_w is given as

$$I_w = \frac{z_1 e^{-i\lambda_1 \beta \overline{R}_0(\overline{u}_1/M)}}{\overline{R}_0}\left\{\frac{1}{\sqrt{1+\overline{u}_1{}^2}}\left(\frac{M}{\beta\sqrt{f^2(y_1') + \overline{R}_0{}^2}} - \frac{\overline{u}_1}{\overline{R}_0}\right) + \frac{i\lambda_1}{M}\left[-\beta\sqrt{1+\overline{u}_1{}^2} + \sum_{i=1}^{N} W_i F(\tau_i)\right]\right\} \tag{22}$$

$$\bar{u}_1 = \frac{M\sqrt{f^2(y_1') + \bar{R}_0^2} + f(y_1')}{\beta \bar{R}_0}$$

$$F(\tau) = \sqrt{\beta^2 + \left[\beta \bar{u}_1 - \frac{iM}{\lambda_1 \bar{R}_0} \tau\right]^2}$$

$$\bar{R}_0 = \sqrt{(y_1 - y_1')^2 + z_1^2}$$

The pressure function equation (9) becomes

$$P(x_1, y_1, z_1) = \frac{1}{4\pi} X_{z_1'} \int_{-y_t}^{+y_t} \int_{x_\ell(y_1')}^{x_t(y_1')} \Delta\varphi_1 \, dx_1' \, dy_1'$$

$$- \frac{1}{4\pi} \psi_{z_1} \int_{-y_t}^{+y_t} e^{i\omega x_t(y_1')} \Delta\varphi_{1_t}(y_1') \, dy_1' \tag{23}$$

Equation (20) is used to evaluate the velocity potential along the line resulting from the intersection of the Y-Z plane through the trailing edge of the wing and the X-Y and X-Z planes bounding the finite difference volume. Equation (16) is then integrated by the trapezoidal rule to determine values ahead of this line and behind this line on the upper, lower, and side boundaries. For example, on the lower boundary when $k = 1$, for points ahead of the trailing edge ($x<1.0$ or $i<i_1$),

$$\varphi_{1_{i-1j1}} = \varphi_{1_{ij1}} \, e^{i\omega(x_i - x_{i-1})} - \left[P(x_i, y_j, z_1)\, e^{i\omega(x_i - x_{i-1})} + P(x_{i-1}, y_j, z_1)\right] \frac{x_i - x_{i-1}}{2} \tag{24}$$

and the equation for points downstream of the trailing edge ($i_1<i$) is

$$\varphi_{1_{ij1}} = \varphi_{1_{i-1j1}} \, e^{-i\omega(x_i - x_{i-1})} + \left[P(x_i, y_j, z_1) + P(x_{i-1}, y_j, z_1)\, e^{-i\omega(x_i - x_{i-1})}\right] \frac{x_i - x_{i-1}}{2} \tag{25}$$

The application of equation (23) to the upstream and downstream boundaries results in the following equations: on the upstream boundary,

$$\varphi_{1_{1jk}} = c_{k1} \varphi_{1_{2jk}} - c_{k2} P_{1jk} \tag{26}$$

and for the downstream boundary,

$$\varphi_{1_{i_{max}jk}} = c_{k3}\,\varphi_{1_{i_{max}-1jk}} + c_{k4}\,P_{i_{max}jk} \tag{27}$$

where

$$P_{1jk} = P(x_1, y_j, z_k)$$

$$P_{i_{max}jk} = P(x_{i_{max}}, y_j, z_k)$$

and

$$c_{k1} = \frac{1 + i\omega\delta_1/2}{1 - i\omega\delta_1/2} \qquad \delta_1 = x_2 - x_1$$

$$c_{k2} = \delta_1/(1 - i\omega\delta_1/2) \tag{28}$$

$$c_{k3} = (1 - i\omega\delta_2/2)/(1 + i\omega\delta_2/2) \qquad \delta_2 = x_{i_{max}} - x_{i_{max}-1}$$

$$c_{k4} = \delta_2/(1 + i\omega\delta_2/2)$$

Equations (25) and (26) may be used to substitute for $\varphi_{1_{1jk}}$ and $\varphi_{1_{i_{max}jk}}$ in equations (1) and (2).

5.0 COMPUTER PROGRAM USAGE

5.1 MACHINE REQUIREMENTS

V174 executes on a CDC 6600 or similarly compatible computer.

5.2 OPERATING SYSTEM

V174 was designed for a KRONOS 2.1 or NOS 1.1 operating system.

5.3 STORAGE ALLOCATION

This program executes in 132000 octal words of computer memory.

5.4 TIMING

Timing is hardware and operating system dependent.

The following example was run on a CDC 6600 with KRONOS 2.1 operating system. The program loads in about 4.5 CP (central processor) seconds. Using an XYZ mesh of 44 by 16 by 26 (18 304 nodes), the program requires about 5 CP seconds per iteration. It needs a like amount of time for each far-field update; 50 iterations of this example with a far-field update every 10 would require:

$$\text{CP seconds} = 4.5 + (50)(5) + (50/10 + 1)(5)$$

or 284.5 decimal seconds. Rounding up the user would place 300 decimal seconds on his job card.

5.5 FILE I/O

The program card of V174 is as follows:

```
Program V174  (INPUT= 1002,OUTPUT=1002,TAPE7,DEBUG,TAPE5=INPUT,
              TAPE6=OUTPUT,TAPE1=1002,TAPE10=1002,
              TAPE11=1002,TAPE12=1002,TAPE13=1002)
```

As noted previously, the buffer sizes of most of these files have been reduced from the default values to save memory space.

5.5.1 FILE UTILIZATION

A considerable saving of core memory, and consequently cost, was achieved by modifying the program. This modification puts only 3 planes of the Phi_1 and Phi_0 matrices in core at a time. These planes are chordwise X-Z planes and are denoted by the J indice (identifying their Y coordinate). Thus, on any one binary file there will be JMAX planes of data.

In core the program identifies the necessary 3 planes as JR (corresponding to J+1–see theory), JC, (corresponding to J), and JL (corresponding to J-1). There are 3 indices available in the incore matrix data space, but each of these will be reused as often as necessary moving JR, JC, and JL. For instance, if the program is calculating the X-Z chordwise plane corresponding to J indice 6 this plane may have been read into the incore storage area plane numbered 3 and would designate that incore plane as JC. Calculation plane corresponding to J = 5 would be in JL which would be stored in the incore data storage plane 1. The next calculation plane JR (corresponding to J=7) would be read into the available incore plane storage area 2.

After calculation plane J = 6 is recalculated, and written to binary file, this plane is now designated JL by the program. The former JR now becomes JC (incore plane area 1) and a plane corresponding to J = 8 is read in and placed in the incore storage area now designated JR (incore storage area 3).

Thus, for calculation of plane J = 6 the incore storage should be as follows:

	Calculation plane	Incore plane storage area
Plane JC	6	3
Plane JR	5	1
Plane JL	7	2
For calculation of plane J = 7:		
Plane JC	7	1
Plane JR	6	2
Plane JL	8	3

Please note that the description applies to the usage of the Phi_0 matrix as well, with the exception that it is not recalculated with each iteration.

The file named TAPE1 contains one steady state velocity potential distribution (Phi_0) from a separate program. This matrix must be present for a wing with thickness (see ref. 3 and input variable list MSTST).

The file named TAPE13 contains the modified Phi_0 matrix from file TAPE1. This matrix is written on the file in the standard form for this program. The initialization overlay recalculates this matrix. During iterations the Phi_0 matrix on this file is read as previously described.

The file named TAPE10 is the file containing the starting data, if any (see input list variable, INC), for the Phi_1 matrix. After a successful execution of the program it will contain the new Phi_1 matrix in place of the old. Its format is standard for this program (sec. 3.5.2).

The files named TAPE11 and TAPE12 are interchanged in function for each iteration of the program. They will contain the scratch Phi_1 matrix in the standard format discussed in section 3.5.2. Initially, one of these will contain the starting Phi_1 matrix. Either may be from TAPE10, a previous run, or a Phi_1 matrix of zeros. The other will then have written on it the Phi_1 calculations from this iteration. For the next iteration these files will be rewound and functions interchanged with the former supply file becoming the receiving file for this iteration.

5.5.2 FILE FORMATS

Binary files

The files TAPE1, TAPE10, TAPE11, TAPE12, and TAPE13 are binary I/O files and all use the same basic structure of format. TAPE1 and TAPE13 are real data (Phi_0 matrix); TAPE10, TAPE11, and TAPE12 are complex with a real- and imaginary-parts written for each element of the matrix (Phi_1).

The structure of these binary files are as follows:

1 (J indice of the first plane)
The I^{th} element at K = 1
.
.
.
The $IMAX^{th}$ element at K = 1
The I^{th} element at K = 2
.
.
.
The $IMAX^{th}$ element at K = 2
.
.
.
.
.
.
The $IMAX^{th}$ element at K = KMAX

2 (J indice of the second plane)
. same structure as the above plane
.
.
.

ORIGINAL PAGE IS
OF POOR QUALITY

.

JMAX (indice of last plane)
I^{th} element at K = 1

.
.
.
.
.
.

$IMAX^{th}$ element at K = KMAX

As mentioned previously the complex binary files will contain a real part and an imaginary part for each element of the Phi_1 matrix.

BCD Files

The BCD files INPUT, OUTPUT, and TAPE7 follow the standard FORTRAN and system formats for that type of file.

BCD files are those which deal with character printing or reading. V174 has three of these; INPUT, OUTPUT, and TAPE7.

INPUT, also called TAPE5, is the file which contains cards or card images. Program card (or card image) input is fully described in section 3.7.

OUTPUT, also called TAPE6, is the file on which the program places the primary printed information. (See sec. 3.8 and app. A.)

TAPE7 is also a print file. The user may disregard it unless he is executing the program on a terminal where the primary OUTPUT print file is to be printed later. It will print a summary during execution telling the user how convergence is proceeding.

Usage of TAPE7 is LGO,IN,OUT,OUTPUT. (See sec. 3.6.)

TAPE7 was primarily used in development of the program. Terminal usage of the program should be limited as terminal execution is usually very expensive.

5.6 CONTROL CARDS

The following control cards can be used to load and execute TEV174 from tape:

```
JOBN,T500,CM132000,P02.
ACCOUNT,ACCTNO,PASWD.   URNAME/PH/M.S./ORG
REQUEST,TAPE,VSN=66XYYY,F=I,LB=KL.
COPYBF,TAPE,LGO.
RETURN,TAPE.
```

GET,TAPE1=URPHI0.
GET,TAPE10=URPHI1.
MAP,FULL.
LGO.
End of Record
Input Cards

The preceding will execute using existing $Phi_0$and Phi_1 distribution files. If either is not available, then adjustments are made in the input cards and the respective GET card is not used.

5.7 PROGRAM INPUT

5.7.1 GENERAL REMARKS

The input to TEV174 is of two forms, disk file/tape input (binary input) and card input (BCD input). Disk file/tape input may consist of input point locations and the Phi_0 and/or Phi_1 distribution. An input Phi_1 distribution is indicated if a previously calculated Phi_1 matrix is to be used to start the iteration process. If the user is starting from scratch, there is no Phi_1 input and the initial Phi_1 distribution is all zeros. Phi_0 is the steady-state distribution from another program. If a flat plate solution is sought, it would not be input.

A description of disk file/tape formats is given in section 5.5.2 and a listing of the input for a sample problem is presented in appendix A.

The card input consists of field dependent input and namelist free field input. The field dependent input is defined in the format column of table 1 as a specific field (i.e., F10.2, A10, I5). The namelist data will be represented in the same column by the namelist name "PARAM."

Some of the features of namelist input are:

1. Card field consists of columns 2 through 80.

2. List consists of a $ list-name in column 2 followed by a series of specifications continued on as many cards as required and terminated by a $.

3. Specifications are of the form:

   a. Vname = Value

   b. Where Vname is an array, Vname = Value1, Value2, . . . ,Valuen

   Where Vname is one of the variable names for the list, value is the associated value(s). Value may be an integer, a floating point number in normal or exponential form, or in the case of a logical variable (specifically the options) of the form.

ORIGINAL PAGE IS
OF POOR QUALITY

.T. or .True. indicating true or on

.F. or .False. indicating false or off

4. Specifications must be separated by commas. There is no comma between the last specification and terminating $.

5. Embedded blanks are allowed except within the $ list-name, variable name, or value. At least one blank must separate the $ list-name and the first specification.

6. The order of appearance of variables on the card(s) is not important; the spelling is.

7. Any or all of the variables may be left out of the list, e.g., $ list-name . . $ is legitimate. This assumes, of course, that there is a legal default value associated with the variable(s) not included in the list.

5.7.2 LIMITATIONS

The following are size limitations within the program.

- $3 \leq IMAX \leq 55$ — X nodes parallel to upstream downstream flow in the XYZ mesh.
- $3 \leq JMAX \leq 33$ — Y nodes spanwise in the XYZ mesh.
- $3 \leq KMAX \leq 26$ — Z nodes vertically in the XYZ mesh.

  Note: The Phi_1 and Phi_0 distributions must also correspond to the limitations on the XYZ mesh.

- $1 \leq NDWING \leq 20$ — The number of Y values in the Y array less than YT. Corresponds to number of values in XLE, XA, and XT.

5.7.3 DATA STACKING

Note: All coordinates are entered as scaled coordinates,

$$X = X_p/b$$

$$Y = \mu * Y_p/b$$

$$Z = \mu * Z_p/b$$

where b is the root semichord and the subscript p means physical coordinate.

Table 1. – User Input Variables

Card number	Variable name	Format	Description
1	Title	8A10	80-character title for this problem
2 to N	FSMACH	PARAM	Mach number
	DELTA	PARAM	Thickness ratio
	THETA	PARAM	Maximum angle of attack in degrees
	OMEGA	PARAM	Angular reduced frequency
	GAMMA	PARAM	Ratio of specific heats for flow medium
	AL	PARAM	Axis of rotation for flapping mode dimensionless physical coordinate
	IMAX	PARAM	Maximum X node count in users mesh
	JMAX	PARAM	Maximum Y node count in users mesh
	KMAX	PARAM	Maximum Z node count in users mesh
	IS	PARAM	Starting X node limit for volume integral for the wing; currently not used
	IE	PARAM	Ending X node limit for volume integral for the wing; currently not used
	KS	PARAM	Starting Y node limit for volume integral for the wing; currently not used
	KE	PARAM	Ending Y node limit for volume integral for the wing; currently not used
	NMAX	PARAM	Maximum number of iterations to be allowed without convergence or divergence
	NA	PARAM	Far-field update cycle control; updates the far field each NA iteration
	ERROR	PARAM	Error difference. – When the maximum difference between Phi_1 distributions of consecutive iterations is less than ERROR, the program stops iterating
	NP	PARAM	Prints pressure distribution every NP interations
	INC	PARAM	Restart variable. – If INC=0, start with the Phi_1 distribution on TAPE10; if INC=0, start with a Phi_1 distribution of zeros.
	ORF	PARAM	Overrelaxation factor used for subsonic nodes to accelerate convergence $1. \leq ORF \leq 2.$
	URF	PARAM	Underrelaxation factor used for supersonic nodes to accelerate convergence $0. < URF \leq 1.$

Table 1.– (Continued)

Card number	Variable name	Format	Description
2 to N (cont)	MSTST	PARAM	When MSTST=0, start iterations with a Phi_0 distribution from a steady-state solution. When MSTST=0, U(I,J,K) is set to K and thickness effects are not included in the analysis. This is the "flat plate" analysis
	ISWEEP	PARAM	This variable along with ILAX determines the order of calculations; with ILAX=0 (row relaxation), ISWEEP has two possible values; (a) ISWEEP=0 indicates rows will be solved from the upper and lower boundary, alternating, in toward the wing; (b) with ISWEEP=0, rows will be solved from lower to upper boundary consecutively with ILAX=1 (column relaxation), ISWEEP has two possible values: (a) with ISWEEP=0, columns will be calculated starting from the trailing edge and moving forward (upstream) then coming back and calculating the nodes back of the trailing edge moving backward (downstream); (b) with ISWEEP=1 (with ILAX=1), columns will be calculated from upstream to downstream boundary
	ILAX	PARAM	With ILAX=0 (see also ISWEEP), relaxation using rows of points is used, the points forming a line parallel to the wing in an X-Z plane; with ILAX=1, relaxation using columns of points is used, the points forming a line perpendicular to the wing in an X-Z plane
	CONPXT CONE6	PARAM PARAM	Constants required for convergence of row relaxation (See refs. 2 and 3.)
	YS	PARAM	Y coordinate of wingtip; scaled value
	YSA	PARAM	Y coordinate of the inside edge of the control surface; scaled value
	TP1MSH	PARAM	This variable determines from what files the XYZ mesh size and the coordinates of each node are read. If TP1MSH=0, read IMAX, JMAX, KMAX, and the XYZ mesh coordinates from input. If TP1MSH=1, read them only from file named TAPE1. If TP1MSH=2, read them from both input file

Table 1. – (Continued)

Card number	Variable name	Format	Description
2 to N (cont)			and file TAPE1. The data overwrites the TAPE1 data. This last preserves file spacing on TAPE1
	LUPSYM	PARAM	If LUPSYM=0, perform a normal problem of full size. If LUPSYM=0 and the angle-of-attack THETA is 0, then assume the nodes above the wing are antisymmetric to those below and calculate only those below
	IPLOT	PRAM	Not used
	NDWING	PARAM	The number of Y nodes on the wing
	IMODE	PARAM	If IMODE=1, a control surface mode is used, and the mode shape deflection is allowed only over the control surface defined by XA, XTE, and YSA. The axis of rotation is parallel to the Y axis at XA. For IMODE=2, a pitch mode is used, and the mode shape deflection is allowed over the entire wing. The axis of rotation is parallel to the Y axis at XA. When IMODE=3, flapping mode, mode shape deflection is allowed over the entire wing; the axis of rotation is parallel to the X axis at Y=AL

End of Namelist Variables

Card number	Variable name	Format	Description
N+1 to M	X	8F10.2	The location coordinates of each of the IMAX X node locations; not input if TP1MSH=1; eight per card
M+1 to K	Y	8F10.2	The location coordinates of each of the JMAX Y node locations; not input if TP1MSH=1; eight per card (scaled values)
K + 1 to L	Z	8F10.2	The location coordinates of each of the KMAX Z node locations; not input if TP1MSH=1; eight per card (scaled values)

Table 1. – (Concluded)

Card number	Variable name	Format	Description
L+1 to P	XLE	8F10.2	The X location at the corresponding Y node of the wing leading edge; NDWING of these are input; eight per card
P+1 to Q	XA	8F10.2	The X location at the corresponding Y node of the aileron hinge; NDWING of these are input; eight per card
Q+1 to R	XTE	8F10.2	The X location at the corresponding Y node of the wing trailing edge; NDWING of these are input; eight per card

5.8 PROGRAM OUTPUT

5.8.1 PROGRAM RESULTS

A listing of the output for a sample program is presented in appendix A.

The printed output of the program consists of an initial block of information printing back the user's input followed by information identifying the program options the user selected.

The X, Y, and Z mesh data come next, read either from cards or binary file (TAPE1). The mesh data are followed by the X locations on the wing of the leading edge, aileron pivot, or pitch axis and the trailing edge. Intermediate information regarding calculated variables and time used at routine calls will follow. This is followed by iteration prints giving data on how convergence to the required error difference is proceeding.

If the program iterates to the maximum number of iterations specified (NMAX), the next data printed will be the complex Phi_1 matrix. If the program stops before NMAX is reached, Phi_1 will not be printed. If it is desired, a follow up run with NMAX=1 will always print the Phi_1 matrix.

Next, and finally, the pressure coefficients above and below the wing will be printed.

Optionally, the user may print the pressure coefficients unextrapolated to the wing surface by setting variable NP to the iteration interval desired.

5.8.2 PROGRAM DIAGNOSTICS

"ERROR DIFFERENCE IS GREATER THAN 100 BETWEEN ITERATIONS. ERROR IS ---------- THE SOLUTION IS DIVERGING." The program checks errors by calculating the difference from iteration to iteration between corresponding nodes, saving the largest for comparison to the user-specified standard. The preceding message indicates the error is becoming larger too rapidly.

"SOLUTION FAILED TO CONVERGE IN ----- ITERATIONS IERR, JERR, KERR, ERRMAX1". ---,---,---,--- indicates the largest error found at the indicated XYZ node location is still larger than the user-specified standard and that the maximum number of iterations has been attained.

"SOLUTION CONVERGED MAXIMUM ERROR IS ----------" indicates the user error standard has been reached and calculation will stop.

"PLANE ERROR THE PLANE READ DOES NOT MATCH THE PLANE DESIRED J = ---- JT ---- IUNIT = ---- KAW=----" indicates an error in the incoming Phi_1 matrix on the indicated file. This error is probably caused by use of the wrong file for TAPE10 (Phi_1).

"INFORMATIVE ERROR - - ISWEEP OPTION MUST BE 2 IF LUPSYM OPTION AND ROW OPTION SELECTED. ISWEEP SET TO 2" indicates user did not select correct option of ISWEEP for row relaxation. This also indicates ISWEEP was reset to the correct value.

"STOP 1" – If this message appears in the dayfile, the program was unable to find the Z nodes just above and just below the wing. This may be caused by a Z node at Z = 0, which is prohibited.

ORIGINAL PAGE IS
OF POOR QUALITY

6.0 COMPUTER PROGRAM DESCRIPTION

Flow diagrams for the program and its subroutines are listed in appendix B.

6.1 OVERLAY STRUCTURE

TEV174 consists of a (0,0) level overlay and four primary level overlays. The (0,0) overlay contains the program driver and several common usage subroutines. The (0,0) driving program called V174 does the following:

1. Calls the (4,0) level overlay to input data and initialize variables and arrays
2. Controls the number of iterations performed either by terminating because of convergence (or divergence) or terminating because the maximum number of iterations has been performed
3. Calls the far-field boundary updating overlay (3,0)
4. Calls the relaxation overlay specified by the user for row relaxation (1,0), specifying which X-Z plane is to be calculated
5. Prints convergence data for each interation
6. Saves the Phi_1 matrix on file TAPE10 after iterations have ceased
7. Calls the final print package routine CPR for pressure differential printing

The (4,0) overlay does the following:

1. Reads inputs and prints them back
2. Sets constants
3. Calculates the body function
4. Calculates the mesh data
5. Initializes the steady-state Phi_0 matrix with a constant or with data from another program
6. Initializes the Phi_1 matrix either with a complex constant or with data from a previous program run

The (1,0) overlay updates an X-Z plane of the Phi_1 matrix by column relaxation. It also causes the print display of the Phi_1 matrix if the maximum number of iterations (NMAX) has been reached.

The (2,0) overlay, like the (1,0) overlay, updates the X-Z plane specified by the (0,0) overlay. It does this by row relaxation instead of column. It will also print the Phi_1 matrix at iteration NMAX.

The (3,0) overlay calculates and updates the nodes on the outside boundaries (farfield update overlay).

6.2 COMMON BLOCK USAGE

Table 2 describes usage of blocks of common variables.

Boeing Commercial Airplane Company
P.O. Box 3707
Seattle, Washington 98124
October 1977

Table 2. – Blocks of Common Variables

Block	Usage
CONST	Control and calculation constants
IMESH	X, Y, and Z mesh constants
WING	Variables describing the wing
CONST2	Control and calculation constants
TIMES	Print time variables
CONE6	Row relaxation constant
TROUB	Troubleshooting variables
ENTR	Column relaxation control and calculation variables used in MATRXCF
EPS	Calculation constants
FARF	Far-field boundary calculation variables
IRELAX	Relaxation variables used in MATRXCF and SRMATCF
JAYS	Phi_1 incore plane designators. – Looking toward the wing from upstream: JL indicates the left X-Z plane. JC indicates the center X-Z plane. JR indicates the right X-Z plane.
ITER	Current iteration number and NMAX
IVOL	Wing integral variables
MATRIX	Matrices used to form the diagonals for solution; used in SRMATCF, MATRXCF, FOURDG, and TRIDIAG
SUBER	Contains two diagonals (see MATRIX) needed for PHICLM calculation used in SRMATCF, FOURDG, MATRXCF, and TRIDIAG
SUBSUB	Contains the fourth diagonal required for row relaxation; used in FOURDG and SRMATCF

Table 2. – (Concluded)

Block	Usage
PHI	Contains the three X-Z planes currently being used by the program (see also JAYS)
XYZ	Contains the X, Y, and Z coordinates of the nodes at which Phi_1 is to be calculated
PRNT	Not used, was a print variable
IRLAXF	Subsonic, supersonic node identification array
ERRS	Error convergence data
IO	File names
FUL	Upper and lower wing function
DEL	Phi_1 array
U	Coefficient of φ_{1xx} term
FXY	Functions of the X, Y, and Z mesh
BIAS	Relaxation coefficients used to speed up convergence
Note: The following common blocks are used only in the far-field boundary overlay (3,0).	
V	Integral evaluation variables
SUM	Not being used in this version

APPENDIX A

SAMPLE INPUT/OUTPUT

```
     STD  LD-UP RECT WNG TRP11 TP1PHO,TP10SD(ST=TPH10SD), 12-10-5 W/5 ITER              77/03/04.

$PARAM
FSMACH  = .875E+00,
DELTA   = .6E-01,
THETA   = .15E+01,
OMEGA   = .6E-01,
GAMMA   = .14E+01,
AL      = .1E+01,
IMAX    = 44,
JMAX    = 16,
KMAX    = 15,
IS      = 0,
IE      = 0,
KS      = 0,
KE      = 0,
NMAX    = 5,
NA      = 3,
ERROR   = .1E-03,
NP      = 10,
INC     = 1,
ORF     = .16E+01,
MSTST   = 0,
ISWEEP  = 0,
NVOL    = 100,
IP      = 0,
ILAX    = 1,
URF     = .7E+00,
CONPXT  = 0.0,
CONE6   = .1E+00,
YS      = .1790712E+01,
YSA     = 0.0,
```

ORIGINAL PAGE IS OF POOR QUALITY

```
TP1MSH  = .1E+01,
LUPSYM  = 1,
IPLCT   = 1,
NDWING  = 12,
IMODE   = 2,
$END
 MSTST=0 SO THIS AIRFOIL HAS FINITE THICKNESS
 THIS IS A COLUMN RELAX      STANDARD
LUPSYM=0 SO THIS IS A LOWER UPPER SYMMETRY RUN
ZERO ANGLE OF ATTACK.IS ASSUMED
 X Y AND Z MESH COORDINATES

   -3.8000   -2.9000   -2.2000   -1.7600   -1.4600   -1.2800   -1.1600   -1.0800   -1.0200    -.9800
    -.9400    -.9000    -.8400    -.7600    -.6800    -.6000    -.5000    -.4000    -.3000    -.2000
    -.1000    0.0000     .1000     .2000     .3000     .4000     .5000     .6000     .7000     .7800
     .8400     .8800     .9200     .9600    1.0000    1.0400    1.1000    1.1800    1.3000    1.4800
    1.7600    2.2000    2.9000    3.8000

    0.0000     .1701     .3402     .5104     .6605     .8506    1.0207    1.1908    1.3609    1.5311
    1.7012    1.8802    2.1489    2.5070    3.0442    3.7605

   -4.7991   -3.2090   -2.1345   -1.4182    -.9455    -.6232    -.4083    -.2650    -.1719    -.1074
    -.0645    -.0358    -.0143     .0143     .0358
WITH   12 NODES ON THE WING THE X VALUES AT THE LEADING EDGE, AILERON, AND TRAILING EDGE ARE --

   -1.0000   -1.0000   -1.0000   -1.0000   -1.0000   -1.0000   -1.0000   -1.0000   -1.0000   -1.0000
   -1.0000   -1.0000

   -1.0000   -1.0000   -1.0000   -1.0000   -1.0000   -1.0000   -1.0000   -1.0000   -1.0000   -1.0000
   -1.0000   -1.0000

    1.0000    1.0000    1.0000    1.0000    1.0000    1.0000    1.0000    1.0000    1.0000    1.0000
    1.0000    1.0000

XK,EPS,XLAM,W1,W2,W7,W9,W11   1.83      .168      .224      .156      .303      .100E-01   .215E-01   8.93
```

```
IMAG,W3,W5,W6,W8,W10   0.0   1.00      .1   0.      0.0   .1C4E-C1   C.0   .196      0.0   .358      0.C   1.14
IMAX1,JMAX1,KMAX1            43          15          13

CP TIME TOT=    22.586 SINCE LAST CALL        .079
```

UPPER AND LOWER BODY FUNCTION

10	.4363	.5236E-03	.4363	.5236E-03	.4363	.5236E-03	.4363	.5236E-03	.4363	.5236E-03
	.4363	.5236E-03	.4363	.5236E-03	.4363	.5236E-03	.4363	.5236E-03	.4363	.5236E-03
	.4363	.5236E-03	.4363	.5236E-03						
11	.4363	.1571E-02	.4363	.1571E-02	.4363	.1571E-02	.4363	.1571E-02	.4363	.1571E-02
	.4363	.1571E-02	.4363	.1571E-02	.4363	.1571E-02	.4363	.1571E-02	.4363	.1571E-02
	.4363	.1571E-02	.4363	.1571E-02						
12	.4363	.2618E-02	.4363	.2618E-02	.4363	.2618E-02	.4363	.2618E-02	.4363	.2618E-02
	.4363	.2618E-02	.4363	.2618E-02	.4363	.2618E-02	.4363	.2618E-02	.4363	.2618E-02
	.4363	.2618E-02	.4363	.2618E-02						
13	.4363	.4189E-02	.4363	.4189E-02	.4363	.4189E-02	.4363	.4189E-02	.4363	.4189E-02
	.4363	.4189E-02	.4363	.4189E-02	.4363	.4189E-02	.4363	.4189E-02	.4363	.4189E-02
	.4363	.4189E-02	.4363	.4189E-02						
14	.4363	.6283E-02	.4363	.6283E-02	.4363	.6283E-02	.4363	.6283E-02	.4363	.6283E-02
	.4363	.6283E-02	.4363	.6283E-02	.4363	.6283E-02	.4363	.6283E-02	.4363	.6283E-02
	.4363	.6283E-02	.4363	.6283E-02						
15	.4363	.8378E-02	.4363	.8378E-02	.4363	.8378E-02	.4363	.8378E-02	.4363	.8378E-02
	.4363	.8378E-02	.4363	.8378E-02	.4363	.8378E-02	.4363	.8378E-02	.4363	.8378E-02
	.4363	.8378E-02	.4363	.8378E-02						
16	.4363	.1047E-01	.4363	.1047E-01	.4363	.1047E-01	.4363	.1047E-01	.4363	.1047E-01
	.4363	.1047E-01	.4363	.1047E-01	.4363	.1047E-01	.4363	.1047E-01	.4363	.1047E-01
	.4363	.1047E-01	.4363	.1047E-01						
17	.4363	.1309E-01	.4363	.1309E-01	.4363	.1309E-01	.4363	.1309E-01	.4363	.1309E-01
	.4363	.1309E-01	.4363	.1309E-01	.4363	.1309E-01	.4363	.1309E-01	.4363	.1309E-01
	.4363	.1309E-01	.4363	.1309E-01						
18	.4363	.1571E-01	.4363	.1571E-01	.4363	.1571E-01	.4363	.1571E-01	.4363	.1571E-01
	.4363	.1571E-01	.4363	.1571E-01	.4363	.1571E-01	.4363	.1571E-01	.4363	.1571E-01
	.4363	.1571E-01	.4363	.1571E-01						
19	.4363	.1833E-01	.4363	.1833E-01	.4363	.1833E-01	.4363	.1833E-01	.4363	.1833E-01
	.4363	.1833E-01	.4363	.1833E-01	.4363	.1833E-01	.4363	.1833E-01	.4363	.1833E-01
	.4363	.1833E-01	.4363	.1833E-01						
20	.4363	.2094E-01	.4363	.2094E-01	.4363	.2094E-01	.4363	.2094E-01	.4363	.2094E-01
	.4363	.2094E-01	.4363	.2094E-01	.4363	.2094E-01	.4363	.2094E-01	.4363	.2094E-01
	.4363	.2094E-01	.4363	.2094E-01						
21	.4363	.2356E-01	.4363	.2356E-01	.4363	.2356E-01	.4363	.2356E-01	.4363	.2356E-01
	.4363	.2356E-01	.4363	.2356E-01	.4363	.2356E-01	.4363	.2356E-01	.4363	.2356E-01
	.4363	.2356E-01	.4363	.2356E-01						
22	.4363	.2618E-01	.4363	.2618E-01	.4363	.2618E-01	.4363	.2618E-01	.4363	.2618E-01
	.4363	.2618E-01	.4363	.2618E-01	.4363	.2618E-01	.4363	.2618E-01	.4363	.2618E-01
	.4363	.2618E-01	.4363	.2618E-01						
23	.4363	.2880E-01	.4363	.2880E-01	.4363	.2880E-01	.4363	.2880E-01	.4363	.2880E-01
	.4363	.2880E-01	.4363	.2880E-01	.4363	.2880E-01	.4363	.2880E-01	.4363	.2880E-01
	.4363	.2880E-01	.4363	.2880E-01						
24	.4363	.3142E-01	.4363	.3142E-01	.4363	.3142E-01	.4363	.3142E-01	.4363	.3142E-01
	.4363	.3142E-01	.4363	.3142E-01	.4363	.3142E-01	.4363	.3142E-01	.4363	.3142E-01
	.4363	.3142E-01	.4363	.3142E-01						
25	.4363	.3403E-01	.4363	.3403E-01	.4363	.3403E-01	.4363	.3403E-01	.4363	.3403E-01
	.4363	.3403E-01	.4363	.3403E-01	.4363	.3403E-01	.4363	.3403E-01	.4363	.3403E-01
	.4363	.3403E-01	.4363	.3403E-01						
26	.4363	.3665E-01	.4363	.3665E-01	.4363	.3665E-01	.4363	.3665E-01	.4363	.3665E-01
	.4363	.3665E-01	.4363	.3665E-01	.4363	.3665E-01	.4363	.3665E-01	.4363	.3665E-01
	.4363	.3665E-01	.4363	.3665E-01						
27	.4363	.3927E-01	.4363	.3927E-01	.4363	.3927E-01	.4363	.3927E-01	.4363	.3927E-01
	.4363	.3927E-01	.4363	.3927E-01	.4363	.3927E-01	.4363	.3927E-01	.4363	.3927E-01
	.4363	.3927E-01	.4363	.3927E-01						
28	.4363	.4189E-01	.4363	.4189E-01	.4363	.4189E-01	.4363	.4189E-01	.4363	.4189E-01
	.4363	.4189E-01	.4363	.4189E-01	.4363	.4189E-01	.4363	.4189E-01	.4363	.4189E-01
	.4363	.4189E-01	.4363	.4189E-01						
29	.4363	.4451E-01	.4363	.4451E-01	.4363	.4451E-01	.4363	.4451E-01	.4363	.4451E-01

	.4363	.4451E-01	.4363	.4451E-01	.4363	.4451E-01	.4363	.4451E-01	.4363	.4451E-01
	.4363	.4451E-01	.4363	.4451E-01						
30	.4363	.4660E-01	.4363	.4660E-01	.4363	.4660E-01	.4363	.4660E-01	.4363	.4660E-01
	.4363	.4660E-01	.4363	.4660E-01	.4363	.4660E-01	.4363	.4660E-01	.4363	.4660E-01
	.4363	.4660E-01	.4363	.4660E-01						
31	.4363	.4817E-01	.4363	.4817E-01	.4363	.4817E-01	.4363	.4817E-01	.4363	.4817E-01
	.4363	.4817E-01	.4363	.4817E-01	.4363	.4817E-01	.4363	.4817E-01	.4363	.4817E-01
	.4363	.4817E-01	.4363	.4817E-01						
32	.4363	.4922E-01	.4363	.4922E-01	.4363	.4922E-01	.4363	.4922E-01	.4363	.4922E-01
	.4363	.4922E-01	.4363	.4922E-01	.4363	.4922E-01	.4363	.4922E-01	.4363	.4922E-01
	.4363	.4922E-01	.4363	.4922E-01						
33	.4363	.5027E-01	.4363	.5027E-01	.4363	.5027E-01	.4363	.5027E-01	.4363	.5027E-01
	.4363	.5027E-01	.4363	.5027E-01	.4363	.5027E-01	.4363	.5027E-01	.4363	.5027E-01
	.4363	.5027E-01	.4363	.5027E-01						
34	.4363	.5131E-01	.4363	.5131E-01	.4363	.5131E-01	.4363	.5131E-01	.4363	.5131E-01
	.4363	.5131E-01	.4363	.5131E-01	.4363	.5131E-01	.4363	.5131E-01	.4363	.5131E-01
	.4363	.5131E-01	.4363	.5131E-01						
35	.4363	.5236E-01	.4363	.5236E-01	.4363	.5236E-01	.4363	.5236E-01	.4363	.5236E-01
	.4363	.5236E-01	.4363	.5236E-01	.4363	.5236E-01	.4363	.5236E-01	.4363	.5236E-01
	.4363	.5236E-01	.4363	.5236E-01						

```
CP TIME TOT=     22.746 SINCE LAST CALL       .160

CP TIME TOT=     22.749 SINCE LAST CALL       .003

CP TIME TOT=     22.946 SINCE LAST CALL       .197

N,IERR,JERR,KERR,ERRMAX1       1      34      1      3      .60E-04
ITER     1 PLANE     0 ERRMAX1=     .6048E-04
ERRMAX =     .9677E-04 ERROR =     .1000E-03

SOLUTION CONVERGED. MAXIMUM ERROR IS    .6048E-04

CP TIME TOT=     25.041 SINCE LAST CALL      2.095
```

MACH NUMBER = .88 OMEGA = .060 AMPLITUDE = .026

PRESSURE COEFFICIENTS

AT CHORD Y(J)= 0.0000 X-- LEADING EDGE= -1.0000 AILERON PIVOT= -1.0000 TRAILING EDGE= 1.0000

I	BELOW AIRFOIL		ABOVE AIRFOIL		ABOVE - BELOW		X
10	0.	0.	0.	0.	.233E+02	-.506E+01	-.960E+00
11	0.	0.	0.	0.	.160E+02	-.348E+01	-.940E+00
12	0.	0.	0.	0.	.150E+02	-.323E+01	-.900E+00
13	0.	0.	0.	0.	.134E+02	-.283E+01	-.840E+00
14	0.	0.	0.	0.	.119E+02	-.241E+01	-.760E+00
15	0.	0.	0.	0.	.104E+02	-.196E+01	-.680E+00
16	0.	0.	0.	0.	.927E+01	-.160E+01	-.600E+00
17	0.	0.	0.	0.	.891E+01	-.141E+01	-.500E+00
18	0.	0.	0.	0.	.894E+01	-.131E+01	-.400E+00
19	0.	0.	0.	0.	.853E+01	-.102E+01	-.300E+00
20	0.	0.	0.	0.	.808E+01	-.673E+00	-.200E+00
21	0.	0.	0.	0.	.899E+01	-.528E+00	-.100E+00
22	0.	0.	0.	0.	.127E+02	-.158E+00	0.
23	0.	0.	0.	0.	.123E+02	.230E+01	.100E+00
24	0.	0.	0.	0.	.668E+01	.367E+01	.200E+00
25	0.	0.	0.	0.	.340E+01	.257E+01	.300E+00
26	0.	0.	0.	0.	.210E+01	.195E+01	.400E+00
27	0.	0.	0.	0.	.146E+01	.157E+01	.500E+00
28	0.	0.	0.	0.	.106E+01	.129E+01	.600E+00
29	0.	0.	0.	0.	.786E+00	.106E+01	.700E+00
30	0.	0.	0.	0.	.600E+00	.883E+00	.780E+00
31	0.	0.	0.	0.	.469E+00	.740E+00	.840E+00
32	0.	0.	0.	0.	.382E+00	.630E+00	.880E+00
33	0.	0.	0.	0.	.290E+00	.503E+00	.920E+00
34	0.	0.	0.	0.	.189E+00	.357E+00	.960E+00
35	0.	0.	0.	0.	0.	0.	.100E+01

AT CHORD Y(J)= .1701 X-- LEADING EDGE= -1.0000 AILERON PIVOT= -1.0000 TRAILING EDGE= 1.0000

I	BELOW AIRFOIL		ABOVE AIRFOIL		ABOVE - BELOW		X
10	0.	0.	0.	0.	.233E+02	-.505E+01	-.980E+00
11	0.	0.	0.	0.	.160E+02	-.347E+01	-.940E+00
12	0.	0.	0.	0.	.150E+02	-.322E+01	-.900E+00
13	0.	0.	0.	0.	.134E+02	-.282E+01	-.840E+00
14	0.	0.	0.	0.	.119E+02	-.240E+01	-.760E+00
15	0.	0.	0.	0.	.104E+02	-.195E+01	-.680E+00
16	0.	0.	0.	0.	.925E+01	-.159E+01	-.600E+00
17	0.	0.	0.	0.	.889E+01	-.140E+01	-.500E+00
18	0.	0.	0.	0.	.893E+01	-.130E+01	-.400E+00
19	0.	0.	0.	0.	.852E+01	-.101E+01	-.300E+00
20	0.	0.	0.	0.	.807E+01	-.662E+00	-.200E+00
21	0.	0.	0.	0.	.898E+01	-.513E+00	-.100E+00
22	0.	0.	0.	0.	.131E+02	-.873E-01	0.
23	0.	0.	0.	0.	.125E+02	.237E+01	.100E+00
24	0.	0.	0.	0.	.636E+01	.366E+01	.200E+00
25	0.	0.	0.	0.	.316E+01	.253E+01	.300E+00
26	0.	0.	0.	0.	.197E+01	.192E+01	.400E+00
27	0.	0.	0.	0.	.138E+01	.155E+01	.500E+00
28	0.	0.	0.	0.	.102E+01	.128E+01	.600E+00

ORIGINAL PAGE IS
OF POOR QUALITY

29	0.	0.	0.	0.	.757E+00	.105E+01	.700E+00
30	0.	0.	0.	0.	.580E+00	.874E+00	.780E+00
31	0.	0.	0.	0.	.455E+00	.733E+00	.840E+00
32	0.	0.	0.	0.	.371E+00	.625E+00	.880E+00
33	0.	0.	0.	0.	.282E+00	.499E+00	.920E+00
34	0.	0.	0.	0.	.183E+00	.354E+00	.960E+00
35	0.	0.	0.	0.	0.	0.	.100E+01

AT CHORD Y(J)= .3402 X-- LEADING EDGE= -1.0000 AILERON PIVOT= -1.0000 TRAILING EDGE= 1.0000

10	0.	0.	0.	0.	.232E+02	-.499E+01	-.980E+00
11	0.	0.	0.	0.	.159E+02	-.343E+01	-.940E+00
12	0.	0.	0.	0.	.149E+02	-.318E+01	-.900E+00
13	0.	0.	0.	0.	.133E+02	-.278E+01	-.840E+00
14	0.	0.	0.	0.	.119E+02	-.236E+01	-.760E+00
15	0.	0.	0.	0.	.104E+02	-.192E+01	-.680E+00
16	0.	0.	0.	0.	.922E+01	-.156E+01	-.600E+00
17	0.	0.	0.	0.	.886E+01	-.137E+01	-.500E+00
18	0.	0.	0.	0.	.889E+01	-.126E+01	-.400E+00
19	0.	0.	0.	0.	.848E+01	-.975E+00	-.300E+00
20	0.	0.	0.	0.	.804E+01	-.627E+00	-.200E+00
21	0.	0.	0.	0.	.895E+01	-.468E+00	-.100E+00
22	0.	0.	0.	0.	.146E+02	.255E+00	0.
23	0.	0.	0.	0.	.130E+02	.264E+01	.100E+00
24	0.	0.	0.	0.	.477E+01	.350E+01	.200E+00
25	0.	0.	0.	0.	.232E+01	.236E+01	.300E+00
26	0.	0.	0.	0.	.157E+01	.182E+01	.400E+00
27	0.	0.	0.	0.	.117E+01	.148E+01	.500E+00
28	0.	0.	0.	0.	.896E+00	.123E+01	.600E+00
29	0.	0.	0.	0.	.683E+00	.102E+01	.700E+00
30	0.	0.	0.	0.	.530E+00	.851E+00	.780E+00
31	0.	0.	0.	0.	.418E+00	.715E+00	.840E+00
32	0.	0.	0.	0.	.342E+00	.610E+00	.880E+00
33	0.	0.	0.	0.	.260E+00	.488E+00	.920E+00
34	0.	0.	0.	0.	.170E+00	.346E+00	.960E+00
35	0.	0.	0.	0.	0.	0.	.100E+01

AT CHORD Y(J)= .5104 X-- LEADING EDGE= -1.0000 AILERON PIVOT= -1.0000 TRAILING EDGE= 1.0000

10	0.	0.	0.	0.	.231E+02	-.469E+01	-.980E+00
11	0.	0.	0.	0.	.158E+02	-.336E+01	-.940E+00
12	0.	0.	0.	0.	.148E+02	-.312E+01	-.900E+00
13	0.	0.	0.	0.	.132E+02	-.272E+01	-.840E+00
14	0.	0.	0.	0.	.118E+02	-.231E+01	-.760E+00
15	0.	0.	0.	0.	.103E+02	-.187E+01	-.680E+00
16	0.	0.	0.	0.	.916E+01	-.151E+01	-.600E+00
17	0.	0.	0.	0.	.880E+01	-.131E+01	-.500E+00
18	0.	0.	0.	0.	.882E+01	-.120E+01	-.400E+00
19	0.	0.	0.	0.	.840E+01	-.912E+00	-.300E+00
20	0.	0.	0.	0.	.798E+01	-.569E+00	-.200E+00
21	0.	0.	0.	0.	.890E+01	-.393E+00	-.100E+00
22	0.	0.	0.	0.	.147E+02	.497E+00	0.
23	0.	0.	0.	0.	.126E+02	.281E+01	.100E+00
24	0.	0.	0.	0.	.398E+01	.343E+01	.200E+00
25	0.	0.	0.	0.	.188E+01	.228E+01	.300E+00
26	0.	0.	0.	0.	.130E+01	.174E+01	.400E+00
27	0.	0.	0.	0.	.998E+00	.141E+01	.500E+00
28	0.	0.	0.	0.	.783E+00	.118E+01	.600E+00
29	0.	0.	0.	0.	.607E+00	.961E+00	.700E+00

30	0.	C.	C.	C.	.475E+00	.820E+00	.780E+00
31	0.	0.	C.	C.	.377E+00	.690E+0C	.840E+00
32	0.	C.	0.	C.	.309E+00	.590E+00	.880E+00
33	0.	0.	C.	C.	.236E+00	.472E+00	.920E+00
34	0.	C.	0.	C.	.154E+00	.335E+00	.960E+00
35	0.	C.	C.	C.	0.	0.	.100E+01

AT CHORD Y(J)= .6805 X-- LEADING EDGE= -1.0000 AILERCN PIVCT= -1.0000 TRAILING EDGE= 1.0C00

10	0.	0.	C.	C.	.229E+02	-.475E+01	-.980E+00
11	0.	C.	C.	C.	.157E+02	-.326E+01	-.940E+00
12	0.	C.	C.	C.	.147E+02	-.302E+01	-.900E+00
13	0.	C.	C.	C.	.131E+02	-.264E+01	-.840E+00
14	0.	C.	C.	C.	.117E+02	-.223E+01	-.760E+00
15	0.	C.	0.	C.	.102E+02	-.179E+01	-.680E+00
16	0.	C.	0.	C.	.906E+01	-.144E+01	-.600E+00
17	0.	0.	C.	C.	.870E+01	-.124E+01	-.500E+00
18	0.	C.	C.	C.	.870E+01	-.112E+01	-.400E+00
19	0.	0.	0.	C.	.826E+01	-.814E+00	-.300E+00
20	0.	C.	0.	C.	.787E+01	-.482E+00	-.200E+00
21	0.	0.	0.	C.	.882E+01	-.279E+00	-.100E+00
22	0.	C.	0.	0.	.145E+02	.843E+00	0.
23	0.	C.	0.	C.	.117E+02	.298E+01	.100E+00
24	0.	C.	C.	C.	.300E+01	.325E+01	.200E+00
25	0.	0.	0.	C.	.148E+01	.213E+01	.300E+00
26	0.	C.	0.	0.	.107E+01	.162E+01	.400E+00
27	0.	C.	C.	C.	.853E+00	.133E+01	.500E+00
28	0.	C.	C.	C.	.685E+00	.112E+01	.600E+00
29	0.	C.	0.	C.	.538E+00	.932E+00	.700E+00
30	0.	0.	0.	0.	.424E+00	.782E+00	.780E+00
31	0.	C.	0.	C.	.338E+00	.659E+00	.840E+00
32	0.	C.	C.	C.	.277E+00	.564E+00	.880E+00
33	0.	C.	0.	C.	.212E+00	.452E+00	.920E+00
34	0.	C.	0.	C.	.138E+00	.321E+00	.960E+00
35	0.	C.	C.	C.	0.	0.	.100E+01

AT CHORD Y(J)= .8506 X-- LEADING EDGE= -1.0000 AILERCN PIVCT= -1.0000 TRAILING EDGE= 1.0000

10	0.	C.	0.	C.	.226E+02	-.457E+01	-.980E+00
11	0.	C.	C.	C.	.155E+02	-.313E+01	-.940E+00
12	C.	C.	C.	C.	.145E+02	-.290E+01	-.900E+00
13	0.	0.	0.	C.	.130E+02	-.252E+01	-.840E+00
14	0.	C.	0.	0.	.115E+02	-.212E+01	-.760E+00
15	0.	C.	0.	C.	.100E+02	-.169E+01	-.680E+00
16	0.	C.	C.	C.	.892E+01	-.134E+01	-.600E+00
17	0.	C.	C.	C.	.854E+01	-.113E+01	-.500E+00
18	0.	C.	C.	0.	.851E+01	-.992E+00	-.400E+00
19	0.	C.	0.	0.	.801E+01	-.670E+00	-.300E+00
20	0.	0.	C.	C.	.764E+01	-.332E+00	-.200E+00
21	0.	C.	0.	C.	.871E+01	-.879E-01	-.100E+00
22	0.	C.	0.	0.	.152E+02	.175E+01	0.
23	0.	C.	C.	C.	.107E+02	.330E+01	.100E+00
24	0.	C.	0.	C.	.672E+00	.251E+01	.200E+00
25	0.	C.	C.	C.	.713E+00	.175E+01	.300E+00
26	0.	C.	0.	C.	.771E+00	.141E+01	.400E+00
27	0.	0.	C.	C.	.699E+00	.120E+01	.500E+00
28	0.	0.	0.	C.	.591E+00	.103E+01	.600E+00
29	0.	C.	0.	C.	.475E+00	.869E+00	.700E+00
30	0.	C.	0.	C.	.378E+00	.734E+00	.780E+00

31	0.	0.	0.	0.	.302E+00	.621E+00	.840E+00
32	0.	0.	0.	0.	.248E+00	.532E+00	.880E+00
33	0.	0.	0.	0.	.190E+00	.427E+00	.920E+00
34	0.	0.	0.	0.	.123E+00	.305E+00	.960E+00
35	0.	0.	0.	0.	0.	0.	.100E+01

AT CHORD Y(J)= 1.0207 X-- LEADING EDGE= -1.0000 AILERON PIVOT= -1.0000 TRAILING EDGE= 1.0000

10	0.	0.	0.	0.	.222E+02	-.432E+01	-.980E+00
11	0.	0.	0.	0.	.152E+02	-.296E+01	-.940E+00
12	0.	0.	0.	0.	.143E+02	-.274E+01	-.900E+00
13	0.	0.	0.	0.	.127E+02	-.237E+01	-.840E+00
14	0.	0.	0.	0.	.113E+02	-.197E+01	-.760E+00
15	0.	0.	0.	0.	.980E+01	-.156E+01	-.680E+00
16	0.	0.	0.	0.	.869E+01	-.122E+01	-.600E+00
17	0.	0.	0.	0.	.831E+01	-.996E+00	-.500E+00
18	0.	0.	0.	0.	.818E+01	-.622E+00	-.400E+00
19	0.	0.	0.	0.	.756E+01	-.466E+00	-.300E+00
20	0.	0.	0.	0.	.718E+01	-.124E+00	-.200E+00
21	0.	0.	0.	0.	.863E+01	.190E+00	-.100E+00
22	0.	0.	0.	0.	.147E+02	.313E+01	0.
23	0.	0.	0.	0.	.655E+01	.345E+01	.100E+00
24	0.	0.	0.	0.	-.106E+01	.113E+01	.200E+00
25	0.	0.	0.	0.	.451E+00	.130E+01	.300E+00
26	0.	0.	0.	0.	.677E+00	.120E+01	.400E+00
27	0.	0.	0.	0.	.638E+00	.107E+01	.500E+00
28	0.	0.	0.	0.	.543E+00	.941E+00	.600E+00
29	0.	0.	0.	0.	.437E+00	.805E+00	.700E+00
30	0.	0.	0.	0.	.347E+00	.684E+00	.780E+00
31	0.	0.	0.	0.	.276E+00	.581E+00	.840E+00
32	0.	0.	0.	0.	.226E+00	.499E+00	.880E+00
33	0.	0.	0.	0.	.172E+00	.401E+00	.920E+00
34	0.	0.	0.	0.	.111E+00	.286E+00	.960E+00
35	0.	0.	0.	0.	0.	0.	.100E+01

AT CHORD Y(J)= 1.1908 X-- LEADING EDGE= -1.0000 AILERON PIVOT= -1.0000 TRAILING EDGE= 1.0000

10	0.	0.	0.	0.	.216E+02	-.401E+01	-.980E+00
11	0.	0.	0.	0.	.148E+02	-.274E+01	-.940E+00
12	0.	0.	0.	0.	.139E+02	-.252E+01	-.900E+00
13	0.	0.	0.	0.	.123E+02	-.217E+01	-.840E+00
14	0.	0.	0.	0.	.109E+02	-.179E+01	-.760E+00
15	0.	0.	0.	0.	.944E+01	-.139E+01	-.680E+00
16	0.	0.	0.	0.	.832E+01	-.105E+01	-.600E+00
17	0.	0.	0.	0.	.791E+01	-.822E+00	-.500E+00
18	0.	0.	0.	0.	.758E+01	-.587E+00	-.400E+00
19	0.	0.	0.	0.	.676E+01	-.200E+00	-.300E+00
20	0.	0.	0.	0.	.647E+01	.978E-01	-.200E+00
21	0.	0.	0.	0.	.805E+01	.468E+00	-.100E+00
22	0.	0.	0.	0.	.985E+01	.245E+01	0.
23	0.	0.	0.	0.	.567E+01	.286E+01	.100E+00
24	0.	0.	0.	0.	.106E+01	.144E+01	.200E+00
25	0.	0.	0.	0.	.958E+00	.126E+01	.300E+00
26	0.	0.	0.	0.	.809E+00	.112E+01	.400E+00
27	0.	0.	0.	0.	.663E+00	.991E+00	.500E+00
28	0.	0.	0.	0.	.533E+00	.870E+00	.600E+00
29	0.	0.	0.	0.	.417E+00	.746E+00	.700E+00
30	0.	0.	0.	0.	.326E+00	.635E+00	.780E+00
31	0.	0.	0.	0.	.257E+00	.540E+00	.840E+00

32	0.	0.	0.	0.	.209E+00	.464E+00	.880E+00
33	0.	0.	0.	0.	.158E+00	.373E+00	.920E+00
34	0.	0.	0.	0.	.997E-01	.266E+00	.960E+00
35	0.	0.	0.	0.	0.	0.	.100E+01

AT CHORD Y(J)= 1.3609 X-- LEADING EDGE= -1.0000 AILERON PIVOT= -1.0000 TRAILING EDGE= 1.0000

10	0.	0.	0.	0.	.207E+02	-.361E+01	-.980E+00
11	0.	0.	0.	0.	.142E+02	-.245E+01	-.940E+00
12	0.	0.	0.	0.	.132E+02	-.225E+01	-.900E+00
13	0.	0.	0.	0.	.117E+02	-.191E+01	-.840E+00
14	0.	0.	0.	0.	.103E+02	-.154E+01	-.760E+00
15	0.	0.	0.	0.	.879E+01	-.115E+01	-.680E+00
16	0.	0.	0.	0.	.765E+01	-.820E+00	-.600E+00
17	0.	0.	0.	0.	.708E+01	-.572E+00	-.500E+00
18	0.	0.	0.	0.	.652E+01	-.303E+00	-.400E+00
19	0.	0.	0.	0.	.567E+01	.364E-01	-.300E+00
20	0.	0.	0.	0.	.566E+01	.276E+00	-.200E+00
21	0.	0.	0.	0.	.737E+01	.797E+00	-.100E+00
22	0.	0.	0.	0.	.657E+01	.195E+01	0.
23	0.	0.	0.	0.	.308E+01	.209E+01	.100E+00
24	0.	0.	0.	0.	.147E+01	.138E+01	.200E+00
25	0.	0.	0.	0.	.107E+01	.116E+01	.300E+00
26	0.	0.	0.	0.	.824E+00	.102E+01	.400E+00
27	0.	0.	0.	0.	.644E+00	.898E+00	.500E+00
28	0.	0.	0.	0.	.504E+00	.790E+00	.600E+00
29	0.	0.	0.	0.	.386E+00	.679E+00	.700E+00
30	0.	0.	0.	0.	.297E+00	.579E+00	.780E+00
31	0.	0.	0.	0.	.232E+00	.493E+00	.840E+00
32	0.	0.	0.	0.	.187E+00	.424E+00	.880E+00
33	0.	0.	0.	0.	.139E+00	.341E+00	.920E+00
34	0.	0.	0.	0.	.851E-01	.243E+00	.960E+00
35	0.	0.	0.	0.	0.	0.	.100E+01

AT CHORD Y(J)= 1.5311 X-- LEADING EDGE= -1.0000 AILERON PIVOT= -1.0000 TRAILING EDGE= 1.0000

10	0.	0.	0.	0.	.192E+02	-.307E+01	-.980E+00
11	0.	0.	0.	0.	.131E+02	-.208E+01	-.940E+00
12	0.	0.	0.	0.	.122E+02	-.189E+01	-.900E+00
13	0.	0.	0.	0.	.106E+02	-.156E+01	-.840E+00
14	0.	0.	0.	0.	.900E+01	-.119E+01	-.760E+00
15	0.	0.	0.	0.	.749E+01	-.827E+00	-.680E+00
16	0.	0.	0.	0.	.647E+01	-.553E+00	-.600E+00
17	0.	0.	0.	0.	.563E+01	-.278E+00	-.500E+00
18	0.	0.	0.	0.	.485E+01	-.223E-01	-.400E+00
19	0.	0.	0.	0.	.436E+01	.189E+00	-.300E+00
20	0.	0.	0.	0.	.467E+01	.418E+00	-.200E+00
21	0.	0.	0.	0.	.588E+01	.114E+01	-.100E+00
22	0.	0.	0.	0.	.407E+01	.151E+01	0.
23	0.	0.	0.	0.	.144E+01	.120E+01	.100E+00
24	0.	0.	0.	0.	.119E+01	.106E+01	.200E+00
25	0.	0.	0.	0.	.924E+00	.948E+00	.300E+00
26	0.	0.	0.	0.	.721E+00	.853E+00	.400E+00
27	0.	0.	0.	0.	.561E+00	.764E+00	.500E+00
28	0.	0.	0.	0.	.435E+00	.679E+00	.600E+00
29	0.	0.	0.	0.	.329E+00	.588E+00	.700E+00
30	0.	0.	0.	0.	.251E+00	.504E+00	.780E+00
31	0.	0.	0.	0.	.192E+00	.430E+00	.840E+00
32	0.	0.	0.	0.	.152E+00	.370E+00	.880E+00

33	0.	0.	0.	0.	.109E+00	.298E+00	.920E+00
34	0.	0.	0.	0.	.609E-01	.212E+00	.960E+00
35	0.	0.	0.	0.	0.	0.	.100E+01

AT CHORD Y(J)= 1.7012 X-- LEADING EDGE= -1.0000 AILERON PIVOT= -1.0000 TRAILING EDGE= 1.0000

10	0.	0.	0.	0.	.161E+02	-.229E+01	-.980E+00
11	0.	0.	0.	0.	.109E+02	-.153E+01	-.940E+00
12	0.	0.	0.	0.	.979E+01	-.134E+01	-.900E+00
13	0.	0.	0.	0.	.796E+01	-.101E+01	-.840E+00
14	0.	0.	0.	0.	.617E+01	-.606E+00	-.760E+00
15	0.	0.	0.	0.	.486E+01	-.404E+00	-.680E+00
16	0.	0.	0.	0.	.410E+01	-.225E+00	-.600E+00
17	0.	0.	0.	0.	.349E+01	-.538E-01	-.500E+00
18	0.	0.	0.	0.	.302E+01	.947E-01	-.400E+00
19	0.	0.	0.	0.	.290E+01	.232E+00	-.300E+00
20	0.	0.	0.	0.	.316E+01	.469E+00	-.200E+00
21	0.	0.	0.	0.	.294E+01	.767E+00	-.100E+00
22	0.	0.	0.	0.	.191E+01	[illegible]	0.
23	0.	0.	0.	0.	.116E+01	.775E+00	.100E+00
24	0.	0.	0.	0.	.863E+00	.714E+00	.200E+00
25	0.	0.	0.	0.	.667E+00	.659E+00	.300E+00
26	0.	0.	0.	0.	.524E+00	.606E+00	.400E+00
27	0.	0.	0.	0.	.405E+00	.553E+00	.500E+00
28	0.	0.	0.	0.	.313E+00	.494E+00	.600E+00
29	0.	0.	0.	0.	.235E+00	.440E+00	.700E+00
30	0.	0.	0.	0.	.175E+00	.383E+00	.760E+00
31	0.	0.	0.	0.	.126E+00	.330E+00	.840E+00
32	0.	0.	0.	0.	.937E-01	[illegible]	.880E+00
33	0.	0.	0.	0.	.552E-01	.232E+00	.920E+00
34	0.	0.	0.	0.	.829E-02	[illegible]	.960E+00
35	0.	0.	0.	0.	0.	0.	.100E+01

CP TIME TOT= 26.065 SINCE LAST CALL 1.024

APPENDIX B

PROGRAM/SUBROUTINE FLOW DIAGRAMS

```
      PROGRAM TEV174 (INPUT=1002,OUTPUT=1002,TAPE7,DEBUG,TAPE5=INPUT,
     A TAPE6=OUTPUT,TAPE1=1002,TAPE10=1002,
     B TAPE11=1002,TAPE12=1002,TAPE13=1002)
```

```
C       PURPOSE
C------------------------------
C
C       OVERALL PROGRAM PURPOSE
C       -----------------------
C       TEV174 INCLUDING OVERLAYS COMPUTES THE UNSTEADY TRANSONIC
C       TRANSONIC PERTURBATION FLOW ABOUT A HARMONICALLY
C       OSCILLATING THREE DIMENSIONAL WING, USING FINITE DIFFERENCE
C       TECHNIQUES.
C
C       OVERLAY PURPOSE
C       ---------------
C       OVERLAY 0,0 DOES THE FOLLOWING:
C       A) SERVES AS THE OVERALL DRIVER.
C       B) SERVES AS THE INITIALLIZATION VARIABLE STORAGE AREA.
C       C) CONTROLS THE ITERATION COUNTER AND TERMINATES AS NECESSARY.
C       D) CHECKS THE ERROR DIFFERENCE BETWEEN ITERATION TO SEE IF
C          CONVERGENCE OR DIVERGENCE HAS OCCURRED AND TERMINATES IF
C          NECESSARY.
C       E) CONTROLS THE FARFIELD BOUNDARY UPDATING.
C       F) CONTAINS UTILITY ROUTINES NEEDED BY THE OTHER OVERLAYS.
C
C       PROGRAM ROUTINE TEV174 PURPOSE
C       ------------------------------
C       THE TEV174 ROUTINE IS THE OVERALL DRIVER AND PERFORMS A TO E ABO
C
```

```
C       AUTHOR T.D BUTLER    LANGUAGE FTN 4.6 420
C
C       REFERNCES
C------------------------------------------------------------------
C
C       1. EHLERS,F.EDWARD, A FINITE DIFFERENCE METHOD FOR THE SOLUTION
C          OF THE TRANSONIC FLOW AROUND HARMONICALLY OSCILLATING
C          WINGS.
C          (BOEING NASA CONTRACT ,NASA CR-2257)
C       2. WEATHERILL,WARREN H.,EHLERS,F.EDWARD,SEBASTIAN,JAMES D.,
C          COMPUTATION OF THE TRANSONIC PERTURBATION FLOW FIELDS
C          AROUND TWO AND THREE DIMENSIONAL OSCILLATING WINGS.
C          (BOEING-NASA CONTRACT, NASA CR-2599)
C
C       DESCRIPTION
C------------------------------------------------------------------
C       PROGRAM ROUTINE TEV174 WILL PERFORM ITS TASKS IN THE FOLLOWING
C       ORDER:
C       A) CALL THE INITIALIZATION OVERLAY FOR INPUT AND OTHER INITIALIZ
C       B) START THE ITERATION LOOP, IT WILL LOOP NMAX TIMES MAXIMUM.
C       C) IF INDICATED FOR THIS ITERATION CALL THE FARFIELD UPDATE
C     OVERLAY.
C       D) DEPENDENT ON INPUT VARIABLE ILAX(SEE PROGRAM INIT)
C          CALL THE ROW RELAXATION OR THE COLUMN RELAXTION CALC-
C          ULATION OVERLAY (SEE REFERENCE 2)
C       E) WRITE ON TAPE THE FINAL XZ PLANE FOR THIS ITERATION.
```

Figure B-1.—Program V174

```
C       F) TEST FOR CONVERGENCE OR DIVERGENCE. TERMINATE THE ITERATION
C          LOOP IF EITHER IS PRESENT.
C       END OF THE ITERATION LOOP
C       G) SAVE THE PHI1 DISTRIBUTION ON FILE TAPE10.
C       H) OUTPUT THE FINAL PRINTS
C       I) EXIT
C       NOTE SUBJECT TO CONVERGENCE/DIVERGENCE CRITERIA DO C TO F
C            NMAX TIMES.
C
C       MODIFICATION HSITORY.
C------------------------------------------------------------------
C
C      TEV174 3-D TRANSONIC SMALL DISTURBANCE FLOW OVER WING
C    VERSION 3-19-75  THREE D OUT OF CORE SOL
C    VERSION 3-15-76 LO-UP SYMMETRY-TB
C    VERSION 5-3-76 THREE-D ROW RELAXATION-TB
C     UNSTEADY TRANSONIC SMALL DISTURBANCE FLOW OVER AIRFOILS
C
C       INPUT
C------------------------------------------------------------------
C       INPUT OF THE INITIAL BCD AND BINARY DATA IS ACCOMPLISHED IN
C       THE INITIALIZATION OVERLAY( PROGRAM INIT IIIDL,4,0)
C
C       OUTPUT
C------------------------------------------------------------------
C       THIS ROUTINE OUTPUTS THE SAVEABLE AND REUSABLE PHI1
C       DISTRIBUTION IN BINARY FORM ON TAPE10.
C       ALSO IT OUTPUTS PRINTED ERROR MESSAGES AND CONVERGENCE
C       DIVERGENCE MESSAGES.
C       OTHER I/O IS ACCOMPLISHED BY THE OVERLAYS AND ROUTINE
C       CPR IN THIS OERLAY.
C       THE OTHER OVERLAYS MAY CALL THE UTILITY ROUTINES IN THIS
C       OVERLAY FOR I/O.
C
C
C
C
C
C
C
C
C       FSMACH      MACH NO.
C       DELTA       THICKNESS RATIO
C       THETA       ANGLE OF ATACK
C       OMEGA       ANGULAR REDUCED FREQUENCY
C       GAMMA       RATIO OF SPECIFIC HEATS FOR AIR
C       AL          HINGE LINE
C       IMAX        MAX X NODE COUNT
C       JMAX        MAX Y NODE COUNT
C       KMAX        MAX Z NODE COUNT
C       IS          STARTING X NODE LIMIT FOR VOL INTEGRAL FOR WING
C       IE          ENDING X NODE LIMIT FOR VOL INTEGRAL FOR WING
C       KS          STARTING Y NODE LIMIT FOR VOL INTEGRAL FOR WING
```

Figure B-1.—(Continued)

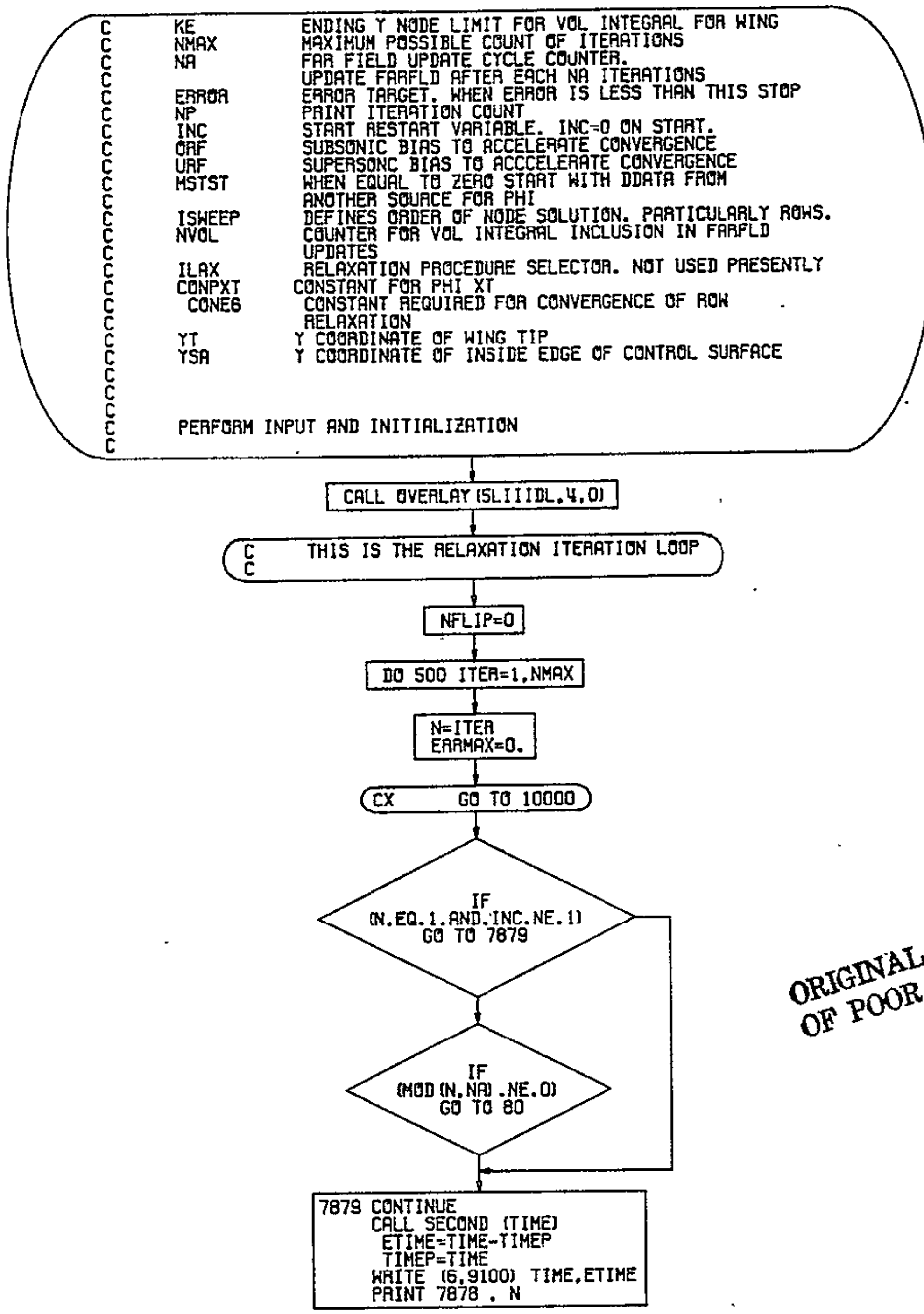

Figure B-1.—(Continued)

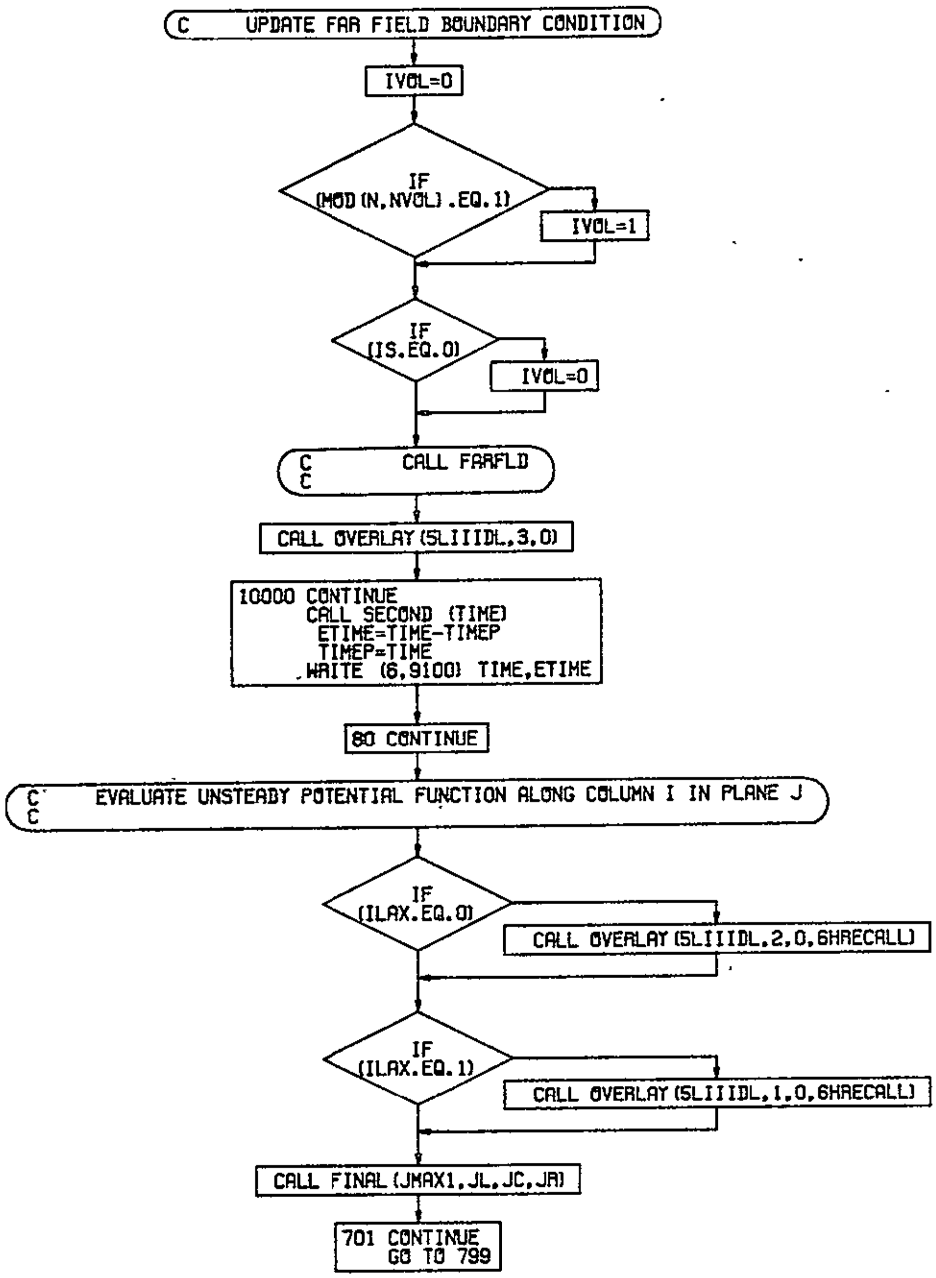

Figure B-1.—(Continued)

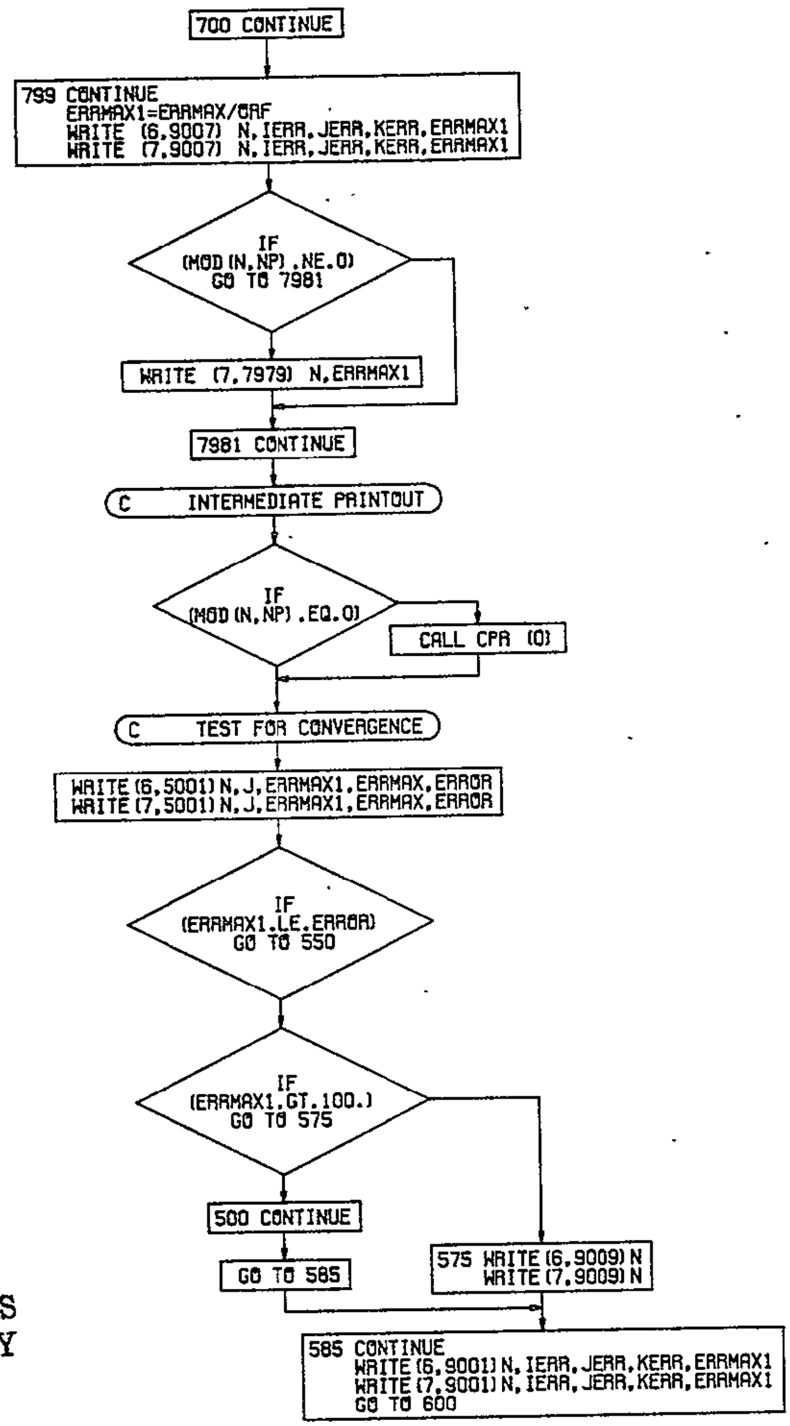

Figure B-1.—(Continued)

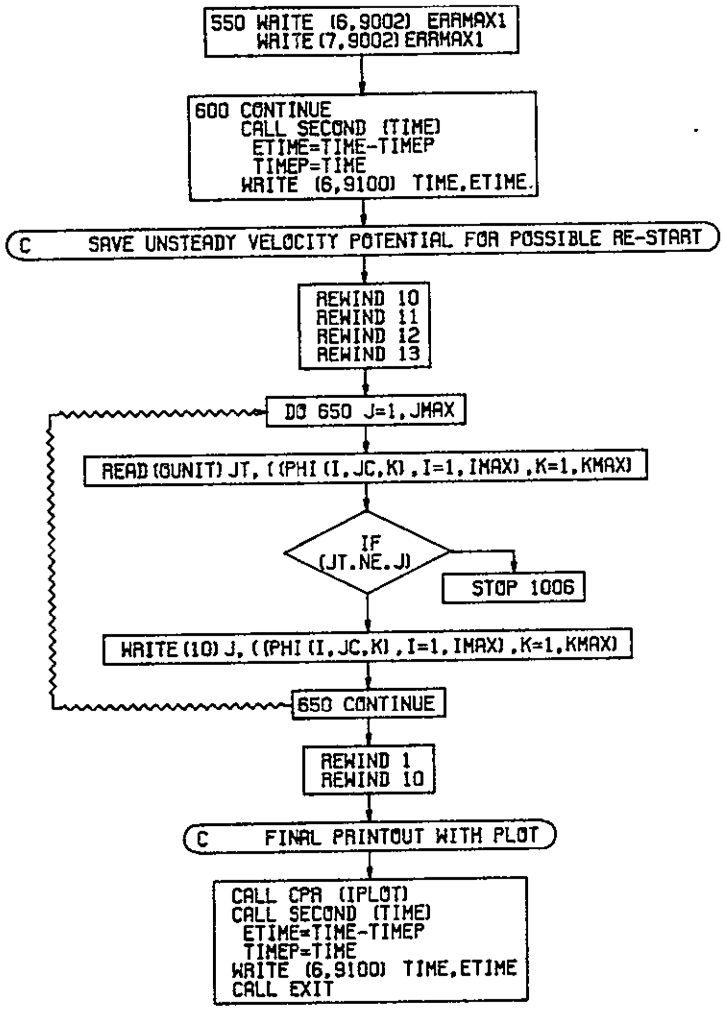

Figure B-1.—(Concluded)

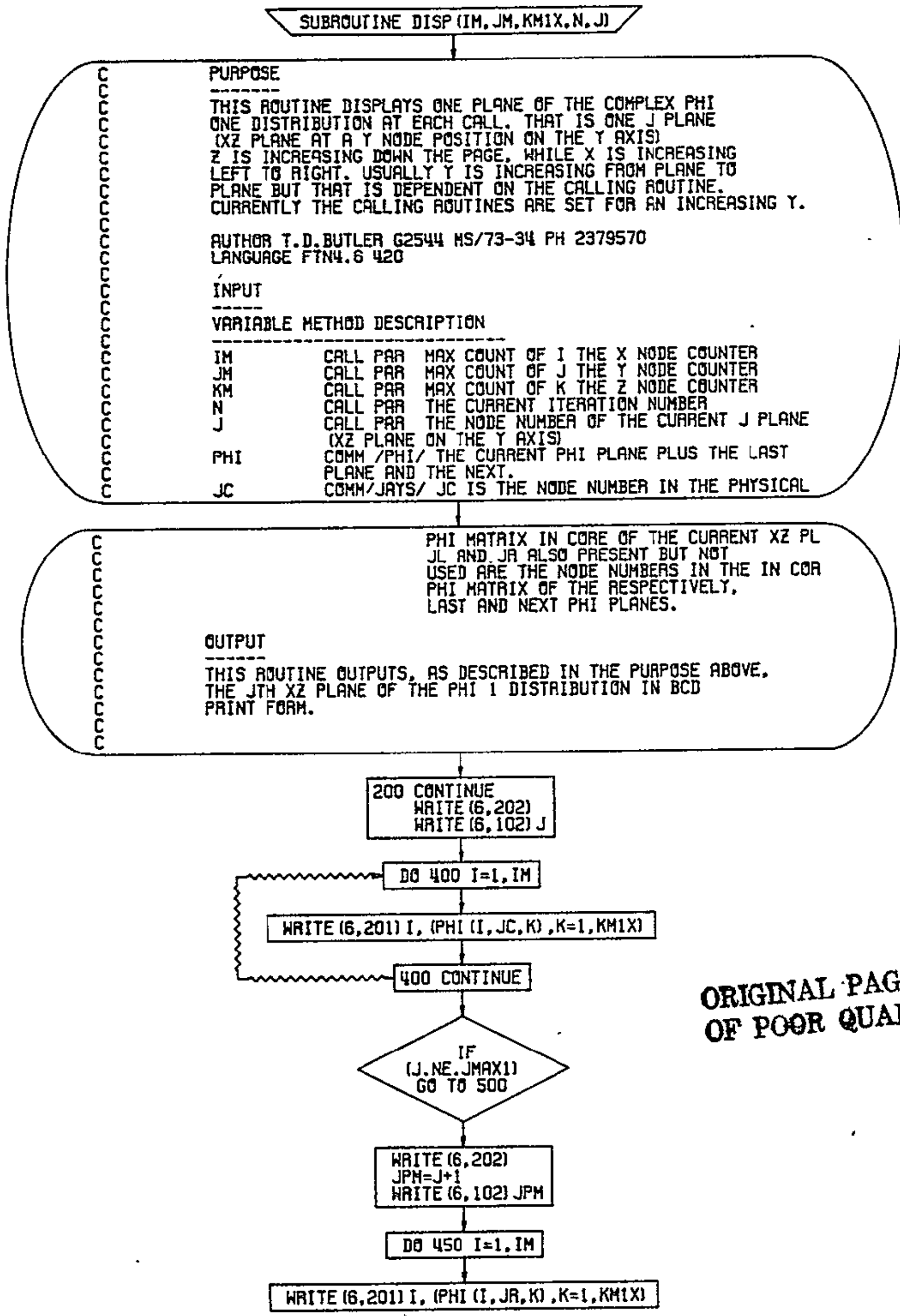

Figure B-2.—Subroutine DISP

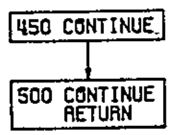

Figure B-2.—(Concluded)

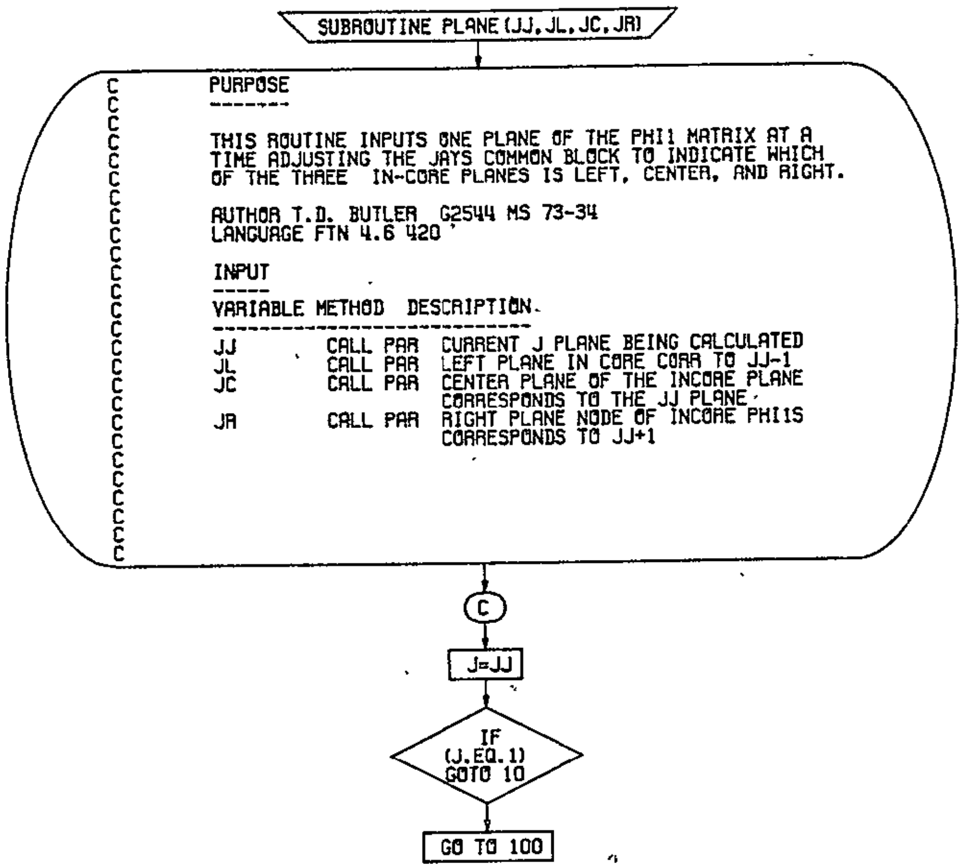

Figure B-3.—Subroutine PLANE

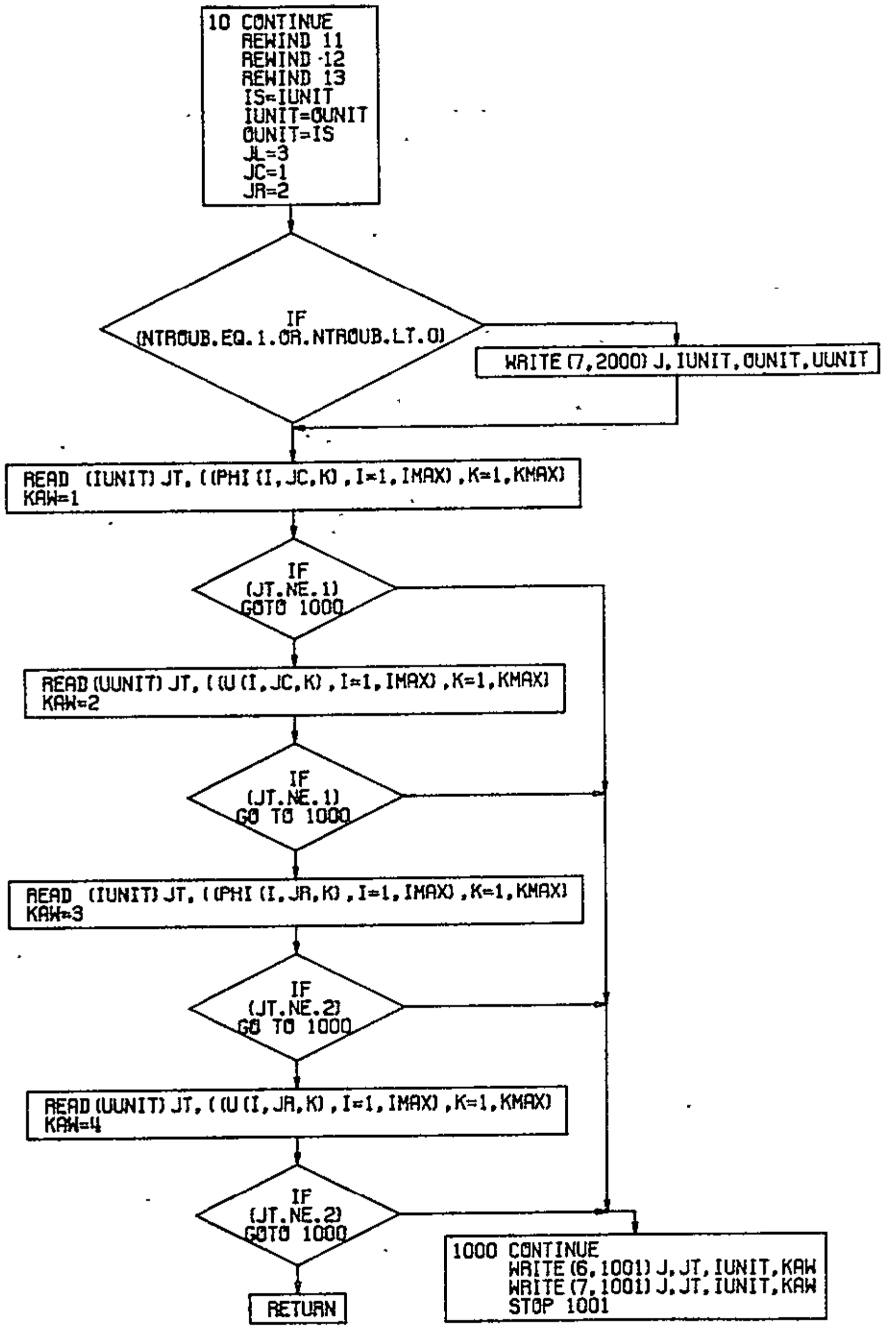

Figure B-3.—(Continued)

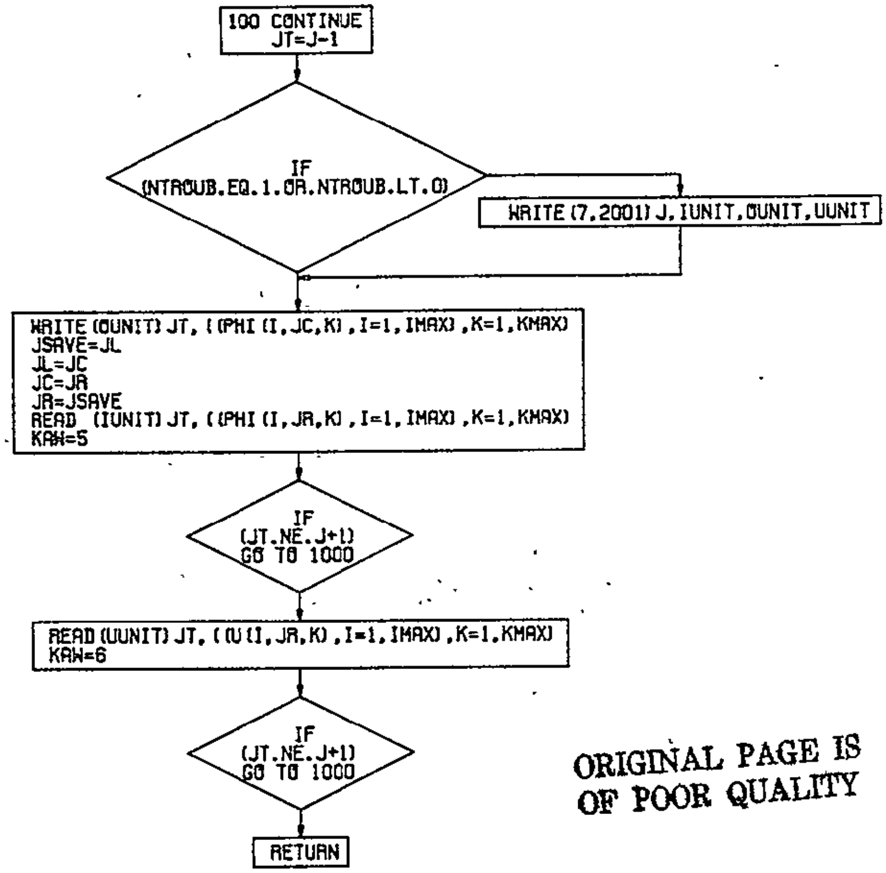

ORIGINAL PAGE IS
OF POOR QUALITY

Figure B-3.—(Continued)

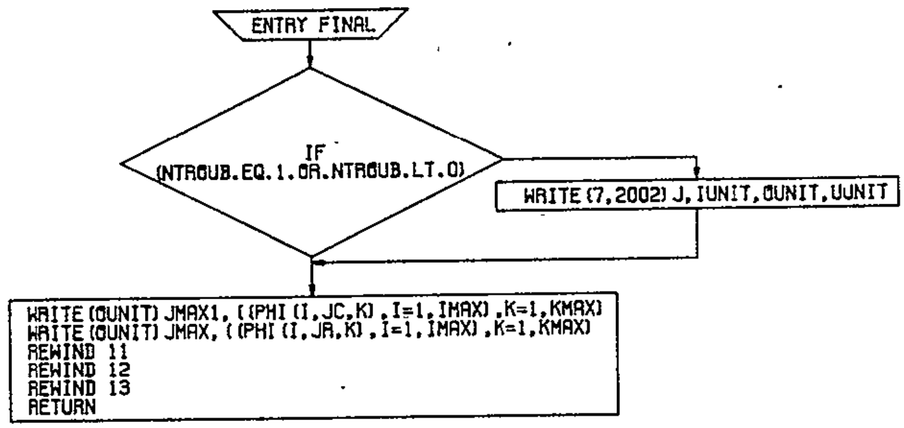

Figure B-3.—(Concluded)

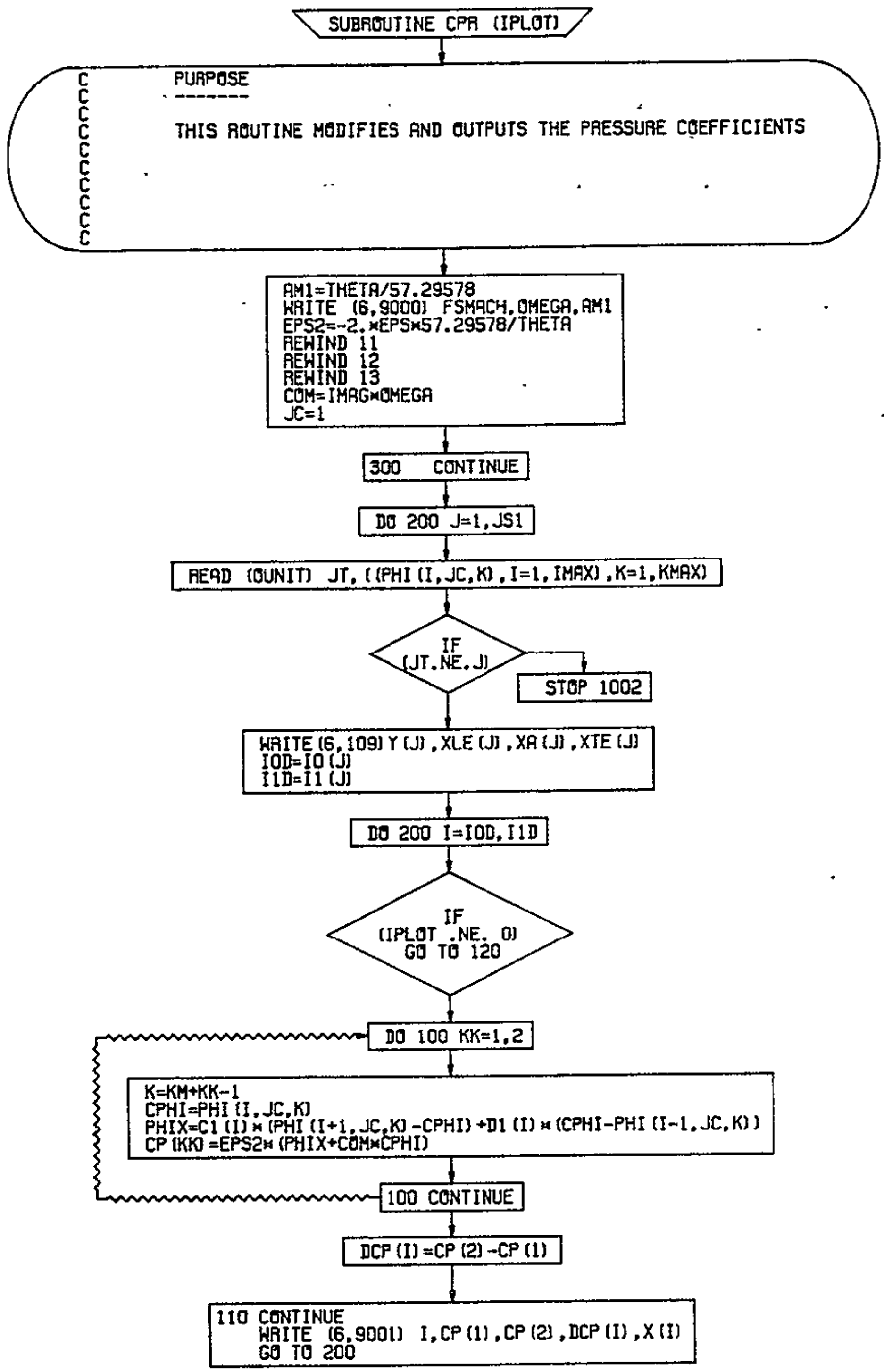

Figure B-4.—Subroutine CPR

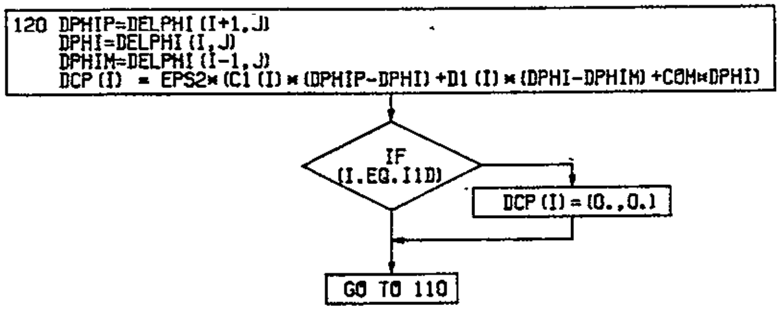

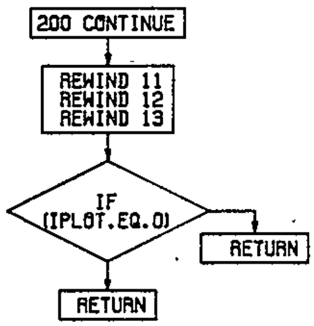

Figure B-4.—(Concluded)

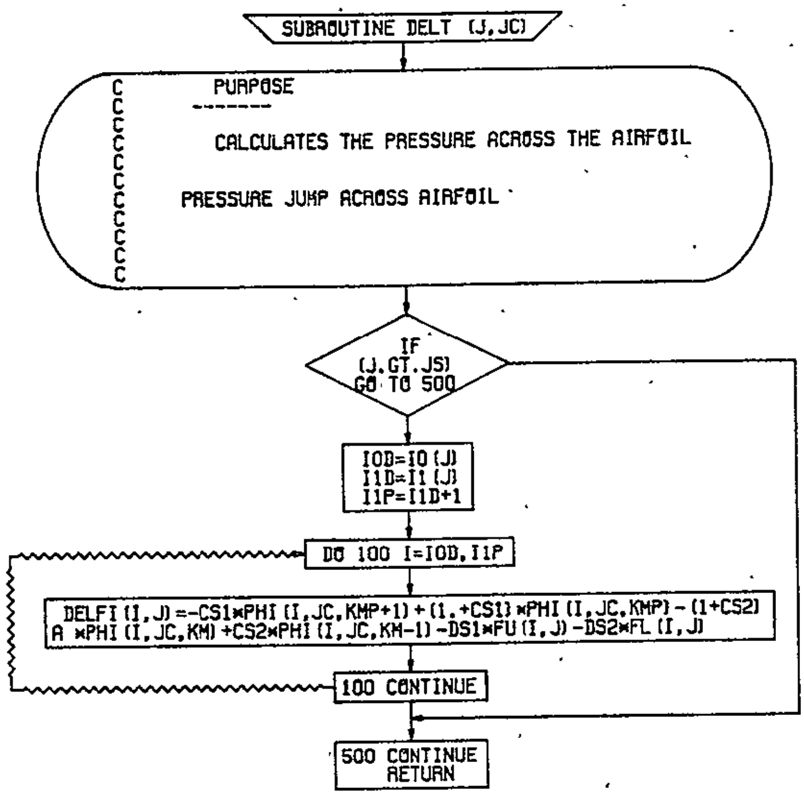

Figure B-5.—Subroutine DELT

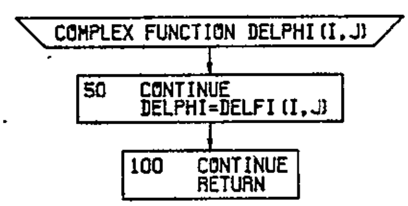

ORIGINAL PAGE IS
OF POOR QUALITY

Figure B-6.—Complex Function DELPHI

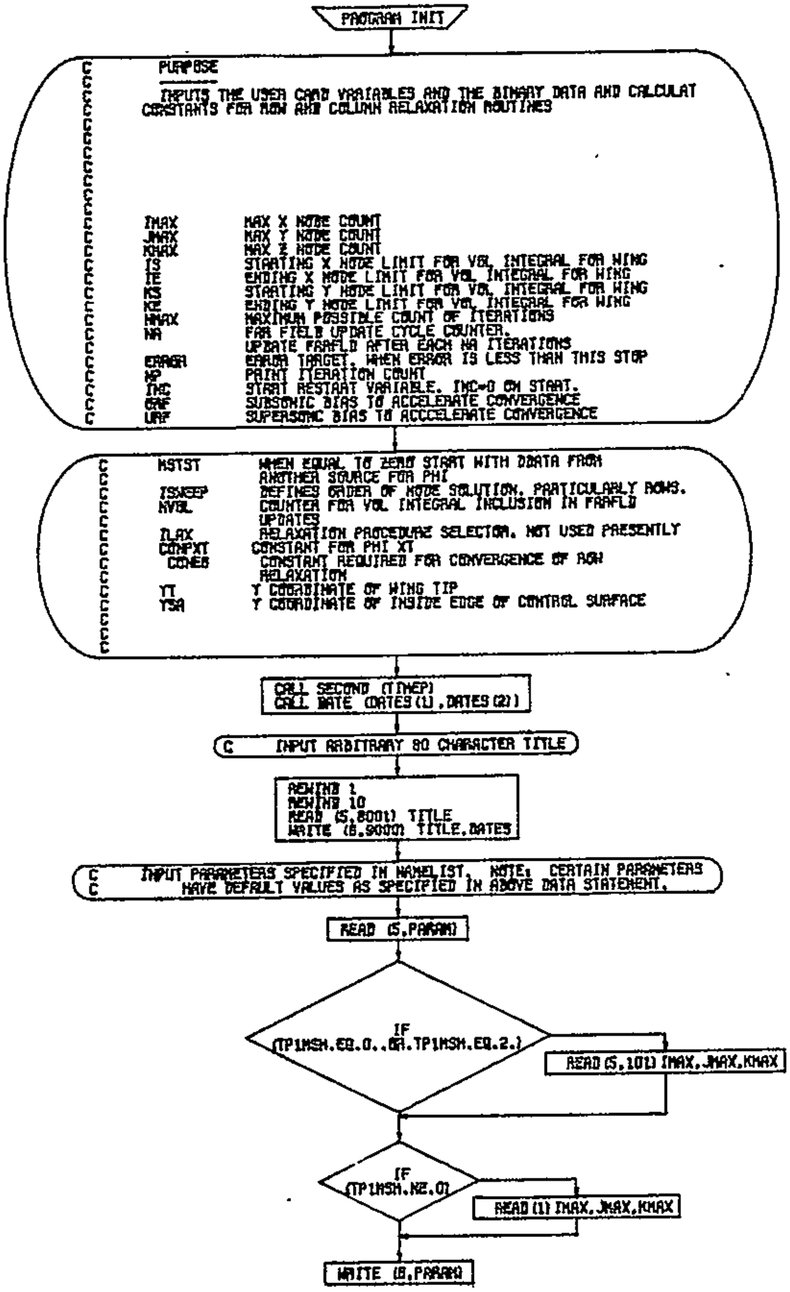

Figure B-7.—Program INIT

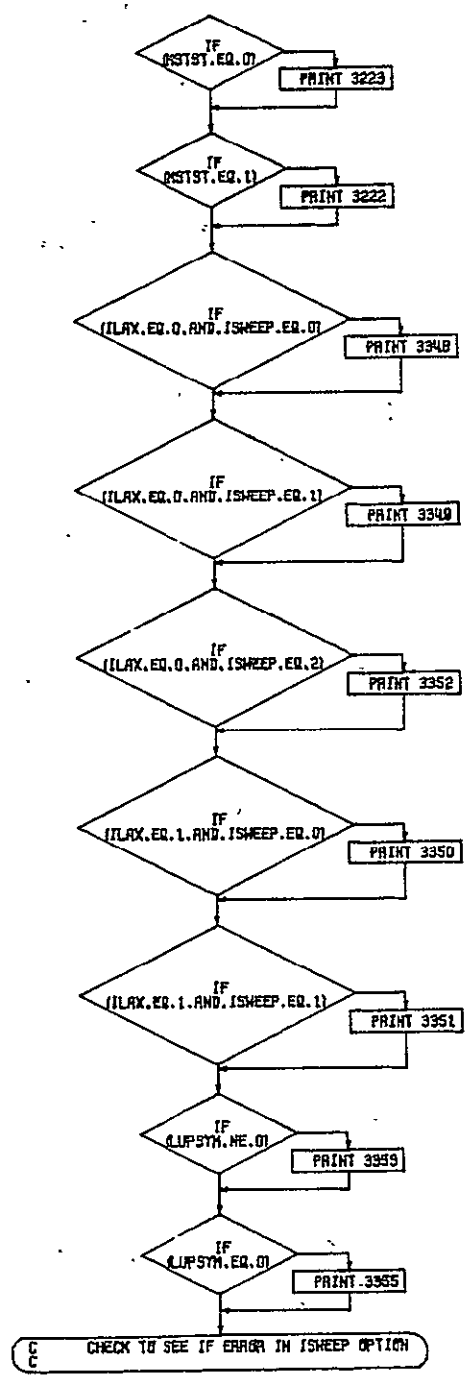

Figure B-7.—(Continued)

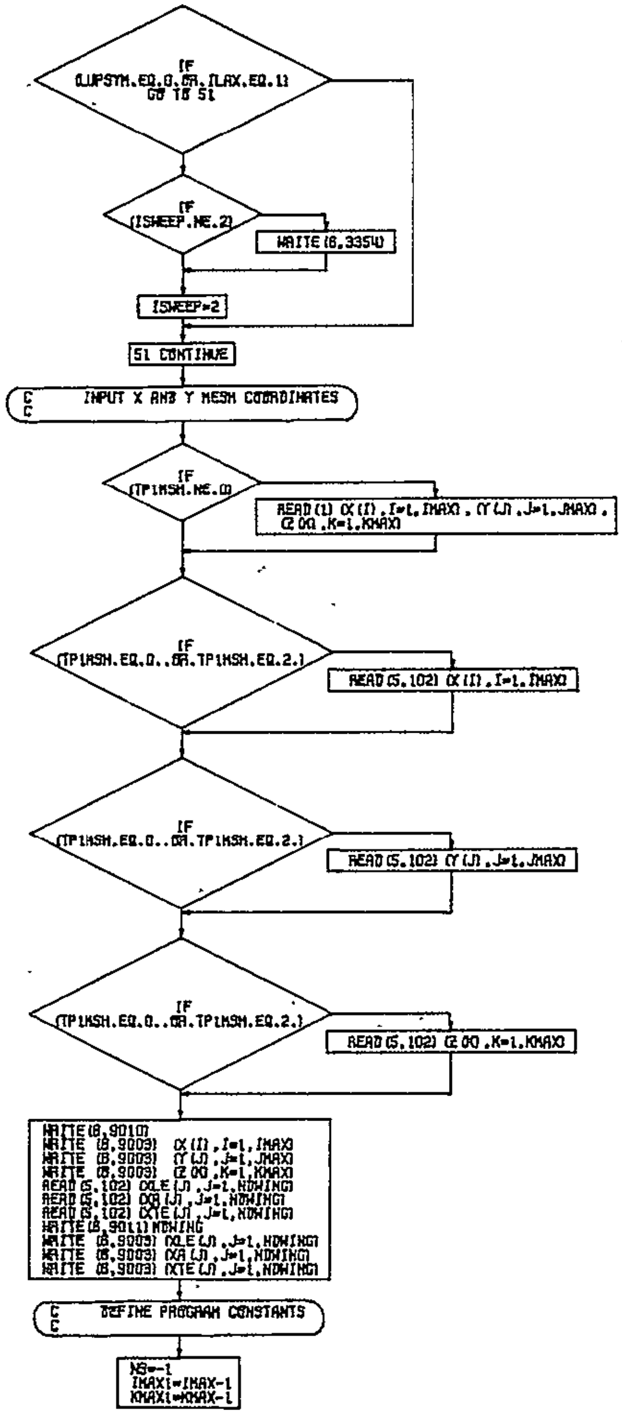

Figure B-7.—(Continued)

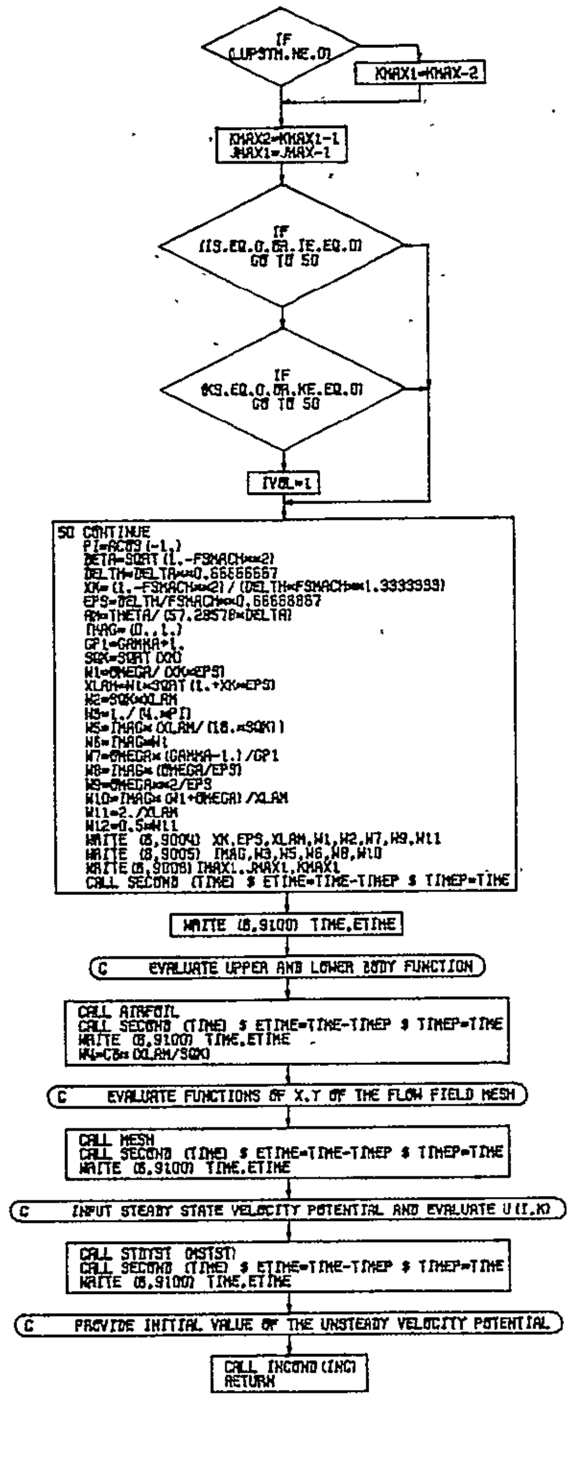

ORIGINAL PAGE IS
OF POOR QUALITY

Figure B-7.—(Concluded)

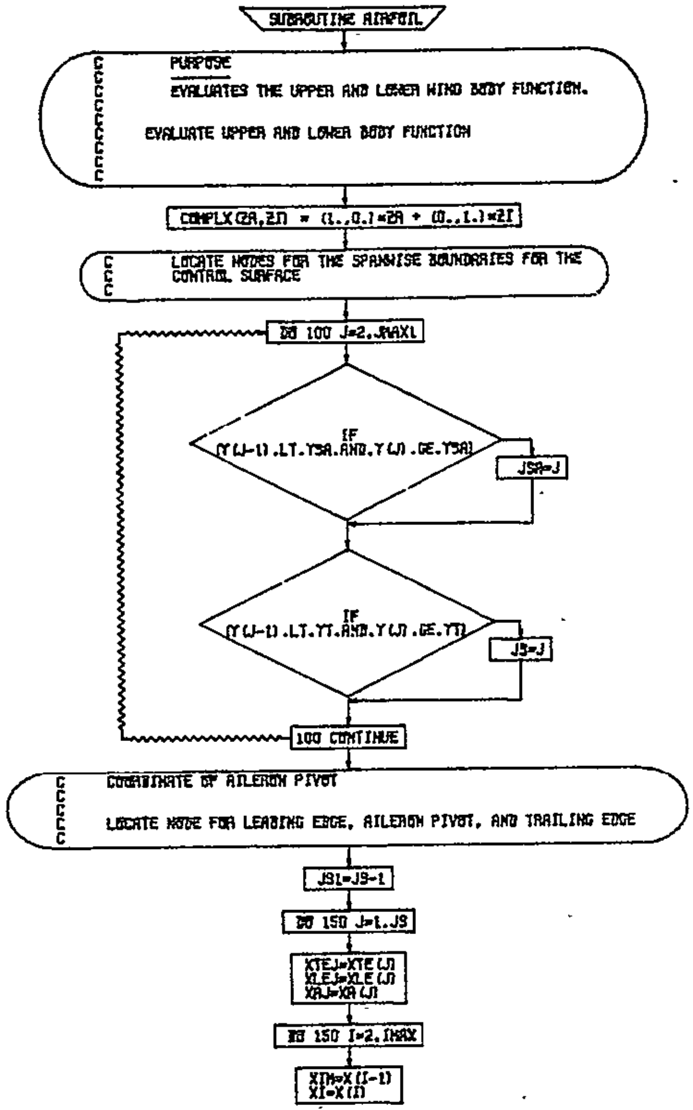

Figure B-8.—Subroutine AIRFOIL

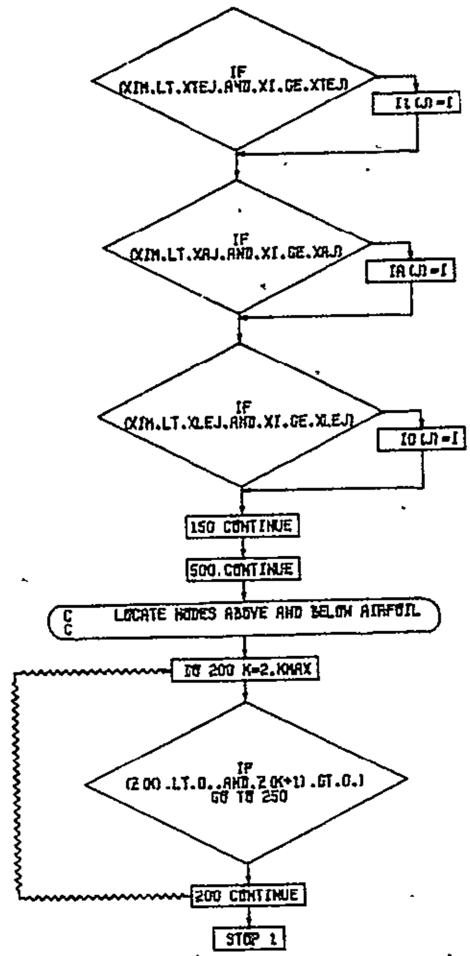

Figure B-8.—(Continued)

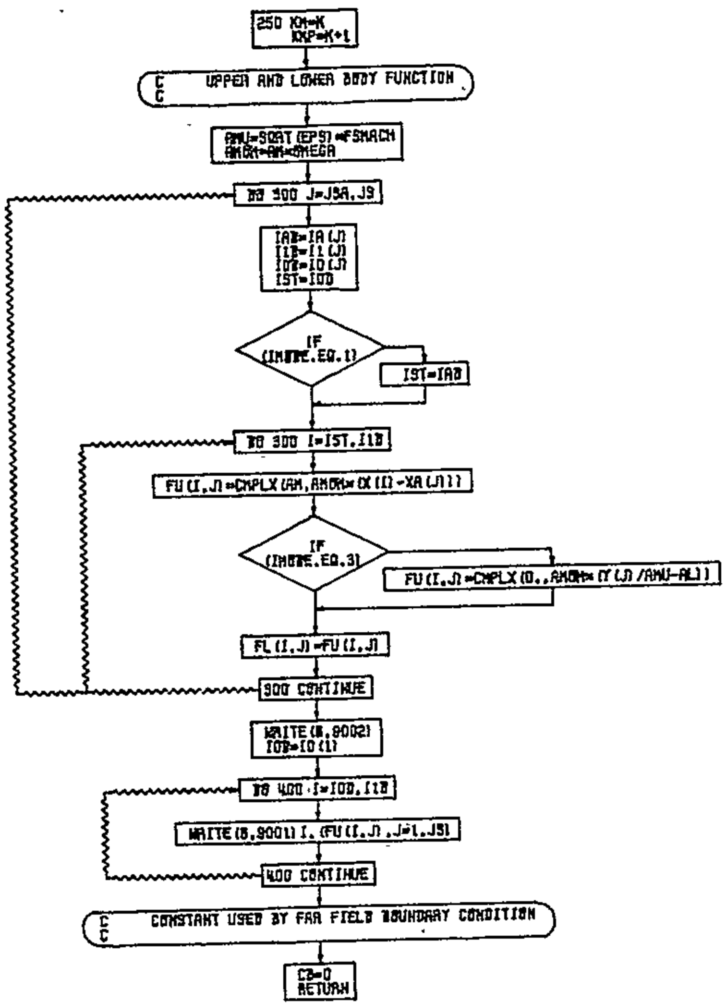

Figure B-8.—(Concluded)

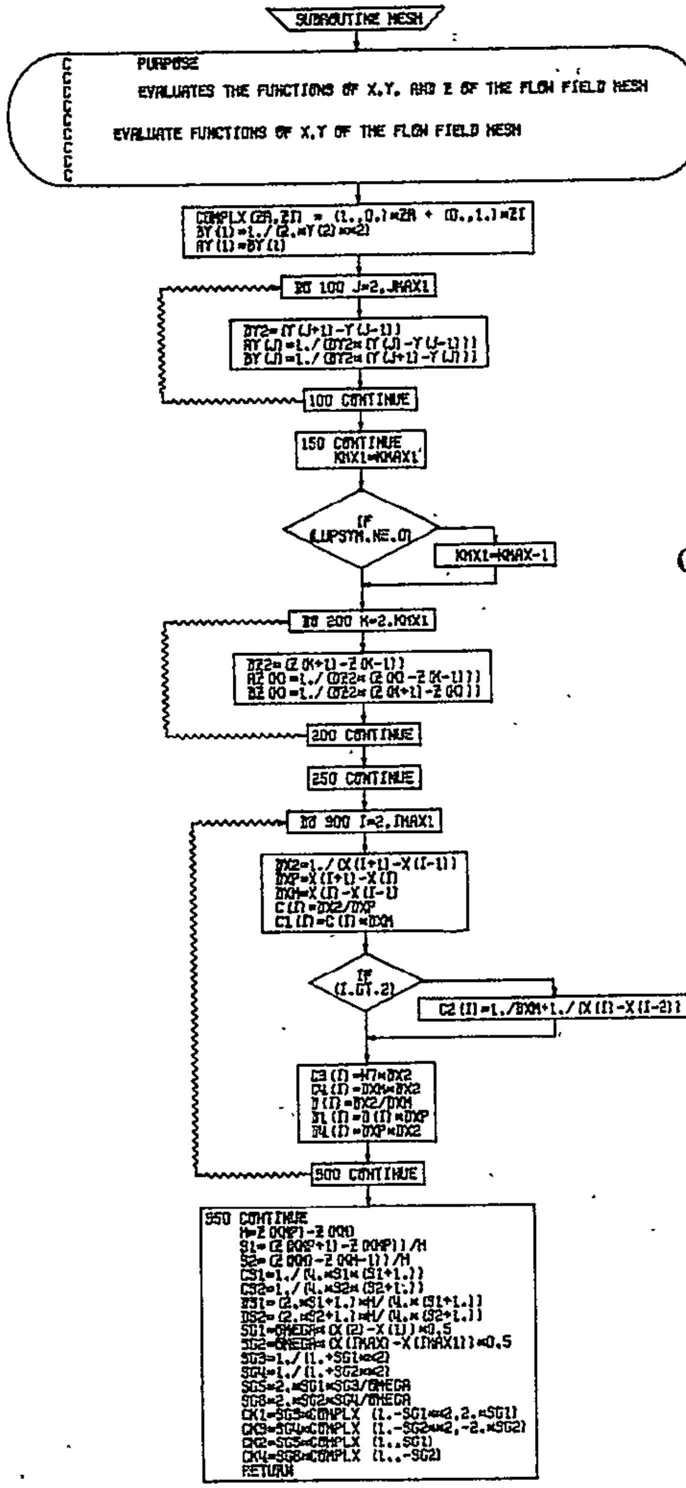

ORIGINAL PAGE IS
OF POOR QUALITY

Figure B-9.—Subroutine MESH

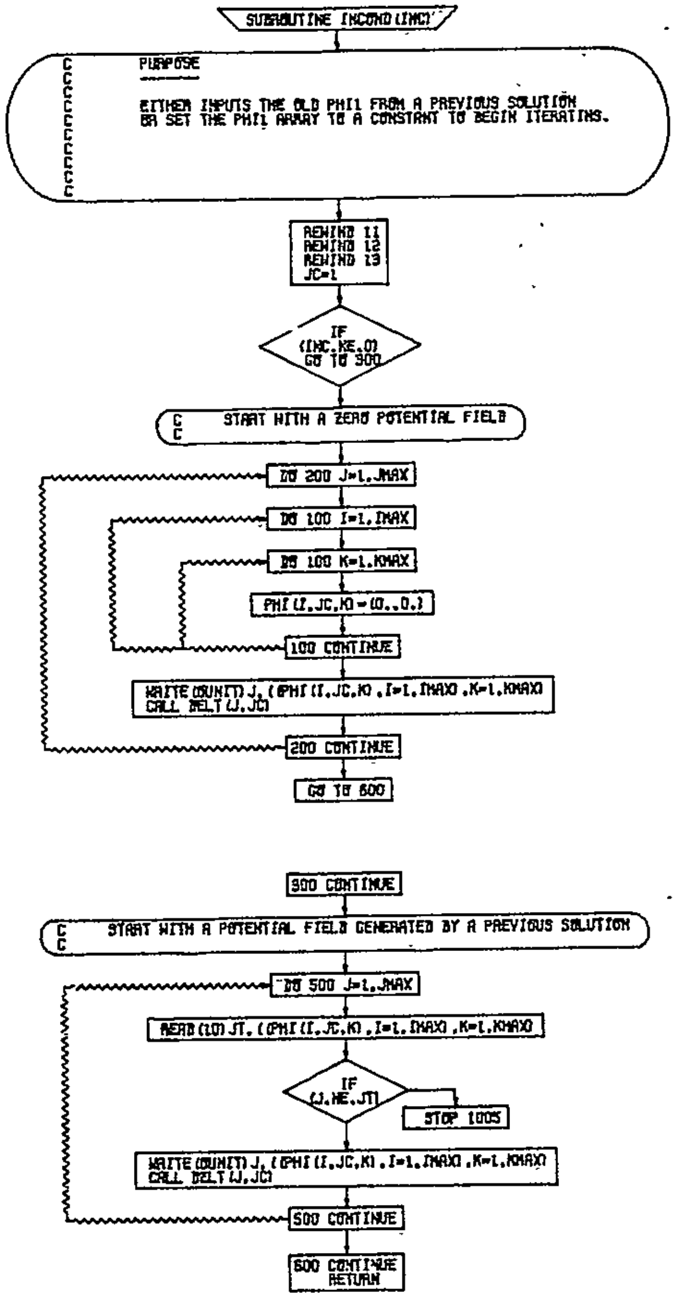

Figure B-10.—Subroutine INCOND

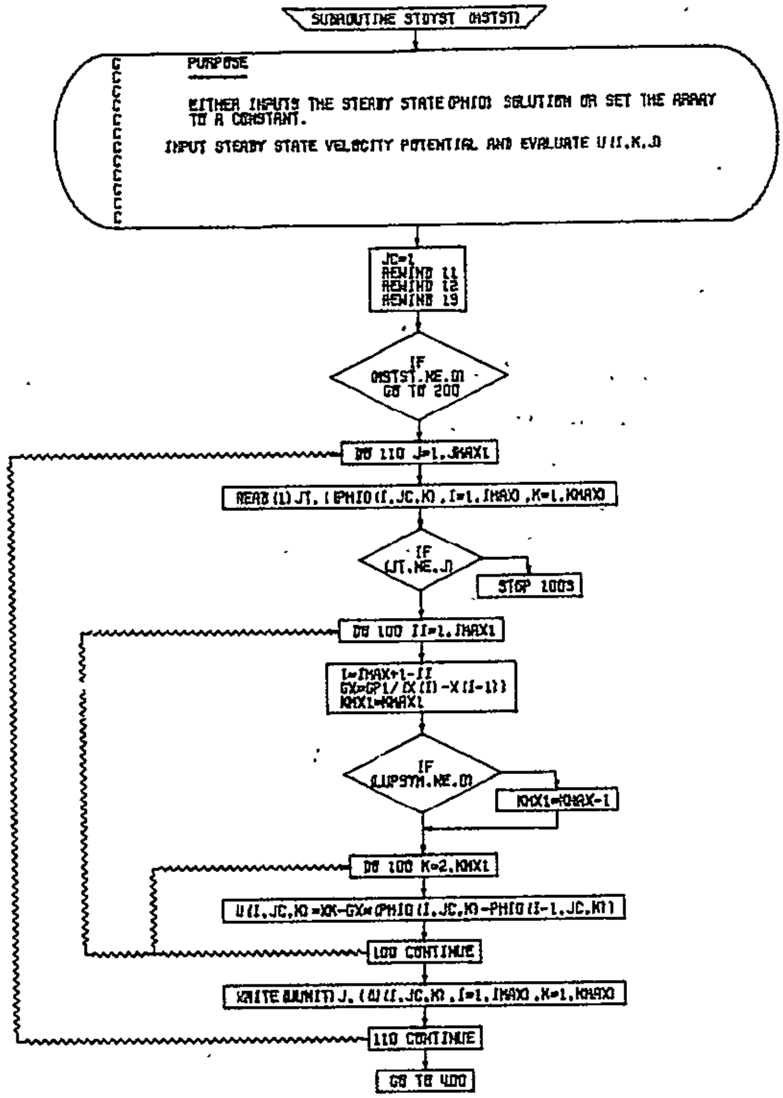

ORIGINAL PAGE IS OF POOR QUALITY

Figure B-11.—Subroutine STDST

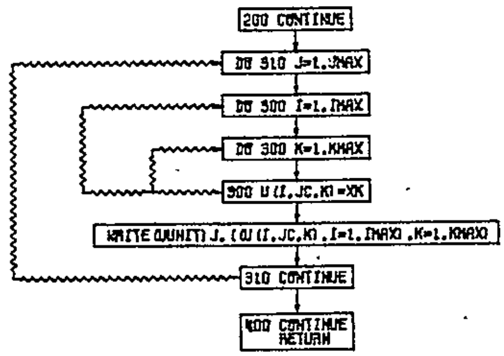

Figure B-11.—(Concluded)

```
PROGRAM COLLAX

C     OVERLAY PURPOSE
C
C     THIS OVERLAY CALCULATES THE CURRENT X-Z PLANE IN COLUMNS
C     THAT IS, COLUMNS OF PHI1 NODES PARALELL TO THE Z AXIS.
C
C     PROGRAM PURPOSE
C
C     THIS PROGRAM IS THE DRIVER FOR THE COLUMN RELAXATION
C     (OR CALCULATION) OVERLAY.
C     IT IS GIVEN A X-Z PLANE TO UPDATE AND THE TWO X-Z PLANES ON
C     EITHER SIDE OF IT (EXCEPT WHEN THE X-Z PLANE BEING CALCULATED
C     IS NEXT TO THE ROOT OR THE OUTSIDE BOUNDARY) FOR
C     FINITE DIFFERENCE UPDATING.
C     IT ALSO CALCULATES THE DIFFERENCE BETWEEN THE NODE JUST
C     CALCULATED AND THE PREVIOUS NODE AND PASSES THAT ON TO THE
C     MAIN DRIVER IN (0,0) FOR DETERMINATION OF CONVERGENCE AND
C     DIVERGENCE OF THE SOLUTION.
C
C     INPUT VAR  FROM    DECSRIPTION
C     PHI        TAPE11  READ BY ROUTINE PLANE INTO THE PHI ARRAY
C                OR      MIDDLE OR J PLANE(PHI(I,J,K)
C                TAPE12

C     JL,JC,JR   COMMON THESE IDENTIFY WHICH PHI J PLANE IS IN WHAT
C                OR     PRAT OF THE PHI ARRAY
C                PASSED
C
C     IMAX1      COMMON MAXIMUM NUMBER OF USER X NODES LESS 1 CALC-
C                       ULATED IN INIT(4,0)
C
C     I1         COMMON ARRAY OF INTEGERS INDICATING THE NODAL
C                       POSITION OF THE TRAILING EDGE.
C
C     ISWEEP     COMMON INPUT VARIABLE CONTROLLING SOL ORDER SEE INIT
C
C     KMAX1      COMMON MAX NUMBER OF USER Z NODES LESS 1. CALC-
C                       ULATED IN INIT.
C
C     IRLAXF     COMMON ARRAY INDICATING COLUMN NODES WHICH ARE
C                       SUPERSONIC AND SUBSONIC
C
C     LUPSYM     COMMON INPUT VARIABLE INDICATING LOWER-UPPER
C                       SYMMETRY.OF NODES DUE TO ZERO ANGLE OF
C                       ATTACK.
C
C     KM         COMMON INDICATES ZODE JUST BELOW THE WING
C
C     KMP        COMMON IDICATES Z NODE JUST ABOVE THE WING

C                       CALCULATED IN INIT.
C
C     IMAX,JMAX, COMMON THESE VARIABLES INDICATE THE MAXIMUM USER
C     AND KMAX          NUMBER OF NODES IN THE,RESPECTIVELY, X,Y,
C                       AND Z AXIS.
C
C     N          COMMON CURRENT ITERATION NUMBER.
C
C     NMAX       COMMON MAXIMUM ALLOWABLE NUMBER OF ITERATIONS
C                       WITHOUT CONVERGENCE OR DIVERGENCE.
C
C     ORF        COMMON BIAS VARIABLE TO SPEED UP CONVERGENCE FOR
C                       SUBSONIC NODES
C
C     URF        COMMON BIAS VARIABLE TO SPEED UP CONVERGENCE FOR
C                        SUPERSONIC NODES.
C
C     OUTPUT VARIABLES IN EXECUTION ORDER
C     VARIABLE FROM   DECSRIPTION
C
C     PHICLM     COMMON CALCULATED IN MATRXCF AND TRIDIAG. THESE ARE
C                       NEW PHI1 S TO REPLACE THE OLD ONES. THIS
C                       ARRAY WILL CONTAIN ONE COLUMN AT A TIME.
C
C     ERR        COMMON THIS VARIABLE CONTAINS THE LARGEST
C                       DIFFERENCE BETWEEN THIS COLUMN JUST DONE

C                             AND THE PREVIOUS VALUE.
C
C     ERRMAX     COMMON SEE ERR
C
C     ERR1       COMMON REAL PART OF ERR
C
C     ERRI1      COMMON IMAGINARY PART OF ERR.
C
C
C     AUTHOR F.EDWARD EHLERS
C     MODIFIER TD BUTLER G2544 73-34 2379570 C
C
      COMMON/PHI/PHI(55,3,28)

DO 310 J=1,JMAX1
```

Figure B-12.—Program COLLAX

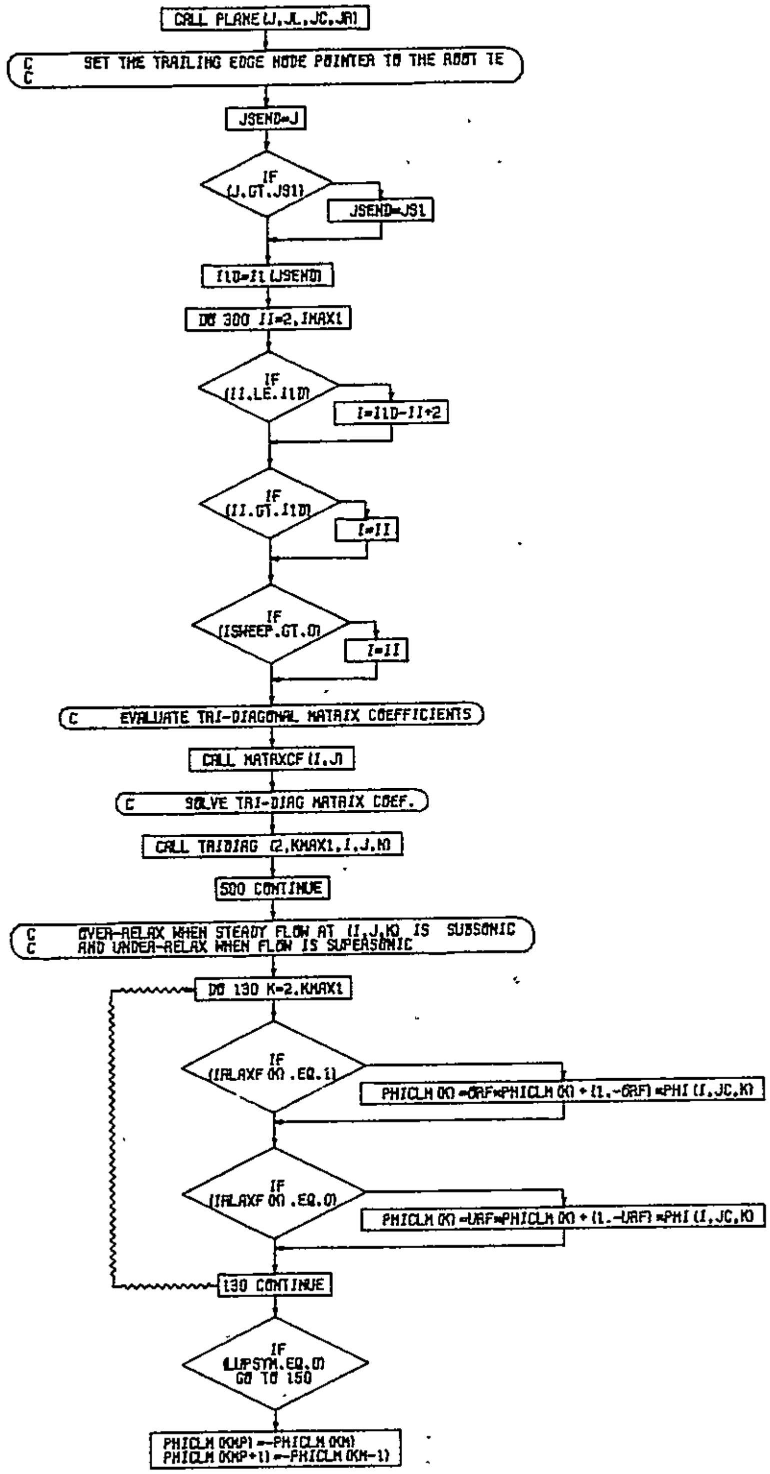

Figure B-12.—(Continued)

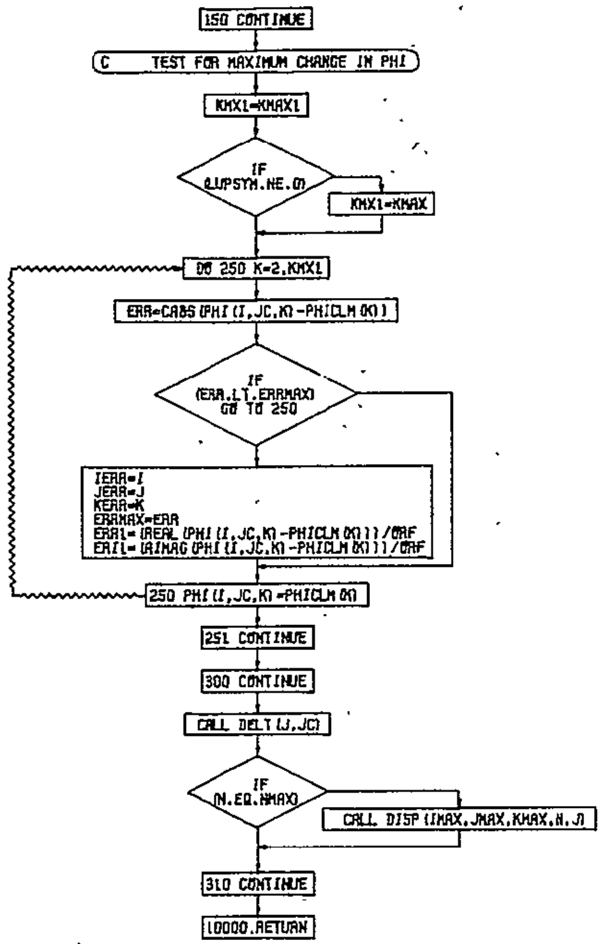

Figure B-12.—(Concluded)

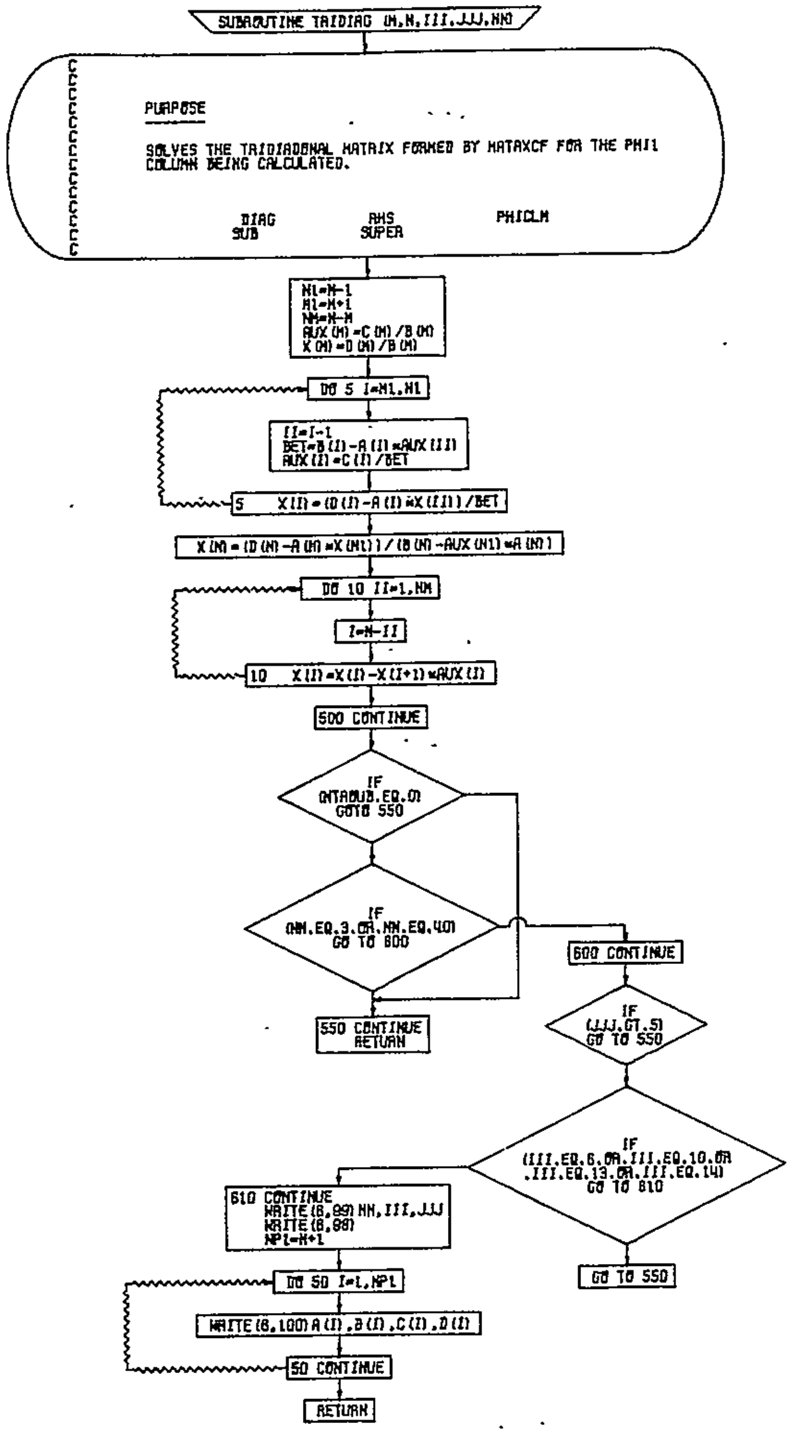

Figure B-13.—Subroutine TRIDIAG

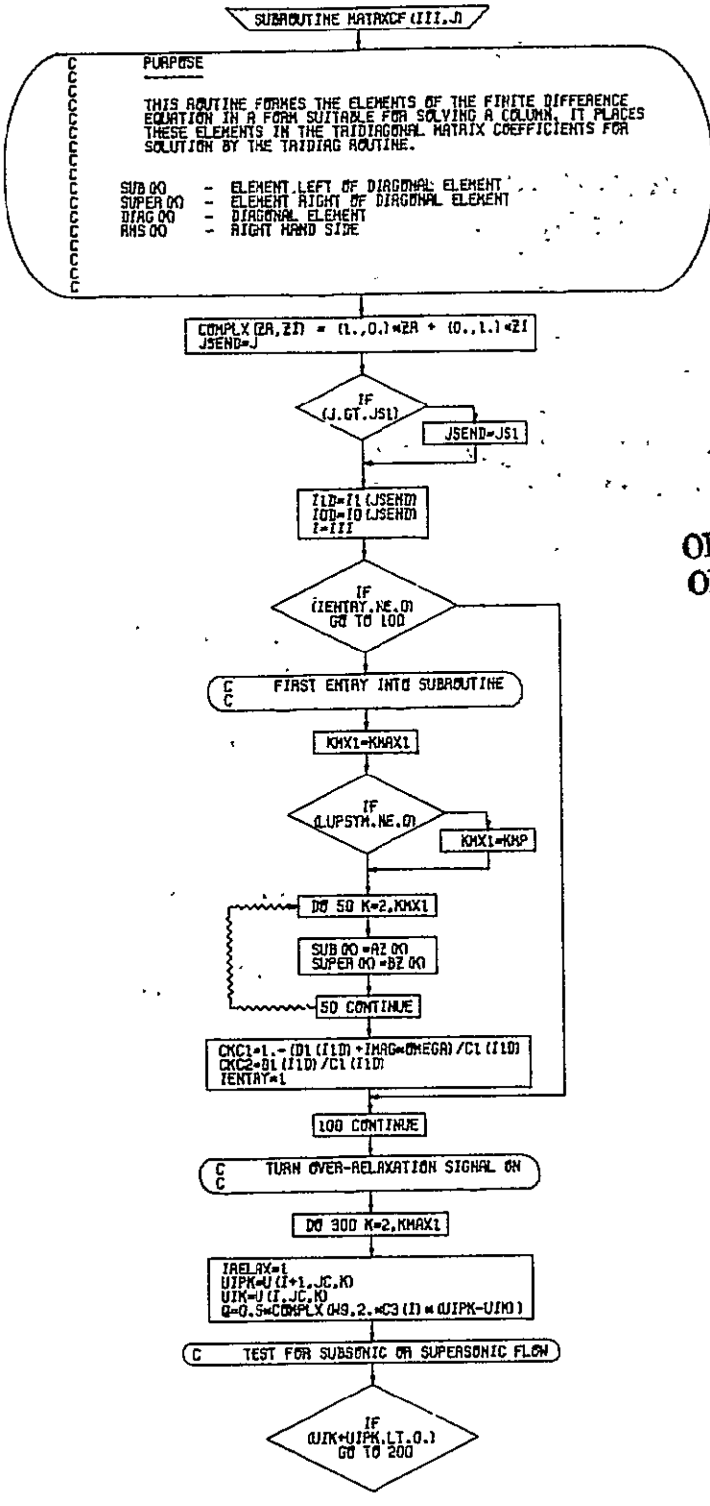

Figure B-14.—Subroutine MATRXCF

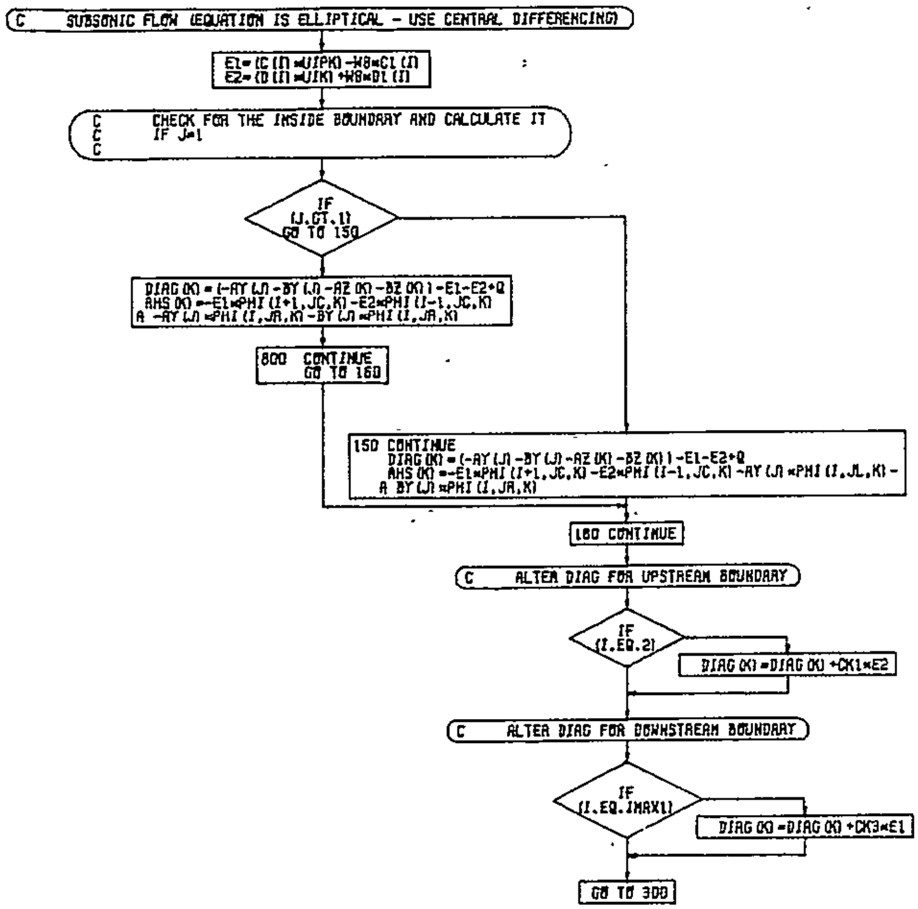

Figure B-14.—(Continued)

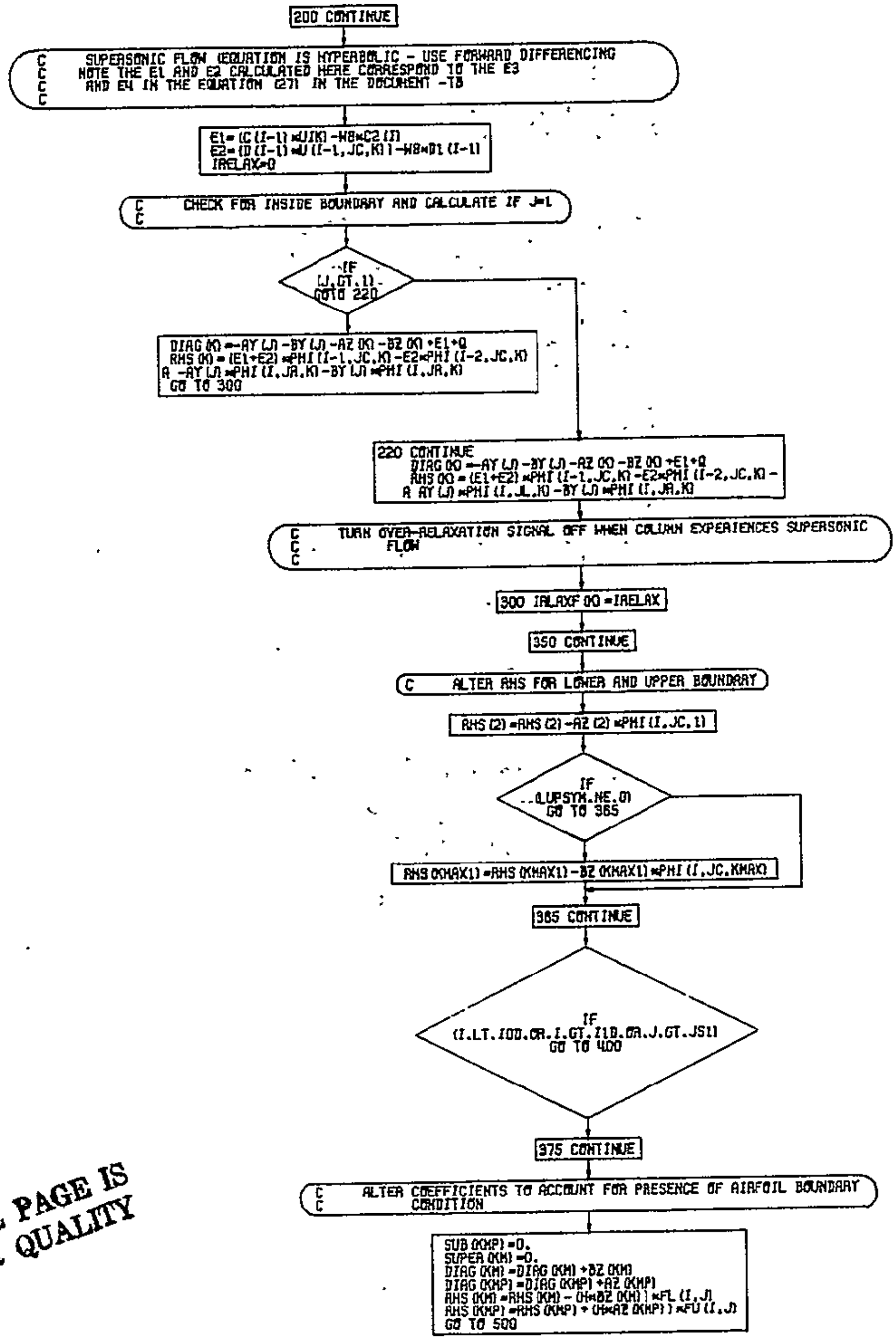

Figure B-14.—(Continued)

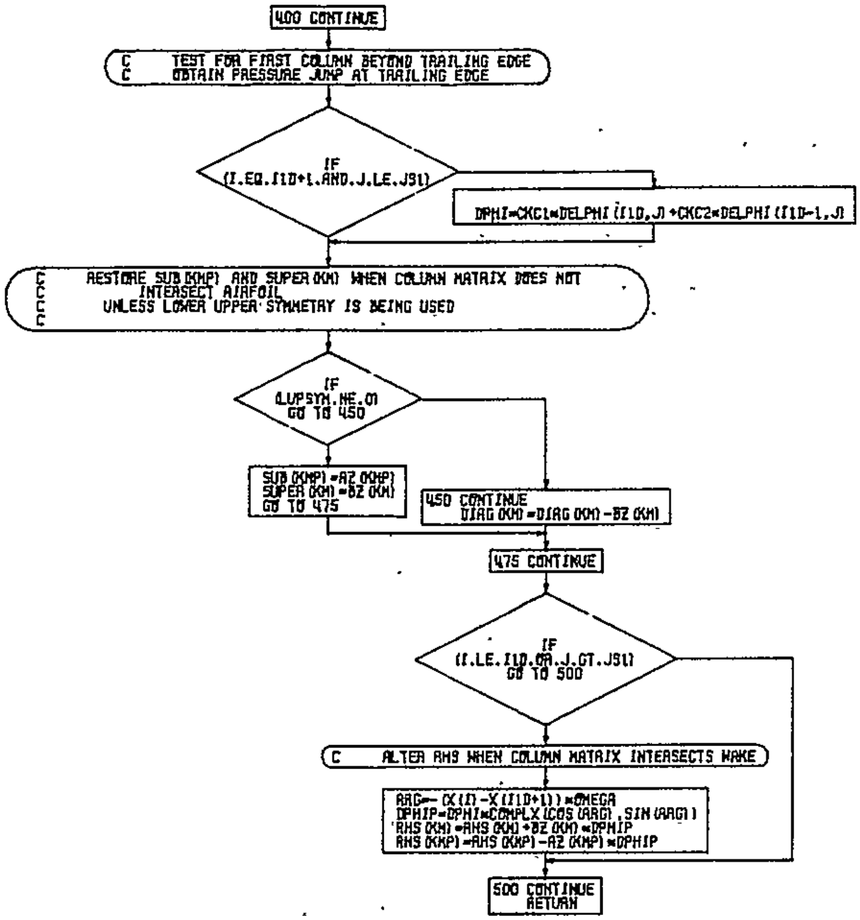

Figure B-14.—(Concluded)

```
PROGRAM ROWLAX

C         OVERLAY PURPOSE
C
C         THIS OVERLAY CALCULATES THE CURRENT X-Z PLANE IN ROWS PARALELL
C         TO THE X AXIS. THAT IS ROW S OF PHI1 NODES.
C
C         PROGRAM PURPOSE
C
C         THIS PROGRAM IS THE DRIVER FOR THE ROW RELAXATION
C         (OR CALCULATION) OVERLAY (2,0)
C         IT IS GIVEN AN X-Z PLANE TO UPDATE AND THE TWO X-Z PLANES
C         ON EITHER SIDE OF IT(EXCEPT WHEN THE X-Z PLANE BEING
C         CALCULATED IS NEXT TO THE ROOT OR THE OUTSIDE BOUNDARY)
C         FOR FINITE DIFFERENCE UPDATING.
C         IT ALSO CALCULATES THE DIFFERENCES BETWEEN THE NODE JUST
C         CALCULATED AND THE PREVIOUS VALUE FOR THAT NODE AND PASSES
C         THAT DIFFERENCE ON TO THE MAIN DRIVER(0,0) WHICH USES
C         IT FOR DETERMINATION OF DIVERGENCE OR CONVERGENCE.
C
C         INPUT VAR  FROM    DECSRIPTION
C         PHI        TAPE11  READ BY ROUTINE PLANE INTO THE PHI ARRAY
C                    OR      MIDDLE OR J PLANE(PHI(I,J,K))

C                    TAPE12
C         JL,JC,JR   COMMON  THESE IDENTIFY WHICH PHI J PLANE IS IN WHAT
C                    OR      PART OF THE PHI ARRAY
C                    PASSED
C         IMAX1      COMMON  MAXIMUM NUMBER OF USER X NODES LESS 1 CALC-
C                            ULATED IN INIT (4,0)
C         I1         COMMON  ARRAY OF INTEGERS INDICATING THE NODAL
C                            POSITION OF THE TRAILING EDGE.
C         ISWEEP     COMMON  INPUT VARIABLE CONTROLLING SOL ORDER SEE INIT
C         KMAX1      COMMON  MAX NUMBER OF USER Z NODES LESS 1. CALC-
C                            ULATED IN INIT.
C         IRLAXF     COMMON  ARRAY INDICATING ROW NODES WHICH ARE
C                            SUPERSONIC AND SUBSONIC
C         LUPSYM     COMMON  INPUT VARIABLE INDICATING LOWER-UPPER
C                            SYMMETRY OF NODES DUE TO ZERO ANGLE OF
C                            ATTACK.
C         KM         COMMON  INDICATES ZODE JUST BELOW THE WING

C         KMP        COMMON  IDICATES Z NODE JUST ABOVE THE WING
C                            CALCULATED IN INIT.
C         IMAX,JMAX, COMMON  THESE VARIABLES INDICATE THE MAXIMUM USER
C         AND KMAX           NUMBER OF NODES IN THE,RESPECTIVELY, X,Y,
C                            AND Z AXIS.
C         N          COMMON  CURRENT ITERATION NUMBER.
C         NMAX       COMMON  MAXIMUM ALLOWABLE NUMBER OF ITERATIONS
C                            WITHOUT CONVERGENCE OR DIVERGENCE.
C         ORF        COMMON  BIAS VARIABLE TO SPEED UP CONVERGENCE FOR
C                            SUBSONIC NODES
C         URF        COMMON  BIAS VARIABLE TO SPEED UP CONVERGENCE FOR
C                            SUPERSONIC NODES.
C         OUTPUT VARIABLES IN EXECUTION ORDER
C         VARIABLE FROM   DECSRIPTION
C         PHICLN     COMMON  CALCULATED IN SRKATCF AND FOURDG. THESE ARE
C                            NEW PHI1 S TO REPLACE THE OLD ONES. THIS
C                            ARRAY WILL CONTAIN ONE ROW AT A TIME.
C         ERR        COMMON  THIS VARIABLE CONTAINS THE LARGEST

C                            DIFFERENCE BETWEEN THIS ROW JUST DONE
C                            AND THE PREVIOUS VALUE.
C         ERRMAX     COMMON  SEE ERR
C         ERR1       COMMON  REAL PART OF ERR
C         ERRI1      COMMON  IMAGINARY PART OF ERR.
C
C         AUTHOR F.EDWARD EHLERS
C         MODIFIER TD BUTLER G2544 73-34 2378570I C
C

DO 310 J=1,JMAX1
```

Figure B-15.—Program ROWLAX

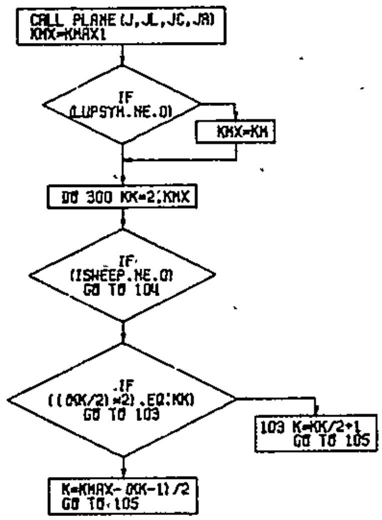

Figure B-15.—(Continued)

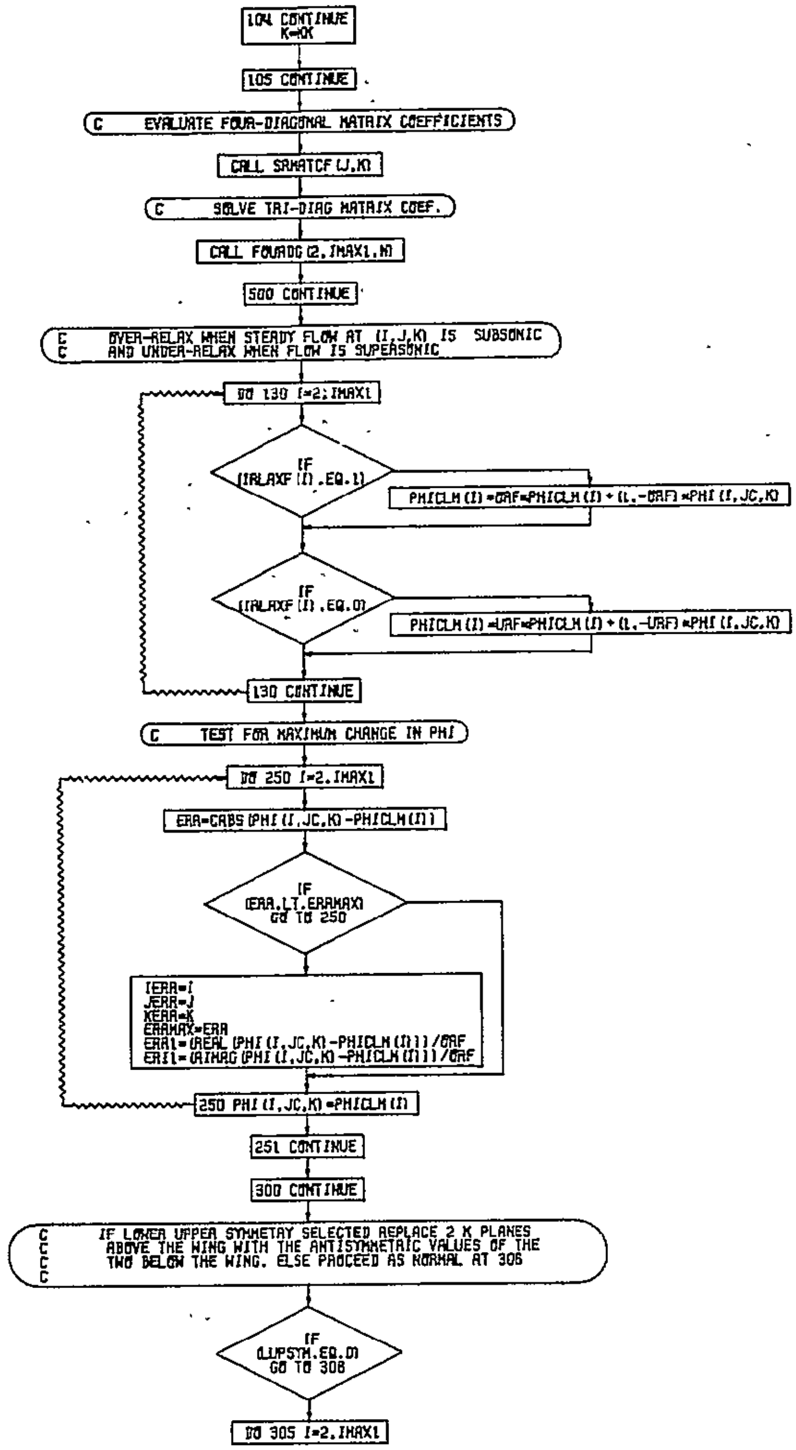

Figure B-15.—(Continued)

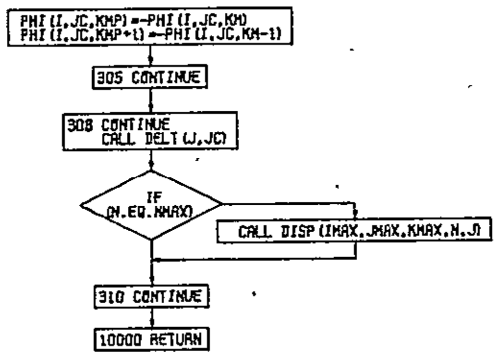

Figure B-15.—(Concluded)

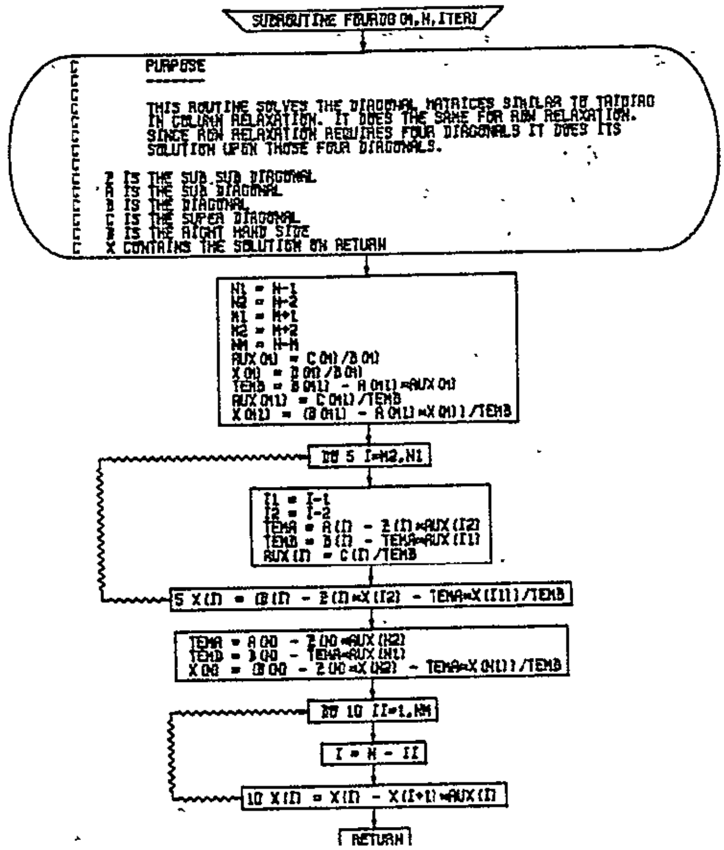

Figure B-16.—Subroutine FOURDG

ORIGINAL PAGE IS
OF POOR QUALITY

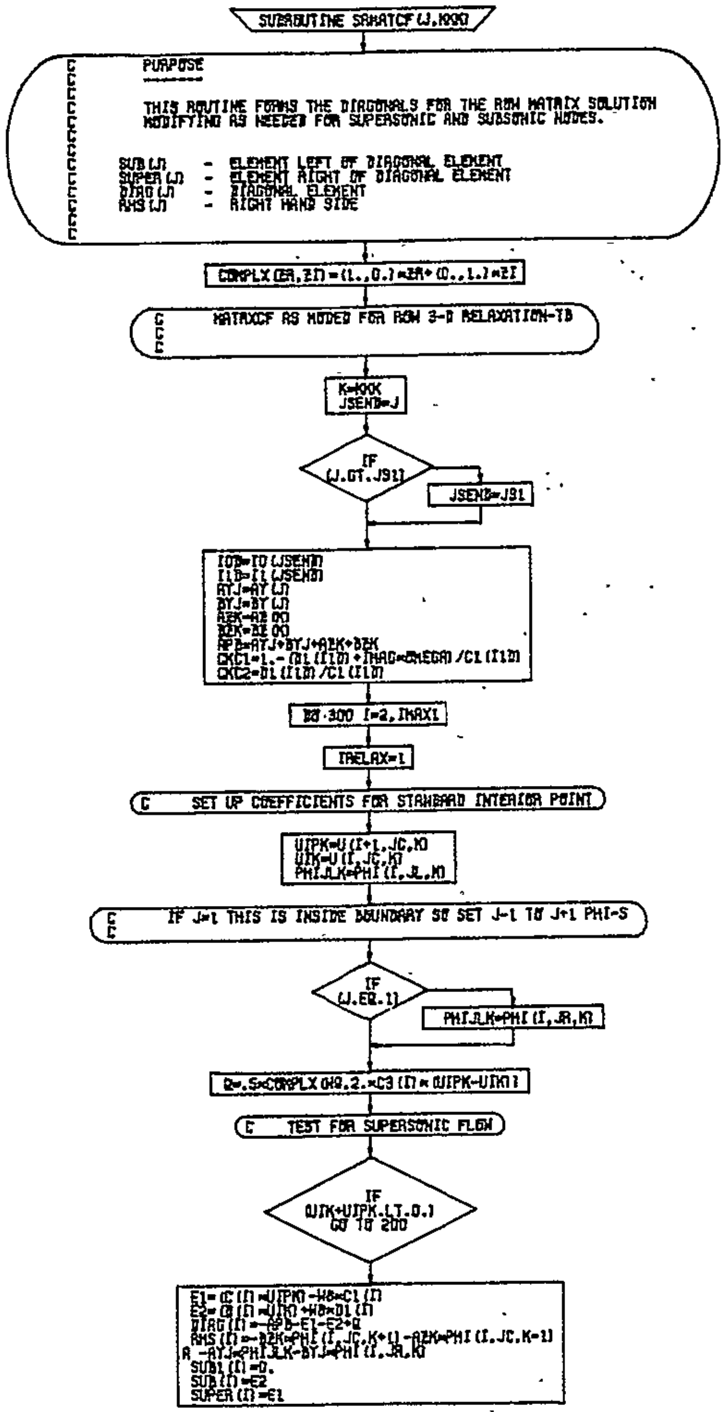

Figure B-17.—Subroutine SRMATCF

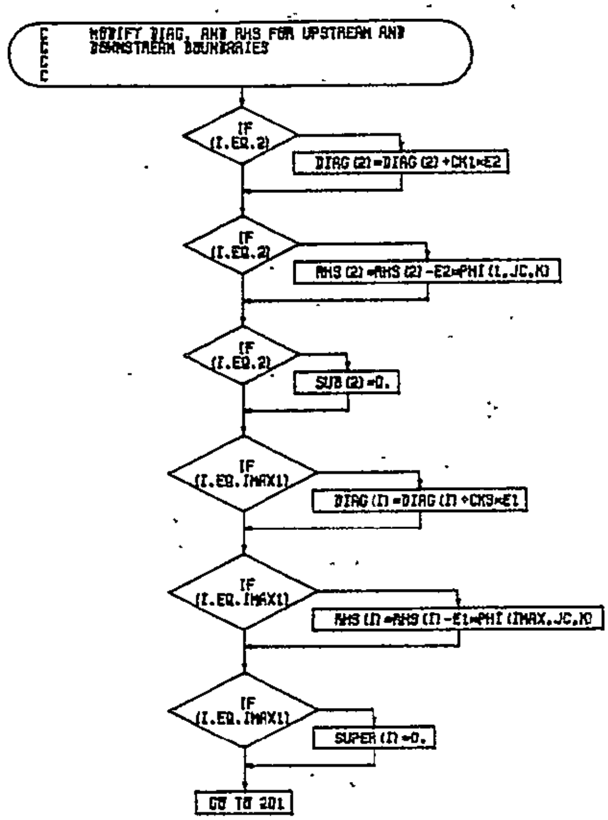

Figure B-17.—(Continued)

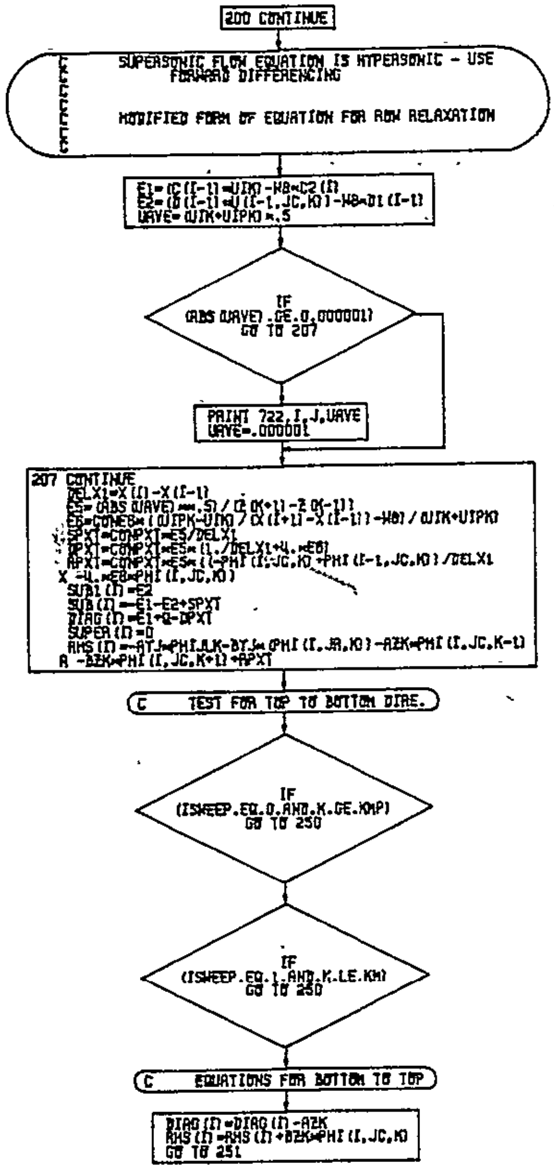

Figure B-17.—(Continued)

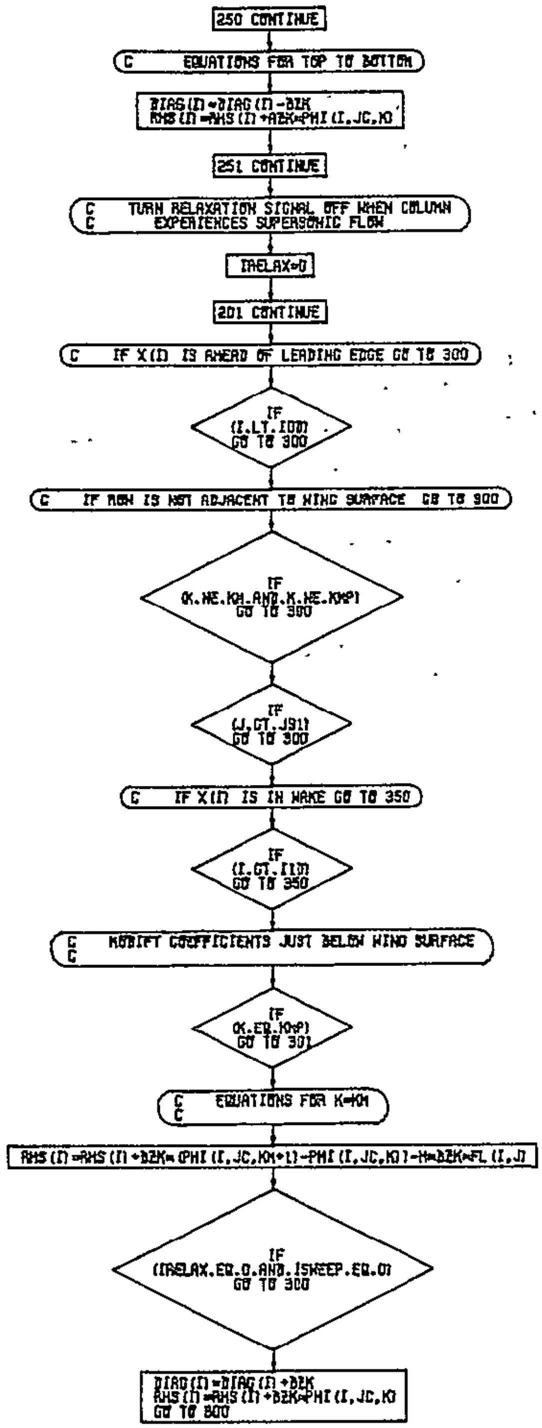

Figure B-17.—(Continued)

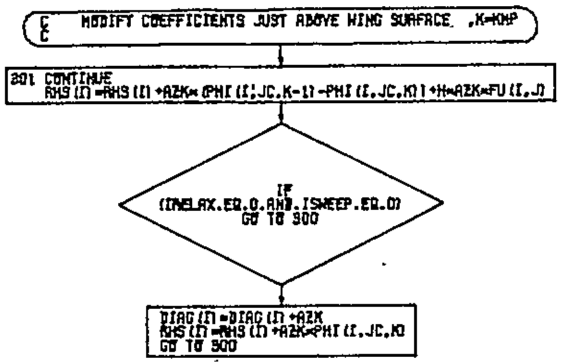

Figure B-17.—(Continued)

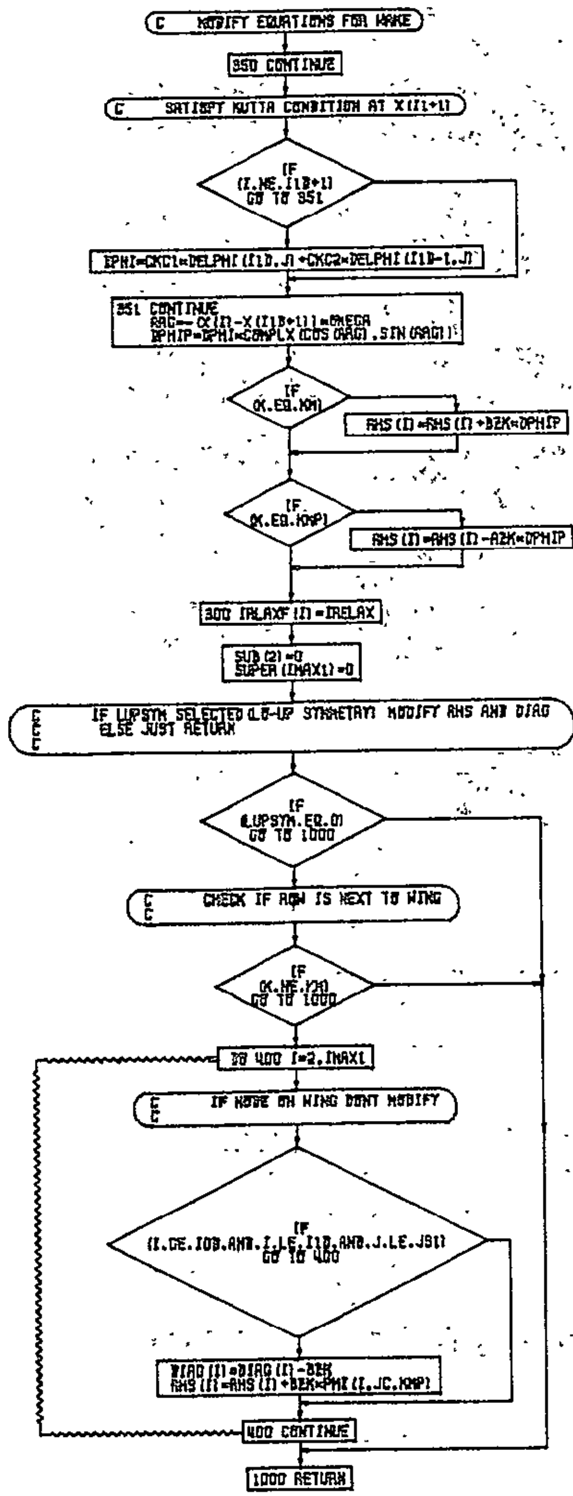

Figure B-17.—(Concluded)

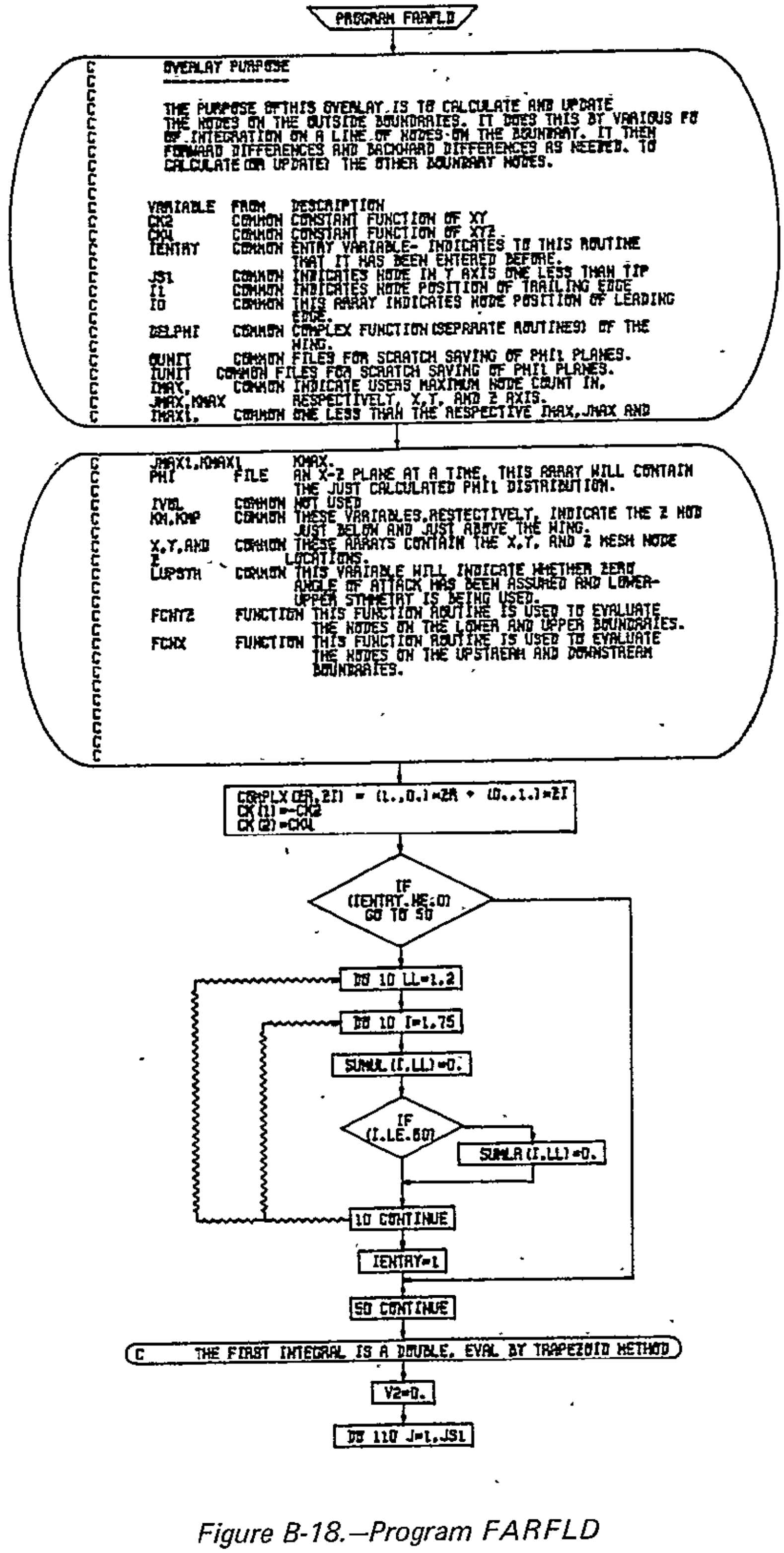

Figure B-18.—Program FARFLD

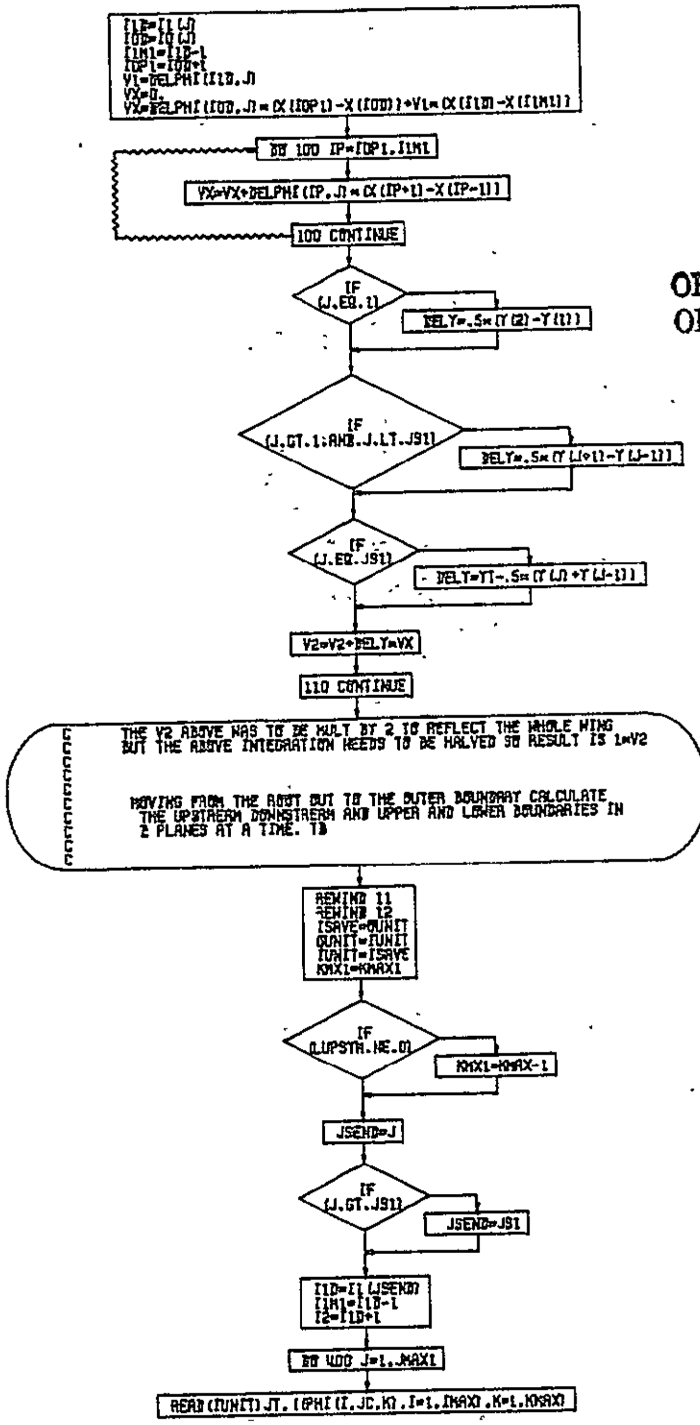

Figure B-18.—(Continued)

ORIGINAL PAGE IS
OF POOR QUALITY

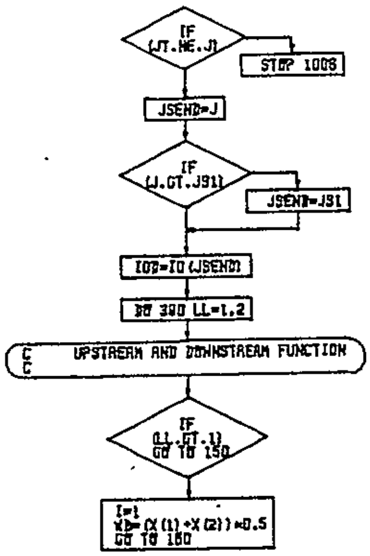

Figure B-18.—(Continued)

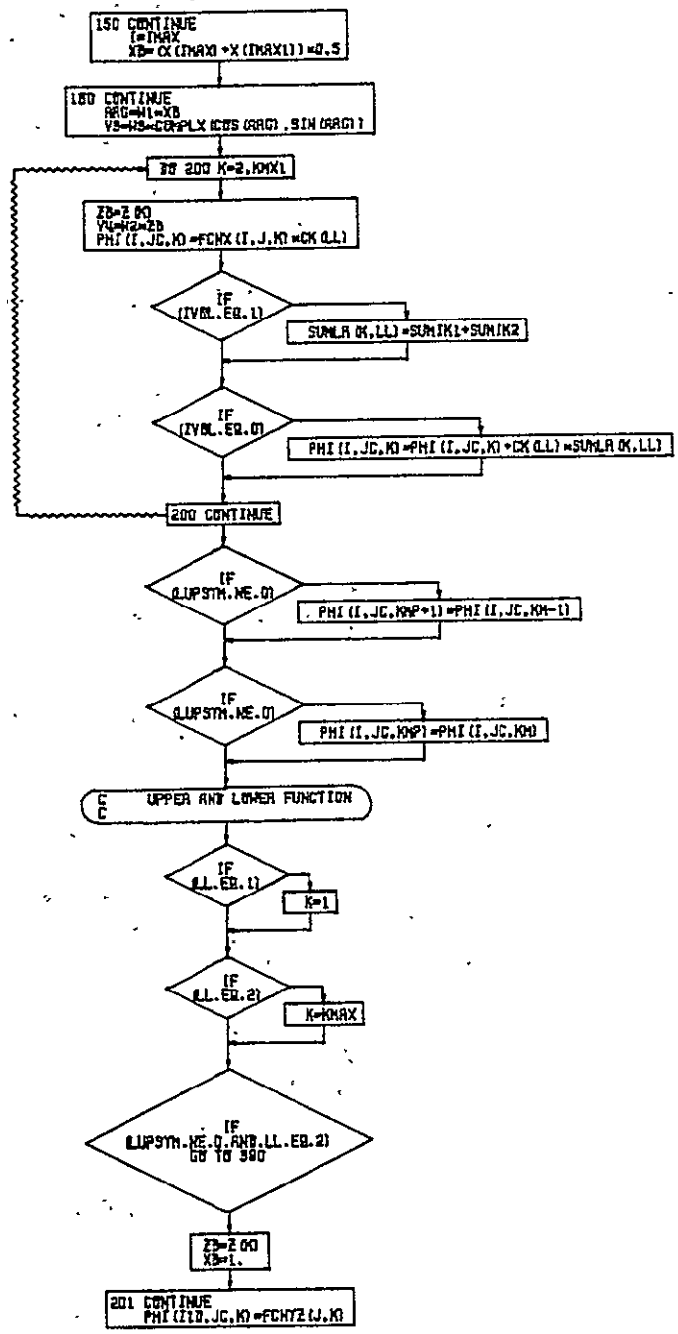

ORIGINAL PAGE IS OF POOR QUALITY

Figure B-18.—(Continued)

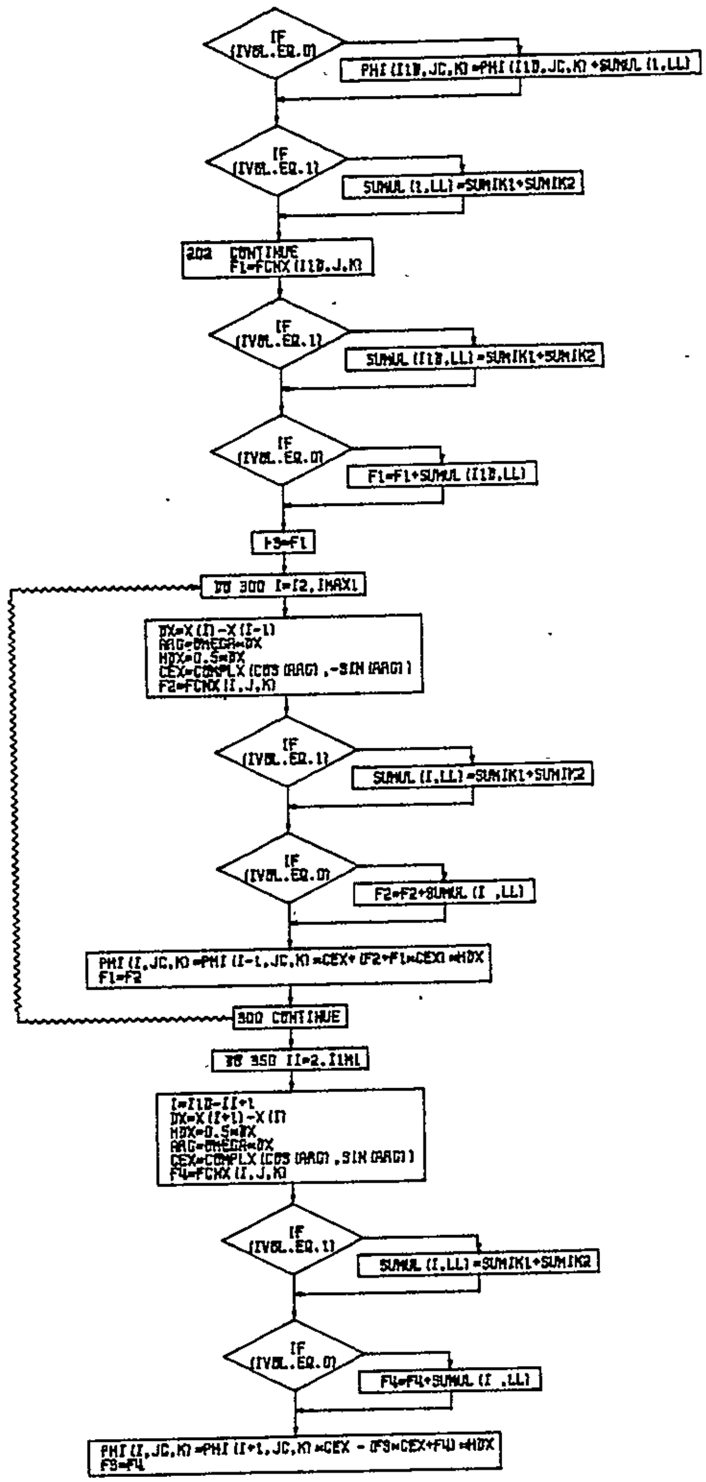

Figure B-18.—(Continued)

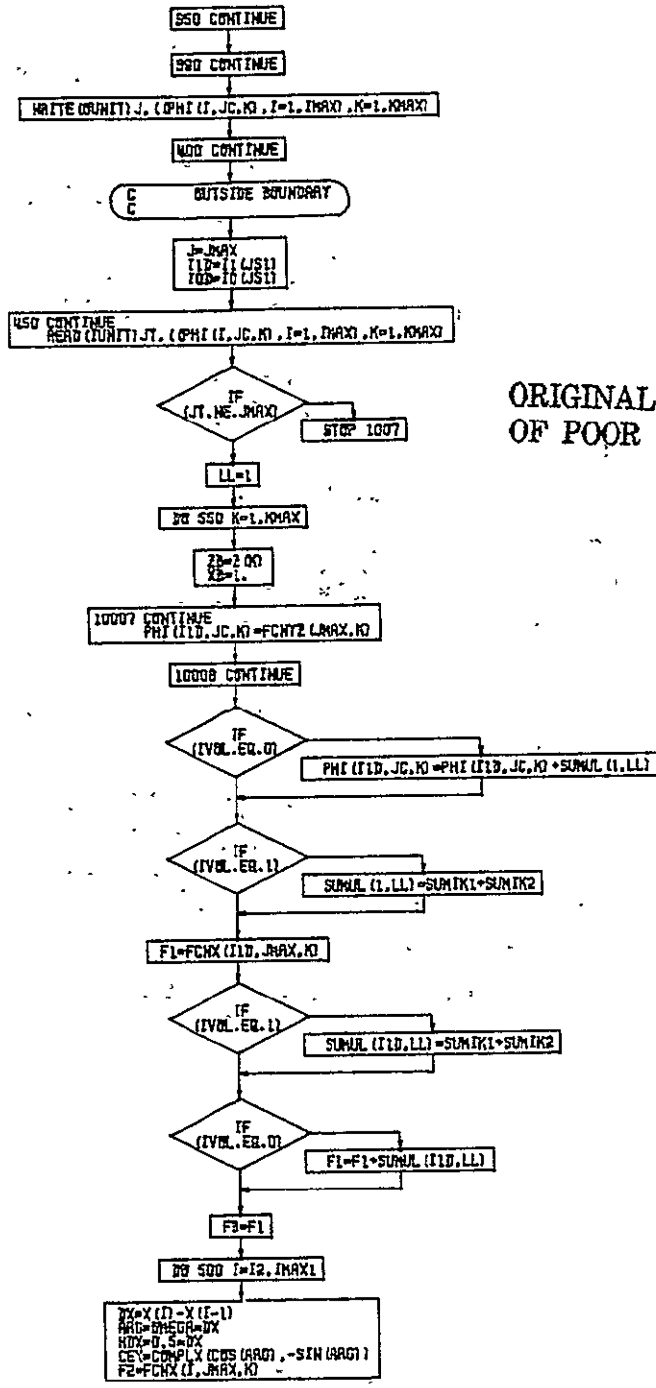

ORIGINAL PAGE IS OF POOR QUALITY

Figure B-18.—(Continued)

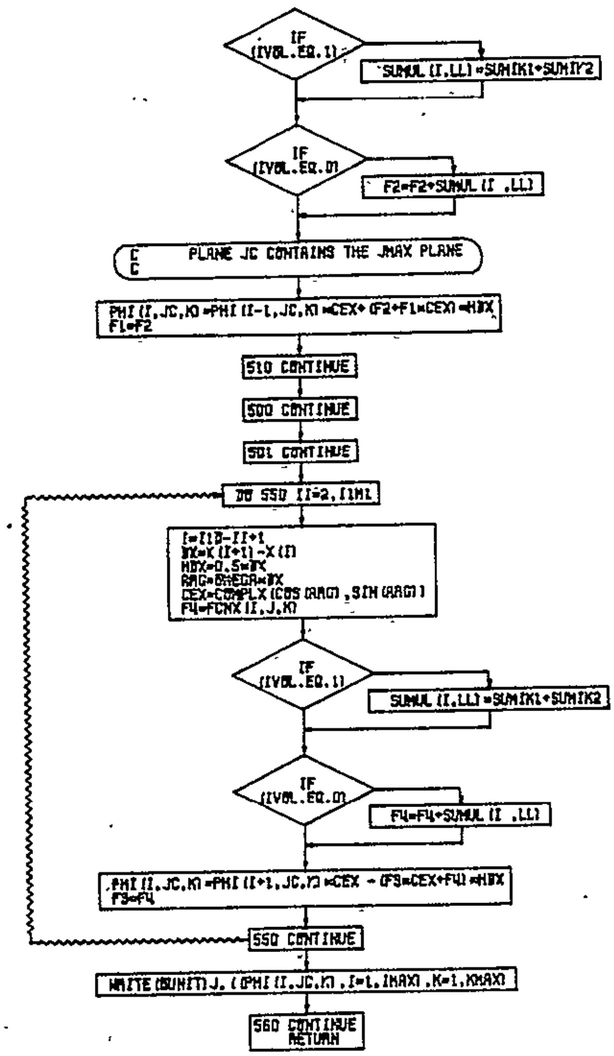

Figure B-18.—(Concluded)

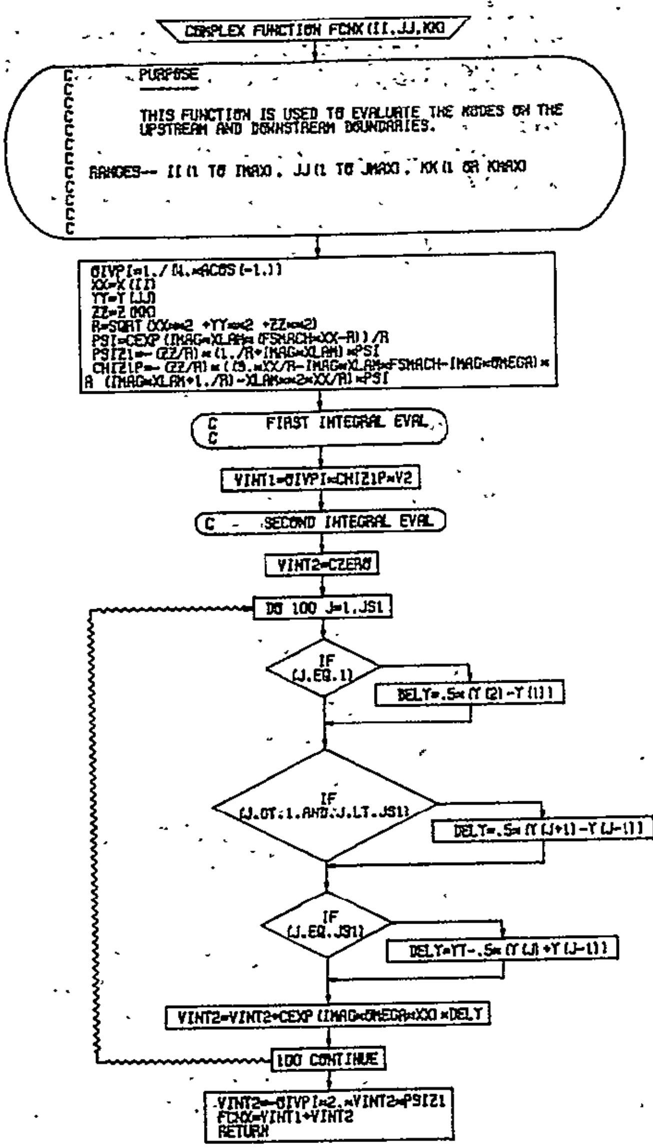

Figure B-19.—Complex Function FCNX

ORIGINAL PAGE IS OF POOR QUALITY

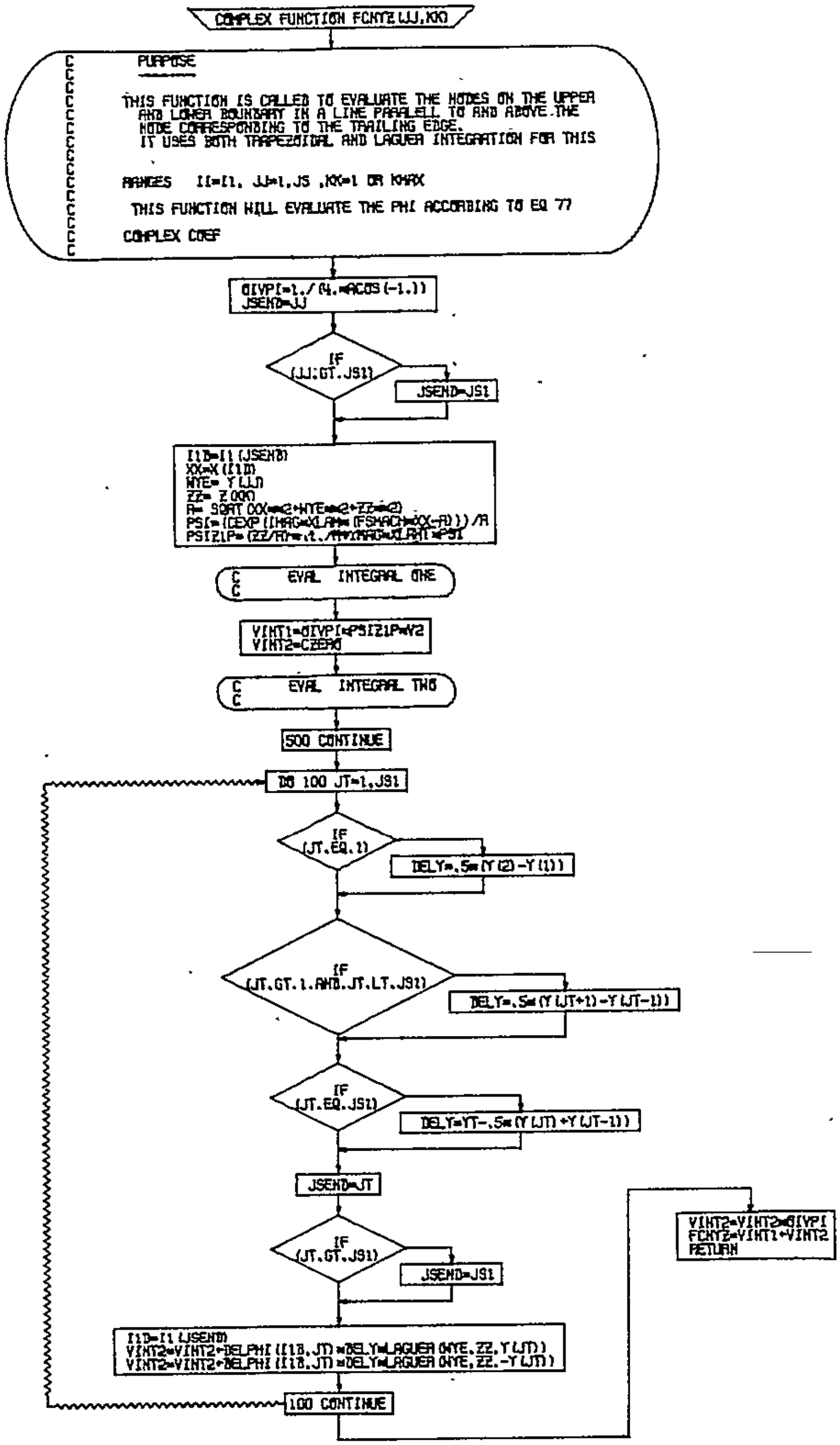

Figure B-20.—Complex Function FCNYZ

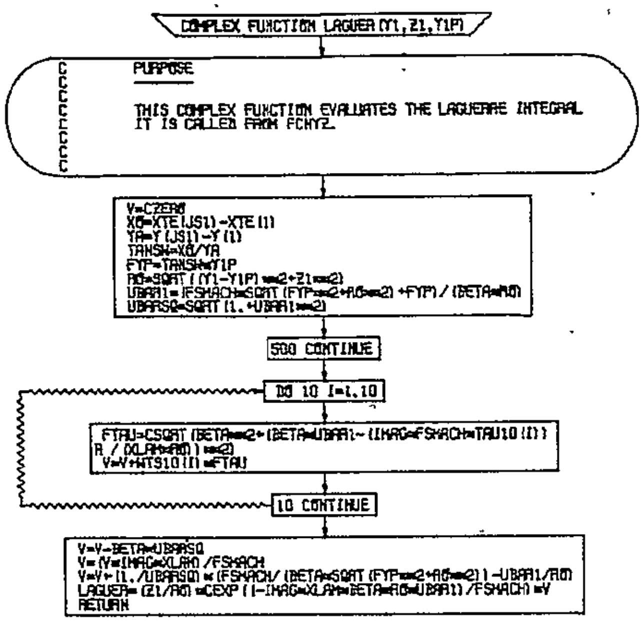

Figure B-21.—Complex Function LAGUER

REFERENCES

1. Ehlers, F. Edward: *A finite Difference Method for the Solution of the Transonic Flow Around Harmonically Oscillating Wings.* NASA CR-2257, January, 1974.

2. Weatherill, Warren H.; Ehlers, F. Edward; and Sebastian, James D.: *Computation of the Transonic Perturbation Flow Fields Around Two- and Three-dimensional Oscillating Wings.* NASA CR-2599, August 1975.

3. Weatherill, Warren H.; Sebastian, James D.; and Ehlers, F. Edwards: *The Practical Application of a Finite Difference Method for Analyzing Transonic Flow Over Oscillating Wings and Airfoils.* NASA CR-14204, September 1977.

4. Ballhaus, W. F.; and Bailey, F. R.: *Numerical Calculation of Transonic Flow About Swept Wings.* AIAA Paper No. 72-677, presented at the AIAA 5th Fluid and Plasma Dynamics Conference, Boston, Massachusetts, June 26-28, 1972.

END

19 JAN. 1978